UNIVERSITY OF KWAZULU-NATAL

SYNTHESIS AND CHARACTERIZATION OF TRIOCTYLAMMONIUM DICARBOXYLATE IONIC LIQUIDS FOR HEAVY METAL EXTRACTION FROM AQUEOUS SOLUTIONS
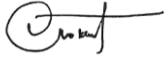

Zaheer Ramjhan
[BScEng, UKZN]

A dissertation submitted in fulfilment of the requirements for the degree of

Master of Science in Engineering, Chemical Engineering

College of Agriculture, Engineering, and Science

University of KwaZulu-Natal

Supervisor: Prof. D. Lokhat

Co-Supervisor: Dr A. Ahmad

January 2020

As the candidate's Supervisor I agree/do not agree to the submission of this thesis. The supervisor must sign all copies after deleting which is not applicable

…………………………..

Prof. D. Lokhat

DECLARATION

I, ……………………………………….………………………., declare that

1. The research reported in this thesis, except where otherwise indicated, is my original research.
2. This thesis has not been submitted for any degree or examination at any other university.
3. This thesis does not contain other persons' data, pictures, graphs or other information, unless specifically acknowledged as being sourced from other persons.
4. This thesis does not contain other persons' writing, unless specifically acknowledged as being sourced from other researchers. Where other written sources have been quoted, then:
a. Their words have been re-written but the general information attributed to them has been referenced
b. Where their exact words have been used, then their writing has been placed in italics and inside quotation marks, and referenced.
5. This thesis does not contain text, graphics or tables copied and pasted from the Internet, unless specifically acknowledged, and the source being detailed in the thesis and in the References sections.

Signed: ………………………….   Date: ………………………….

ACKNOWLEDGEMENTS

ABSTRACT

Five hydrophobic trioctylammonium-based ionic liquids (ILs) functionalized with phthalate, succinate, adipate, suberate, and sebacate anions were synthesized for heavy metal extraction from aqueous solutions. The ILs were characterized using ^{1}H NMR, ^{13}C NMR, and FT-IR spectroscopy, with FT-IR spectroscopy confirming the synthesis of the ILs. The thermal stability of the ILs was investigated using thermogravimetric analysis, and the synthesized ILs had decomposition temperatures between 205 and 222 °C. Of the five synthesized ILs, [HTOA][phthalate], [HTOA][adipate], and [HTOA][sebacate] were liquid at room temperature (18 °C) with [HTOA][succinate] and [HTOA][suberate] having melting points of 20 and 26 °C, respectively. The temperature dependences of density, viscosity, and electrical conductivity for the liquid ILs were investigated in the temperature range of 293.15–333.15 K and modelled using a linear model, the Vogel–Fulcher–Tammann model, and the Arrhenius model, respectively. [HTOA][phthalate], [HTOA][adipate], and [HTOA][sebacate] were highly viscous, having viscosities of 734.3, 3369.7, and 2471.7 mPa s, respectively, at 25 °C. The addition of a molecular solvent was shown to be effective in reducing the viscosity as IL mixtures of [HTOA][phthalate], [HTOA][adipate], and [HTOA][sebacate] with 10 wt.% methanol had viscosities of 82.8, 250.7, and 193.5 mPa s, respectively, at 25 °C. Walden plots were prepared to investigate the extent of proton transfer in the liquid IL systems. Analysis of these plots indicated that these ILs had low ionicities. The efficacy of [HTOA][phthalate] and [HTOA][adipate] as extraction solvents in liquid-liquid extraction of Cd(II), Cu(II), and Zn(II) from aqueous solutions was then determined by investigating the effect of extraction time on the extraction process, with four extraction times being used: 5, 15, 30, and 60 min. [HTOA][suberate] was not water stable and was not investigated further. [HTOA][adipate] performed better than [HTOA][phthalate], having extraction efficiencies of 85, 67 and 69% for Cd(II), Cu(II), and Zn(II), respectively, after 60 min. In comparison, [HTOA][phthalate] had extraction efficiencies of 85, 53, and 37% for Cd(II), Cu(II), and Zn(II), respectively, after 60 min. The lower performance of [HTOA][phthalate] may be due to the steric hindrance exerted by the benzene ring present in the phthalate ion. Both ILs showed a higher affinity for Cd(II), with extraction efficiencies for Cd(II) being significantly higher than those for Cu(II) and Zn(II). The recyclability of the [HTOA][adipate] was investigated by using 0.1 M EDTA solution as the regenerating agent. The EDTA solution was effective in extracting Cd(II) and Cu(II), with back-extraction efficiencies of 89 and 82%, respectively. Its extraction of Zn(II) was less effective with a back-extraction efficiency of 41% being achieved.

TABLE OF CONTENTS

LIST OF FIGURES

LIST OF TABLES

NOMENCLATURE

Symbol	Description	Units
A_0	Density model parameter	g cm^{-3}
A_1	Density model parameter	$\text{g cm}^{-3}\ \text{K}^{-1}$
B	Viscosity model parameter (VFT)	K
C	Concentration	mg L^{-1}
D_i	Distribution ratio for metal i	
E_{es}	Energy of the electrostatic interactions	J
E_{sr}	Energy of the short-range interactions	J
E_i	Extraction efficiency for metal i	%
E_η	Activation energy for dynamic viscosity	kJ mol^{-1}
E_σ	Activation energy for electrical conductivity	kJ mol^{-1}
F_e	The magnitude of the electrostatic force between two ions	N
m	Mass	g
n_D	Refractive index	
R	Ideal gas constant	
R^2	Coefficient of determination	
s	Standard deviation	
T	Temperature	°C or K
T_m	Melting point	°C
T_o	Viscosity model parameter (VFT)	K
T_{onset}	Onset temperature of decomposition	°C
$u(x)$	Uncertainty of x	
$U(x)$	Expanded uncertainty of x	
V	Volume	L

Greek letters

δ	Chemical shift	ppm
η	Viscosity	mPa s
η_0	Viscosity model parameter (VFT)	mPa s
η_∞	Viscosity at infinite temperature (Arrhenius)	mPa s
Λ	Molar conductivity	S cm^2 mol^{-1}
$\bar{\nu}_{\max}$	Wavenumber of maximum absorption peaks	cm^{-1}
ρ	Density	g cm^{-3}
σ	Electrical conductivity	μS cm^{-1}
σ_∞	Electrical conductivity at infinite temperature (Arrhenius)	μS cm^{-1}

Subscript	Description
IL	Ionic liquid
aq	Aqueous

Abbreviation	Description
HTOA	Trioctylammonium
IL	Ionic liquid
LLE	Liquid-liquid extraction
MTOA	Methyltrioctylammonium
PIL	Protic ionic liquid
TOA	Trioctylamine
VFT	Vogel–Fulcher–Tammann
wt.%	Weight percent

CHAPTER 1 INTRODUCTION

1.1 Background and rationale

Heavy metals are metals with relatively high densities and potential toxicity. These include cadmium, lead, mercury, arsenic, chromium, copper, nickel, and zinc. Industries such as metal forming, electroplating, and battery manufacturing industries produce industrial wastewater containing high concentrations of heavy metals, resulting from numerous processes such as cooling and cleaning (Thomas et al., 1986). This wastewater cannot be discharged directly into the environment due to the non-biodegradable and toxic nature of the heavy metals present in the effluent. For instance, high concentrations of lead can harm aquatic life while also causing anaemia and neurological disturbances in humans (Akpor et al., 2014; WHO, 2010). Furthermore, discharge into wastewater treatment works (WWTWs) is also problematic in that high concentrations of heavy metals can reduce plant efficiency (Theodore et al., 2008).

In order to protect the environment and ensure WWTWs operate efficiently, various laws and regulations were promulgated to ensure the quality of discharged effluent is acceptable (Theodore et al., 2008). For example, the U.S. Environmental Protection Agency (EPA) developed Effluent Guidelines which are industry-specific regulations to control the quality of industrial wastewater discharged. Locally, the South African Department of Water and Sanitation and Department of Environmental Affairs (DEA) accomplishes this through various regulations and national guidelines that require industries to obtain permits to discharge industrial effluent (DEA, 2014). These regulations compel industries to pretreat industrial wastewater prior to discharge in order to prevent damage to the environment and WWTWs.

The pretreatment technology that is generally used is chemical precipitation (Gunatilake, 2015). Chemical precipitation involves treating the wastewater with precipitating agents, followed by physically separating the metal precipitates formed utilizing either sedimentation or filtration (Thomas et al., 1986). While this process is relatively simple and effective, disadvantages include large chemical usage and production of chemical sludge which requires further treatment (Theodore et al., 2008; Barakat, 2011). Other possible techniques include ion exchange, adsorption, and electrolysis. However, while possessing some advantages, these techniques are limited due to their operating costs (Barakat, 2011). Due to the disadvantages

present in existing pretreatment methods, a great deal of research has been conducted to create cost-effective and efficient pretreatment technologies.

Recently, liquid-liquid extraction (LLE) utilizing ionic liquids as extraction solvents has emerged as a promising technique for heavy metal removal (Stojanovic and Keppler, 2012). Ionic liquids (ILs) are defined as ionic compounds with melting points below 100 °C (Wilkes, 2002) or, more generally, as liquids which are comprised entirely of ions (MacFarlane et al., 2009). ILs possess low vapour pressures and wide liquidus ranges. As such, they compete favourably against molecular solvents commonly used in LLE processes (Stojanovic and Keppler, 2012).

The ILs generally investigated incorporate quaternary ammonium or phosphonium cations and carboxylic acid derived anions. This is due to the resulting hydrophobicity achieved from the long alkyl chains on the cation and the functionality achieved from N, O, or S, which coordinate to the metal ions in order to remove them from solution, usually found on the anion. Although numerous studies have reported good results utilizing quaternary ammonium and phosphonium ILs (Valdés Vergara et al., 2014; Platzer et al., 2017a), few studies have investigated the use of their protic counterparts. Protic ionic liquids (PILs), which are formed by proton transfer reactions between a Brønsted acid and a Brønsted base, have some advantages over quaternary ILs in that their synthesis is simpler, does not involve the use of halogen impurities, and utilizes inexpensive starting materials (Janssen et al., 2016; Al Kaisy et al., 2017a).

Recently, Janssen et al. (2016) have shown that PILs synthesized from trioctylamine perform well in extracting copper from aqueous solutions and concluded that PILs might be highly suitable extraction solvents. However, a difficulty encountered with PILs is the extent to which the proton transfer reaction occurs. Stoimenovski et al. (2010) have shown that the degree of proton transfer in systems involving tertiary amines is low. They attributed this to there being no hydrogen bonding sites in tertiary amines (Stoimenovski et al., 2010). However, they concluded that the presence of hydrogen bonding sites in either the cation or anion precursor would greatly affect the extent to which proton transfer occurs. Proton transfer is also a function of the difference in acid dissociation constants of the acid and base. Therefore, the degree of proton transfer tends to be higher in systems in which acids and bases have increased acidities and basicities, respectively (Yoshizawa et al., 2003).

The present study aimed to synthesize and characterize trioctylammonium PILs incorporating dicarboxylate anions and evaluate their efficacy as extraction solvents in liquid-liquid extraction of Cd(II), Cu(II), and Zn(II) from aqueous solutions. Dicarboxylic acids were selected as anion precursors because of their increased acidity compared to monocarboxylic acids, their additional hydrogen bonding site provided by the second –OH group, and their functionality achieved by the O atoms in the carboxyl group. Trioctylamine was used as the cation precursor due to the hydrophobicity gained from its long alkyl chains. In order to achieve the proposed aim, several objectives will have to be met. These are delineated below:

- Synthesis of trioctylammonium dicarboxylate ILs from commercially available trioctylamine and selected dicarboxylic acids.
- Characterization of the prepared ILs using ^{1}H NMR, ^{13}C NMR, and FT-IR spectroscopy as well as TGA analysis.
- Investigation of the physical properties of the prepared ILs.
- Investigation of the extent to which proton transfer occurs using transport property data of the prepared ILs.
- Evaluation of the efficacy of the studied ILs for heavy metal removal by investigating the effect of extraction time on the extraction process.
- Determination of the recyclability of the prepared ILs after extraction.

1.2 Dissertation outline

Chapter 1 is a general introduction to the project, covering the background and rationale as well as the objectives of the project. In Chapter 2, a comprehensive literature review is presented. The literature review details the synthesis procedures used to prepare the studied ILs, the procedures used to determine the IL's efficacy as extraction solvents, and a concise overview of the use of ILs as extraction solvents in heavy metal extraction.

A thorough description of the materials and the procedure used to prepare the studied ILs are presented in Chapter 3. The procedures and instruments used to investigate the physical properties of the ILs, carry out the spectroscopic characterization, and conduct the extraction studies are also given. A succinct description of the procedures followed in carrying out the metal ion extraction studies is then presented.

Chapter 4 presents the results of the characterization and extraction studies, together with a discussion critically analysing these results. Finally, the major conclusions drawn from the project are presented in Chapter 5.

The appendices include the detailed syntheses, characterization results, spectroscopic spectra, and physical property data of the prepared ILs. Calibration data and raw concentration data for the metal ion extraction studies are also included. This section also includes the uncertainty analysis procedure followed in calculating the uncertainties for the quantitative data.

CHAPTER 2 LITERATURE REVIEW

2.1 Introduction

Ionic liquids (ILs) are a new class of solvents defined as a molten salt with a melting point below 100 °C (Wilkes, 2002). Early research in ILs was driven by the possible design of "low-temperature molten salts" for use as electrolytes in thermal batteries, in order to gain the advantages of (high-temperature) molten salts at lower temperatures. Later, a significant development in the field was the synthesis of air and water stable ILs by Wilkes and Zaworotko (1992) from commonly used 1-ethyl-3-methylimidazolium and hexafluorophosphate, tetrafluoroborate, and nitrate anions (Wilkes, 2002).

Afterwards, the IL field grew rapidly with numerous ILs being synthesized and applications being explored. This growth is attributed to the supposed "greenness" of ILs, arising from their negligible vapour pressure, and their possible replacement of the commonly used volatile organic compounds (VOCs) (MacFarlane et al., 2017). While their greenness is currently an active research topic, ILs still draw considerable interest due to their unique physico-chemical properties. ILs possess wide liquidus ranges, good electrochemical and thermal stabilities, and unique solvation properties. As a result, ILs have been applied in numerous fields including biomass processing (MacFarlane et al., 2017), electrochemistry (Ohno, 2011), and reaction chemistry (Wasserscheid and Welton, 2008).

The focus of this literature review is on the application of ILs as extraction solvents for heavy metal removal from industrial wastewater. The literature review first discusses the physical properties of ILs relevant to liquid-liquid extraction (LLE). The standard synthesis methods are then reviewed, followed by a concise overview of the different ways ILs have been utilized in heavy metal extractions. A discussion on the ions chosen for the current work is then presented.

2.2 Properties of ionic liquids

ILs are composed of ions, generally an organic cation and an inorganic anion (Wilkes, 2003). The desirable properties of ILs, such as their low melting points, are attributed to their constituent ions. Researchers, noting this fact, have selected different combinations of ions such that the properties of the synthesized ILs are suitable for particular applications. Figure 2-1 shows some of the commonly used ions.

Cations

Alkylmethylimidazolium
$[C_n\text{mim}]^+$

Alkyldimethylimidazolium
$[C_n\text{dmim}]^+$

N-alkylpyridinium
$[C_n\text{py}]^+$

Tetraalkylammonium
$[N_{nmop}]^+$

Tetraalkylphosphonium
$[P_{nmop}]^+$

Trialkylammonium
$[HTOA]^+$

$R_{1,2,3,4} = \text{alkyl}$

Anions

Acetate
$[Ac]^-$

Chloride
$[Cl]^-$

Bromide
$[Br]^-$

Iodide
$[I]^-$

Nitrate
$[NO_3]^-$

Hexafluorophosphate
$[PF_6]^-$

Bis(trifluoromethanesulfonyl)imide
$[NTF_2]^-$

Tetrafluoroborate
$[BF_4]^-$
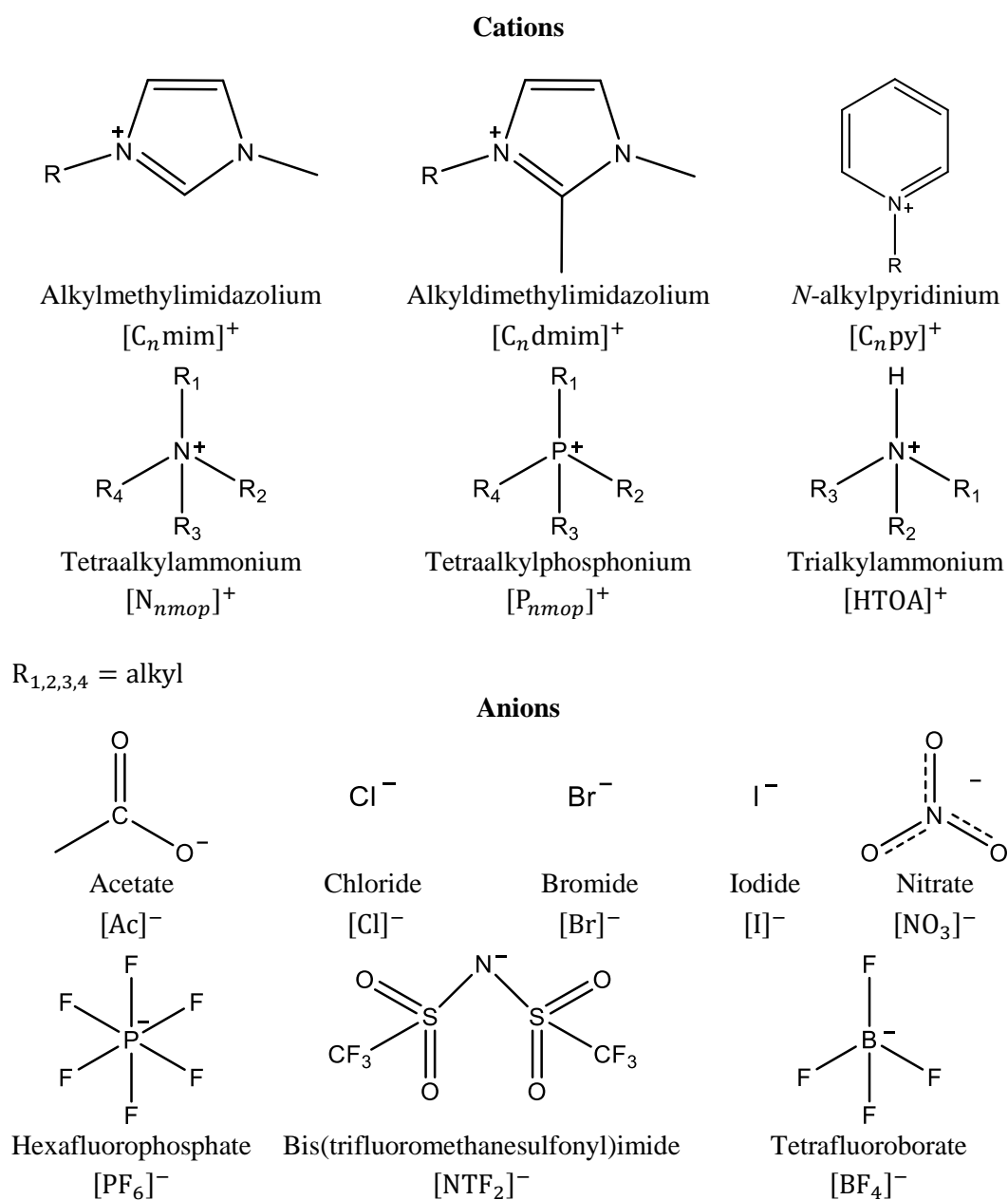
Figure 2-1 Commonly used cations and anions in ionic liquids.

The properties of ILs that are of general interest include the melting point, the density, the viscosity, the electrical conductivity as well as the hydrophobicity of the IL. The following sections describe how the constituent ions in an IL affect the properties previously mentioned.

2.2.1 Melting point

The melting point of ILs is largely governed by the lattice energy of the ionic solid. ILs with lower lattice energies are energetically less stable, and therefore possess lower melting points (MacFarlane et al., 2017). The lattice energy can be thought of as the sum of the energies of the electrostatic interactions, E_{es}, and the short-range interactions, E_{sr}. The dominant term in the lattice energy is the energy of the electrostatic interactions, which result from the individual electrostatic interactions of the constituent ions. The magnitude of the electrostatic force between two ions, F_e, is calculated using Coulomb's Law, given by Eq. 2.1.

$$F_e = \frac{k_e q_1 q_2}{r^2} \tag{2.1}$$

where k_e is Coulomb's constant, q_1 and q_2 are the charges of ion 1 and 2, respectively, and r is the distance between the ions. The electrostatic energy, which is the sum of all the individual attractive and repulsive interactions, is attractive and given by Eq. 2.2.

$$E_{es} = \frac{M q_{cation} q_{anion}}{4\pi \epsilon_0 d_{min}} \tag{2.2}$$

where M is the Madelung constant, d_{min} is the minimum distance, q_{cation} and q_{anion} are the charges of the anion and cation, respectively, and ϵ_0 is the permittivity. Eq. 2.2 shows that ILs with larger ions or ions with smaller charge densities have lower E_{es}, resulting in lower melting points. This was shown by Yang et al. (2015) who investigated the melting points tetrabutylphosphonium based ILs incorporating straight-chain carboxylate anions with chain lengths between 2 and 18. ILs incorporating[CH_3COO]$^-$, [C_3H_7COO]$^-$, [$C_5H_{11}COO$]$^-$ anions had melting points of 54.5, 37.9, and 40.7 °C, respectively. ILs incorporating anions with larger chain lengths (C_8–C_{18}) were liquid at room temperature.

However, E_{sr}, resulting from Van der Waals forces, π-π stacking, and hydrogen bonding, increases as the size of the ions increase. Therefore, increasing the size of the ions would only reduce the melting point of ILs while the short-range interactions are less significant. This was also shown by Yang et al. (2015) when investigating the melting points of trihexyl(tetradecyl)phosphonium ILs. ILs incorporating $[C_7H_{15}COO]^-$, $[C_9H_{19}COO]^-$, $[C_{11}H_{23}COO]^-$, and $[C_{13}H_{27}COO]^-$ anions had melting points of –74.6, –26.5, –12.9, and 0.7 °C, respectively. This illustrated that an increase in the size of the anion increases the melting point. However, these interactions are generally significant in large, branched organic cations.

A simple way then to prepare low-melting ILs is to use larger ions (cations or anions). This has led to the wide use of the common tetraalkylphosphonium and tetraalkylammonium cations, which are also cheaper than imidazolium cations (Wasserscheid and Welton, 2008).

2.2.2 Density

The densities of ILs can vary as they are dependent on the ions used. The densities of ammonium and phosphonium ILs incorporating carboxylate anions typically range between 0.8 and 1 g cm^{-3}, with the majority of the ILs being less dense than water. This can be seen in Table F-2 in Appendix F.

The density of an IL generally decreases as the size of its ions increases. Rocha et al. (2016) investigated the densities of ILs incorporating tetraalkylammonium based cations and fatty acid anions. Their results showed that the density of an IL decreases as the number of carbons in the anion or cation increases. They explained this result by considering the molecular volume of the ion and noting that larger ions would occupy a larger volume and would, therefore, have a lower density.

The density of an ionic liquid is not known to be highly sensitive to temperature (Wasserscheid and Welton, 2008). However, a linear model, Eq. 2.3, is commonly used to investigate the dependence of density on temperature.

$$\rho = A_0 + A_1 T \tag{2.3}$$

where ρ is the density, T is the temperature, and A_0 and A_1 are model parameters.

2.2.3 Viscosity

ILs are generally viscous. The large organic cations, which lower the melting point, also increase the viscosity due to their size and the resulting increase in intermolecular interactions (Van der Waals forces and hydrogen bonding). Thus, the commonly used quaternary phosphonium and ammonium ILs are very viscous. having viscosities from 1000 mPa s to greater than 4000 mPa s, as shown in Table F-2 in Appendix F.

This drawback is alleviated by mixing the IL with a molecular solvent, as solvent addition is noted to reduce the viscosity significantly. Litaiem and Dhahbi (2012) showed this by investigating the viscosities of binary mixtures of the common Aliquat 336 with dimethyl carbonate (DMC). The addition of a molecular solvent was shown to be effective in reducing the viscosity as an IL mixture containing 10 wt.% DMC had a viscosity of 534.7 mPa s at 298 K. This viscosity was significantly lower than the viscosity of pure Aliquat 336 which was 2391.4 mPa s at the same temperature.

The viscosity of an IL is highly sensitive to temperature. As a result, heating is a commonly used method to reduce the viscosity of an IL. The two commonly used models to correlate the effect of temperature on IL viscosity are the Vogel–Fulcher–Tammann (VFT) and Arrhenius models (Anouti et al., 2010; Rocha et al., 2016; Li et al., 2013), which are given by Eq. 2.4 and Eq. 2.5, respectively.

$$\eta = \eta_0 \exp\left[\frac{B}{T - T_0}\right] \tag{2.4}$$

where η is the viscosity, T is the temperature, and η_0, B and T_0 are the model parameters.

$$\eta = \eta_\infty \exp\left[\frac{E_\eta}{RT}\right] \tag{2.5}$$

where η_∞ is the viscosity at infinite temperature, E_η is the activation energy for dynamic viscosity, and R is the ideal gas constant.

2.2.4 Electrical conductivity

As ILs are ionic, one would expect that these solvents possess high electrical conductivities. However, due to significant ion-pairing or the formation of neutral aggregates, the electrical conductivities of ILs are significantly lower than that of a purely ionic substance (MacFarlane et al., 2017). As conductivity is also dependent on viscosity, ILs with high viscosities possess low conductivities.

The electrical conductivity of an IL is sensitive to temperature, and the Arrhenius model, Eq. 2.6, is commonly used to represent the dependence of electrical conductivity on temperature.

$$\sigma = \sigma_\infty \exp\left[\frac{-E_\sigma}{RT}\right] \tag{2.6}$$

where σ_∞ is the electrical conductivity at infinite temperature, E_σ is the activation energy for electrical conductivity, and R is the ideal gas constant.

2.2.5 Hydrophobicity

As with all IL properties, the hydrophobicity of an IL is dependent on both the cation and anion. Generally, large, non-coordinating, charge diffuse anions produce hydrophobic ILs (Cocalia et al., 2008). As a result, fluorinated ions, namely $[PF_6]^{-1}$, $[Tf_2N]^-$ and $[BF_4]^-$, were initially used to synthesize hydrophobic ILs. However, ILs incorporating fluorinated anions have been shown to be prone to hydrolysis, thus limiting their use in aqueous systems (Wasserscheid and Welton, 2003).

An alternative to the use of fluorinated anions is the use of quaternary ammonium and phosphonium cations containing long alkyl chains. The long alky chains increase the organic character of the IL, resulting in water immiscibility. This was shown by Yang et al. (2015), who synthesized two sets of fatty-acid based ionic liquids from tetrabutylphosphonium ($[P_{4444}]^+$) and trihexyl(tetradecyl)phosphonium ($[P_{66614}]^+$) cations. ILs containing the more organic $[P_{66614}]^+$ were hydrophobic while those containing $[P_{4444}]^+$ were not. Due to their desirable hydrophobic nature, quaternary ammonium and phosphonium cations are widely

used in the synthesis of hydrophobic ILs (Valdés Vergara et al., 2014; Parmentier et al., 2015b; Platzer et al., 2017a).

2.3 Synthesis of ionic liquids

2.3.1 Synthesis of protic ionic liquids

Protic ionic liquids are formed by the proton transfer reaction between a Brønsted acid and a Brønsted base, as shown by Eq. 2.7.

$$HA + B \rightleftharpoons [BH]^+[A]^- \tag{2.7}$$

For the reaction of tertiary amines reacting with dicarboxylic acids,

$$NR_3 + HCOO(CH_2)_n COOH \rightleftharpoons [HNR_3]^+[HCOOR'COO]^- \tag{2.8}$$

where R is an alkyl group. The reaction is relatively simple and carried out using simple laboratory glassware. However, a potential difficulty encountered with PIL syntheses is the exothermicity of the proton transfer reaction (MacFarlane et al., 2017). Proton transfer reactions are highly exothermic and require adequate heat removal to ensure that the products do not decompose. The exothermic effects are generally alleviated with the slow addition of the acid, constant stirring, and the use of an oil-bath to maintain a constant temperature and remove heat. The synthesis is usually carried out in a multi-neck flask equipped with a dropping funnel to facilitate the acid addition (Al Kaisy et al., 2017a). A solvent is also sometimes used to act as a heat sink, allowing for adequate temperature control.

In reactions involving a solid acid, the kinetics are much slower due to the slow uptake of solid into in liquid phase of the base (Burrell et al., 2010). For these reactions, no heat removal is generally required, and the reaction may be carried out in a round bottom flask at room temperature with continuous stirring (Janssen et al., 2016). A solvent is generally not used as removal of the solvent tends to remove some of the ions as well (Burrell et al., 2010; MacFarlane et al., 2017).

Purification of PILs is generally difficult as purification methods tend to remove some of the ions as well. An effective method to ensure the synthesis of high purity ILs is to purify all starting materials prior to use (MacFarlane et al., 2017).

2.3.2 Synthesis of aprotic ionic liquids

While not carried out in the current work, the synthesis of aprotic ILs is briefly discussed in order to show the differences between aprotic and protic ILs. The synthesis of aprotic ILs consist of two steps: formation of the aprotic cation and anion exchange to incorporate the desired anion. Quaternization, which is the alkylation of tertiary amines or phosphines using alkyl halides, is generally used to synthesize the aprotic cation (Gordon and Muldoon, 2008).

$$NR_3 + R'-X \rightarrow [NR_3R']^+X^- \qquad (2..9)$$
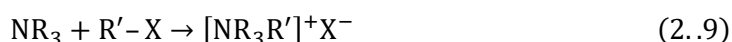
where R' is an alkyl group, and X is a halogen. Anion exchange is generally carried out *via* metathesis reactions utilizing Brønsted acids.

$$[NR_3R']^+X^- + H^+[A]^- \rightarrow [NR_3R']^+[A]^- + HX \qquad (2.10)$$
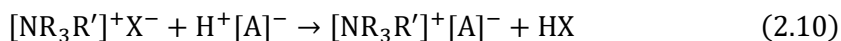
As can be seen from the above reactions, the synthesis of PILs is simpler, requiring one reaction step. Aprotic syntheses also utilize haloalkanes for the alkylation reaction. As a result, halogen impurities remain in the IL. These impurities can affect the properties of the IL as well as poison catalysts (Wagner and Hilgers, 2008).

2.3.3 Characterization of ionic liquids

Product confirmation is usually carried using ^{1}H NMR, ^{13}C NMR, and FT-IR spectroscopy. ^{1}H NMR spectroscopy is used in identifying the deprotonation of monocarboxylic acids through the absence of the characteristic signal of the hydrogen in the carboxyl group of the carboxylic acid (Leyma et al., 2016). FT-IR spectroscopy is useful since the relative shifts of absorption bands in the product and the reactants are generally used to confirm strong proton transfer (Stoimenovski et al., 2012).

2.4 Ionic liquids in heavy metal extraction

Early application of ILs in heavy metal extraction consisted of a two-step process. Chelating agents (extractants) were first added to the aqueous solutions to coordinate to the metal ions, forming a metal complex. These complexes were then extracted from the aqueous phase using a hydrophobic IL (Dietz, 2006). This particular application received much interest as the IL solvents performed much better than molecular solvents that were used in the same manner. In addition, ILs were considered more environmentally benign than molecular solvents. Successful extractants included the dicyclohexano-18-crown-6 crown ether, with imidazolium-based ILs being used as the extracting phase (Dietz, 2006).

Two different extraction mechanisms were proposed for the second step of the process, depending on the type of extractant used. The first mechanism, proposed for acidic and anionic extractants, involved ion-exchange of the metal complex with either the cation or the anion of the IL. The second mechanism, proposed for neutral extractants, involved neutral extraction of the metal complex into the IL phase. Neutral extraction was the favoured extraction mechanism since the ion-exchange mechanism would involve the loss of an ion, usually the cation, to the aqueous phase (Stojanovic and Keppler, 2012) However, subsequent analyses revealed that ion-exchange was the extraction mechanism for both extractants (Dietz, 2006). This was unfavourable as IL cations are usually toxic (Stojanovic and Keppler, 2012). Furthermore, regeneration of the IL would be expensive.

A solution to promote the neutral extraction mechanism was to increase the hydrophobicity of the cation by either fluorinating the alkyl chain on the cation or increasing its chain length. However, this approach was not effective in reducing ion-exchange. Furthermore, the resulting performance of the ILs was significantly lower (Dietz, 2006). The use of ILs together with an extractant would, therefore, be unfeasible for industrial applications as the process would not be cost-effective. Moreover, the extraction process would also be environmentally harmful as cations would remain in the aqueous phase.

2.5 Task-specific ionic liquids

A more favourable approach than the IL-extractant method is the use of task-specific ionic liquids (TSILs), which are defined as ionic liquids in which a functional group is attached to the cation or anion of the IL (Davis, 2003). Visser et al. (2002) synthesized TSILs by appending metal ion coordinating groups to imidazolium cations for extraction of Hg(II) and Cd(II) from aqueous solutions. The appended urea-, thiourea-, and thioether groups coordinated to the metal ions, thereby extracting them into the IL phase. In this approach, the extractants were fixed to the IL phase. The authors concluded that metal ion extraction in this manner would reduce the loss of extractant to the aqueous phase, a significant problem encountered with the earlier application. Furthermore, the prepared ILs also showed good extractive capability, indicating that the functionalization was effective.

TSILs, therefore, function as the extractant and the solvent, significantly simplifying and improving the IL-extractant approach. Since then, numerous studies have explored the use of TSILs, yielding promising results. The TSILs initially studied comprised a task-specific cation for functionality, and a fluorinated anion for hydrophobicity (Visser et al., 2002). The extra synthesis steps in preparing the task-specific cation resulted in these TSILs being more expensive to synthesize (Visser et al., 2002). As a result, recent studies have focused on the use of quaternary ammonium and phosphonium cations and carboxylate anions. In these ILs, hydrophobicity is achieved through the long alkyl chains of the cation, and functionality is achieved through the anion, usually with the O atoms in the carboxyl group.

The standard procedure used to investigate the extractive ability of an IL involves agitating the IL phase and a neutral aqueous phase containing the metal ions. After agitation, the phases are separated, and the metal ion concentration in the aqueous is determined. Two measures are commonly used to determine the efficiency with which the ILs extract the metal ions. The first is the extraction efficiency, E, defined by Eq. 2.11.

$$E(\%) = \left(\frac{C_{\text{aq}}^0 - C_{\text{aq}}}{C_{\text{aq}}^0} \right) \times 100 \qquad (2.11)$$

where C^0_{aq} and C_{aq} are the initial and final metal ion concentrations in the aqueous phase, respectively. The second measure is the distribution ratio, D, defined by Eq. 2.12

$$D = \left(\frac{C^0_{\text{aq}} - C_{\text{aq}}}{C_{\text{aq}}}\right)\left(\frac{V_{\text{aq}}}{V_{\text{IL}}}\right) \qquad (2.12)$$

where V_{aq} and V_{IL} are the volumes of the aqueous and the IL phase, respectively.

Numerous studies have reported favourable results with the use of quaternary ammonium and phosphonium ILs. Parmentier et al. (2013) investigated the extractive ability of tetraoctylammonium based ILs functionalized with oleate and linoleate anions. They efficiently extracted Mn(II), Fe(II), and Zn(II) from aqueous solutions, obtaining extraction efficiencies in excess of 99% for all metals after 2 h.

In a different study, Valdés Vergara et al. (2014) synthesized several methyltrioctylammonium (MTOA) and methyltrihexylammonium ILs incorporating carboxylate and dicarboxylate anions for extraction of Co(II), Cu(II), Ni(II), Pb(II), and Zn(II) from neutral aqueous solutions. These ionic liquids showed good extraction efficiencies, with MTOA oxalate obtaining extracting efficiencies above 88% for all metal ions after 15 min. The authors also compared the extractive capability of the synthesized ILs against the commercial MTOA thiosalicylate. The synthesized ILs achieved higher extraction efficiencies than the commercial IL, an IL designed specifically for Cu(II) extraction.

In a later study, Valdés Vergara et al. (2015) investigated the use of MTOA camphorate and MTOA dodecanedioate for extraction of Cd(II), Cu(II), and Pb(II) from neutral aqueous solutions. Both ILs obtained good results, with extraction efficiencies above 80% for all metal ions after 30 min. MTOA dodecanedioate performed better than MTOA camphorate in extracting Cu(II). The authors stated that the increased performance of MTOA dodecanedioate was due to the arrangement and number of carbon atoms in the dodecanedioate anion. The dodecanedioate anion contained more carbon atoms in a linear arrangement as opposed to the camphorate anion, which contained fewer carbon atoms in a cyclic arrangement. They concluded that the steric hindrance exerted by the carbon ring present in the camphorate anion affected the extraction process.

Many researchers add CaCl$_2$ to the aqueous phase before extraction to increase the ionic strength of the solution. This is done to promote the extracting ability and improve the water solubility of the IL (Stojanovic et al., 2010). Leyma et al. (2016) investigated the use of several ammonium and phosphonium based ILs functionalized with thiosalicylate derived anions for extraction of Zn(II), Cd(II) and Cu(II) from 0.1 M CaCl$_2$ aqueous solution. Good extraction efficiencies were obtained for all the ILs when extracting Cd(II) and Cu(II) after 24 h.

In a recent study, Platzer et al. (2017a) investigated several MTOA and methyltrioctylphosphonium based ILs as extracting agents for Cu(II) and Cd(II) from 0.1 M CaCl$_2$ aqueous solution. The extraction efficiencies of the thioglycolate functionalized ILs for Cd(II) were in excess of 90% after 30 min.

2.5.1 Extraction mechanism for TSILs

While neutral extraction by the anion is generally assumed to be the extraction mechanism for TSILs, the extraction mechanism is still an active research topic. Platzer et al. (2017a) investigated the extraction mechanism of thioglycolate based IL in extracting Cu(II) and Cd(II). They used FT-IR spectroscopy to confirm coordination of Cd(II) to the thioglycolate anions, confirming that neutral extraction had occurred.

Parmentier et al. (2013) investigated the extraction mechanism for oleate and linoleate based ILs. The authors used the change in chloride concentration of the aqueous phase to conclude that the dominant extraction mechanism was neutral extraction and not ion-exchange. However, in a subsequent study with tetraoctylphosphonium oleate, Parmentier et al. (2015b) stated that ion-exchange of anionic chloro complexes was one possible mechanism.

Valdés Vergara et al. (2015) investigated the extraction mechanism for MTOA camphorate and MTOA dodecanedioate. Noting that the anions are highly hydrophobic, they proposed the neutral extraction mechanism shown in Figure 2-2. Here, M denotes the metal ion, and Y denotes the counter ion of the metal salt (Cl$^-$, NO$_3^-$, SO$_4^{2-}$).

$$2R_4N^+ \quad OOC\!-\!C_nH_m\!-\!COOH + 3M^{2+}Y^{2-} + 2H_2O \longrightarrow$$

$$R_4N^+\,Y^{2-}\,M^{2+}\,{}^-OOC\!-\!C_nH_m\!-\!C \overset{O}{\underset{O}{\diagdown}}\ominus\ \ M^{2+}\ \ominus \overset{O}{\underset{O}{\diagup}} C\!-\!C_nH_m\!-\!COO^-\,M^{2+}\,Y^{2-}\,{}^+NR_4 + 2H_3O^+ + Y^{2-}$$
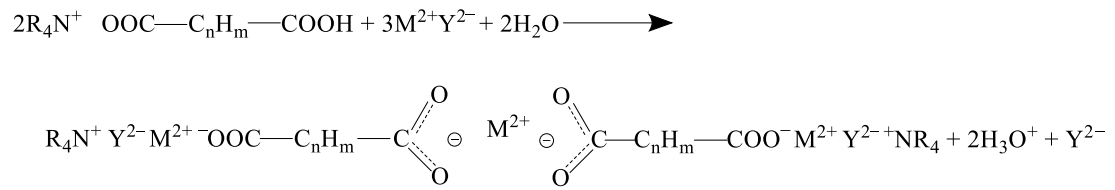
Figure 2-2 Extraction mechanism for MTOA dodecanedioate and MTOA camphorate. Adapted from Valdés Vergara et al. (2015).

In this mechanism, the nitrogen of the quaternary ammonium as well as the carboxyl group of the anion coordinate to the metal ions, with no ion-exchange occurring. It can be concluded from the different studies that the extraction mechanism is not fixed and may change depending on the cation and anion of the IL.

.

2.6 Trioctylammonium ionic liquids

Few studies have investigated the use of PILs in aqueous extractions. In the studies which report their use, the hydrophobic HTOA cation is used. Katsuta and Tamura (2018) extracted Pd(II) and Pt(II) from dilute acidic media using HTOA based ILs incorporating nitrate and chloride ions. As nitrate and chloride anions are not known to impart hydrophobicity, the resulting hydrophobicity was achieved through the use of the HTOA cation. Interestingly, the authors also showed that the HTOA based ILs were more hydrophobic than the corresponding MTOA based ones, which have greater organic character.

As previously mentioned, recent extraction studies utilize ILs containing a quaternary ammonium or phosphonium cation for hydrophobicity, and a carboxylate anion for functionality. As shown in section 2.3.2, these ILs are synthesized in a two-step process, with the hydrophobic cation synthesized in the first step and the functional anion introduced in the second step. With HTOA ILs, the HTOA cation and the functional anion may be synthesized in a single step. Recently, Janssen et al. (2016) showed that in addition to being easily synthesized, these ILs could also be functionalized for metal ion extraction. The authors investigated the extractive capability of HTOA based ILs containing straight-chain carboxylate ions. They achieved extraction efficiencies greater than 75% and concluded that HTOA ILs might be effective extraction solvents.

However, there are two disadvantages encountered with PILs which need mentioning. The first is the potential instability of protic cations in comparison to quaternary ones. Quaternary ammonium cations are more stable than their protic counterparts. This is due to N–C bonds being more stable than N–H ones. However, protic cations would only be reactive in basic media. In acidic media, as is the case with industrial effluent, the stability of the HTOA cation would not be a problem. This is shown in the studies by Katsuta et al. (2011), Katsuta et al. (2012), Katsuta and Tamura (2018), in which metal extraction was from hydrochloric acid solutions.

The second difficulty experienced with PILs is that the proton transfer reaction for these ILs is often incomplete (MacFarlane et al., 2017). As the proton transfer reaction is a neutralization reaction, it is a function of the difference in acid dissociation constants of the acid and base

($\Delta \mathrm{p}K_{\mathrm{a}}^{\mathrm{aq}}$). As a result, the extent of the proton-transfer reaction tends to be higher in systems in which acids and bases have increased acidities and basicities, respectively (Yoshizawa et al., 2003). One method then to ensure the reaction goes to completion it to use stronger acids and stronger bases.

Stoimenovski et al. (2010) investigated the proton transfer reaction for primary amines and tertiary amines. Their results indicated the extent of proton transfer for tertiary amines is much lower than that for primary amines. They attributed this result to there being no hydrogen bonding sites in tertiary amines, as hydrogen bonding sites help stabilize the anion by providing a good solvating environment (Stoimenovski et al., 2010). However, they noted that the presence of hydrogen bonding sites on either the cation or anion would favour PIL formation, significantly affecting the extent to which the proton transfer reaction occurs.

2.6.1 Walden plot

A simple method to investigate the extent of the proton transfer reaction is to prepare a Walden plot (Yoshizawa et al., 2003). The Walden plot is a measure of the ionicity of the PIL (MacFarlane et al., 2009). A high degree of ionicity is characteristic of systems with strong proton transfer. A Walden plot is prepared by plotting the log of the molar conductivity against that of the inverse of the viscosity. According to the Walden rule given by Eq. 2.13, the resulting curve is a straight line. This curve is then compared to a reference curve, usually that for a 0.01 M KCl solution (MacFarlane et al., 2009). Walden curves below the reference would be characteristic of systems with low ionicity, with those above being characteristic of highly ionic systems.

$$\Lambda_{\mathrm{m}} \eta = k \tag{2.13}$$

where Λ_{m} is the molar conductivity, η is the viscosity, and k is a temperature-dependent constant. However, as significant ion-pairing or formation of neutral aggregates may occur, the extent of proton transfer in a PIL may be high even though the ionicity is low (MacFarlane et al., 2017).

2.7 Ions used in the present study

In the present study, HTOA was selected as the cation for the following previously mentioned reasons. Firstly, the HTOA cation imparts hydrophobicity to the IL, which is essential for LLE solvents involving aqueous systems. Secondly, ILs containing this cation may be synthesized in a simple one-step reaction. Finally, the cost of trioctylamine was relatively competitive compared to the cost of the commonly used IL precursors (Davis, 2003).

Dicarboxylate anions were chosen to functionalize the HTOA ILs. The anions selected are shown in Figure 2-3. These anions were selected for several reasons. Firstly, these anions are also hydrophobic, having poor solubilities in water. As the hydrophobicity of an IL is dependent on both the cation and anion, the selected anions would also need to be hydrophobic. Secondly, the dicarboxylic acid precursors possess increased acidities compared to monocarboxylic acids due to inductive electron withdrawal (Bruice, 2016). In addition, compared to monocarboxylic acids, dicarboxylic acids possess an additional hydrogen bonding site provided by the additional COOH group. Both of the above features promote strong proton transfer, as mentioned in the previous section. Thirdly, dicarboxylate anions possess functionality for metal ion extraction through their two carboxyl groups. Finally, the cost of the utilized dicarboxylic acids was also relatively competitive compared to the cost of the commonly used IL precursors.

[phthalate]⁻   [succinate]⁻   [adipate]⁻

[suberate]⁻   [sebacate]⁻
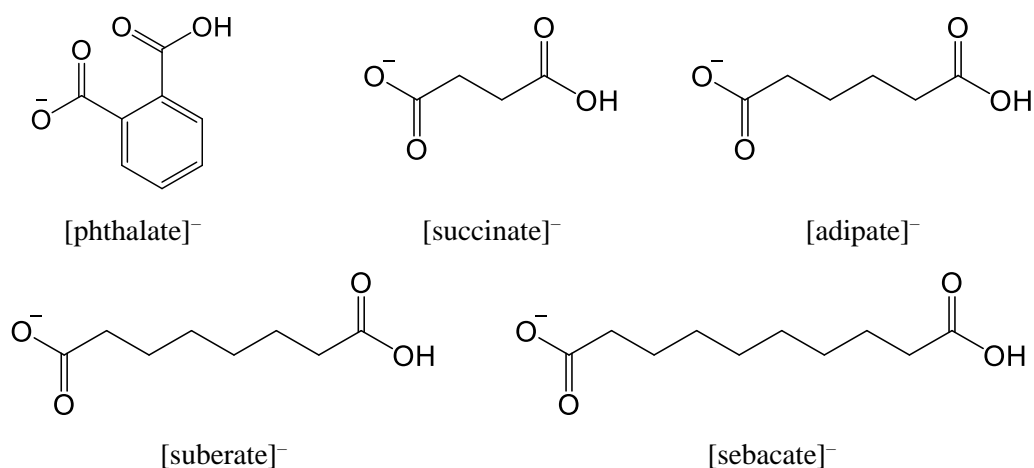
Figure 2-3 The dicarboxylate anions used in the present study.

.

2.8 Regeneration of ionic liquids

IL recyclability is an important factor which needs to be considered when determining the suitability of ILs as extracting solvents. Treatment with acidic solutions is generally used to strip the metal ions from the IL phase, thereby regenerating the IL. The standard measure of the effectiveness of the regenerating agent is the back-extraction efficiency, given by Eq. 2.14.

$$S(\%) = \left(\frac{C_{IL}^0 - C_{IL}}{C_{IL}^0}\right) \times 100 \tag{2.14}$$

where C_{IL}^0 and C_{IL} are the metal ion concentrations in the IL phase before and after back-extraction, respectively.

Leyma et al. (2016) investigated the regenerative properties of several ionic liquids synthesized from Aliquat 336 and Cyphos IL 101 with EDTA, HCl and HNO_3 solutions as stripping agents. HNO_3 worked best in back-extracting Cd(II) from the IL phase.

In another study, Platzer et al. (2017a) conducted back-extraction studies of Cd(II) from MTOA hexylsulfanyl acetate utilizing 0.5 M HNO_3, 0.5 M HCl, and 0.5 M ETDA solutions as regenerating agents. 0.5 M HNO_3 solution was effective in stripping Cd(II) from the IL phase, obtaining a back-extraction efficiency of 72% for Cd(II). 0.5 M HCl and 0.5 M ETDA solutions were not effective. In a later study, Platzer et al. (2017b) conducted back-extraction studies of Zn (II) from methyltrioctylphosphonium hexylsulfanyl acetate utilizing 0.5 M HNO_3, 0.5 M HCl, and 0.5 M H_2SO_4 solutions as stripping agents. Their results indicated 0.5 M HCl and H_2SO_4 were effective in stripping Zn(II) ions.

However, the use of acid solutions has also been shown to protonate the carboxylate anions of the IL. Parmentier et al. (2015a) showed that treatment with H_2SO_4, CH_3CO_2H, and HCl was not suitable in regenerating tetraoctylammonium oleate, as the acids protonated the oleate anion. They concluded that chemical regeneration using acids should be avoided as the direct reuse of the IL would not be possible with using acidic regenerating agents. In the same study, they also concluded that electro-deposition is not suitable for ILs due to the high resistance and viscosities of ILs (Parmentier et al., 2015a).

In a different study, Janssen et al. (2016) obtained promising results with the use of 0.1 M EDTA solution to regenerate [HTOA][octanoate] after Cu(II) extraction. They obtained back-extraction efficiencies in excess of 76%.

CHAPTER 3 EXPERIMENTAL METHOD

3.1 Materials

Trioctylamine (98%), phthalic acid (≥99.5%), succinic acid (99%), adipic acid (99%), suberic acid (98%), and sebacic acid (99%) were purchased from Sigma Aldrich. Atomic absorption spectroscopy standards for cadmium, chromium, copper, lead, and zinc (1000 mg/L in 0.5M HNO_3) were purchased from Laboquip. Nitric acid (65%, AR grade), $CaCl_2 \cdot 2H_2O$ (≥99%), $EDTA \cdot 2H_2O$ (disodium salt, ≥99%), potassium chloride (≥99%), NaOH (≥97%), cadmium nitrate tetrahydrate (98%), chromium nitrate (III) nonahydrate (99%), copper(II), nitrate hemi(pentahydrate) (98%), lead nitrate (≥99%), and zinc nitrate hexahydrate (≥99%) were purchased from Sigma Aldrich. Chloroform-D1 (≥ 99.96%) was purchased from Merck. All reagents and solvents were used without further purification.

3.2 Synthesis of ionic liquids

Five ILs, namely trioctylammonium phthalate [TOAH][phthalate], trioctylammonium succinate [TOAH][succinate], trioctylammonium adipate [TOAH][adipate], trioctylammonium suberate [TOAH][suberate], and trioctylammonium sebacate [TOAH][sebacate], were synthesized *via* neutralization reactions between trioctylamine (TOA) and the corresponding acid according to a similar procedure used by Janssen et al. (2016). TOA and a slight excess of the corresponding acid were added to a round bottom flask. The mixture was then stirred for 24 h at room temperature using a magnetic stirrer. Afterwards, the mixture was left to settle for 2 h, and the IL phase was removed from the unreacted starting materials and then dried over silica gel for 24 h. The reactions were carried out without the addition of a solvent. No significant heat effects were noticed. Detailed syntheses of the prepared ILs are provided in Appendix A.

3.3 Characterization of ionic liquids

This section explains the procedures followed and instruments used to characterize the synthesized ILs.

3.3.1 Spectroscopy

^{1}H NMR spectra were recorded on a Bruker Avance III 400 MHz spectrometer in CDCl$_3$ using CHCl$_3$ as the standard at 7.24 ppm. ^{13}C NMR spectra were recorded on the same instrument in CDCl$_3$ using the solvent as the standard at 77.0 ppm. FTIR spectra were obtained on a Shimadzu IRPrestige-21 FTIR spectrophotometer equipped with an attenuated total reflectance (ATR) accessory.

3.3.2 Thermal analysis

Thermogravimetric analyses (TGA) and differential thermal analyses (DTA) were carried out on a Shimadzu DTG-60AH, using aluminium crucibles under a continuous nitrogen flow of 20 mL min^{-1}. Sample masses were between 15 and 20 mg. A heating rate of 10 °C min^{-1} was used for both TGA and DTA.

3.3.3 Density

Density measurements were carried out on an Anton Paar DSA 5000 M Density meter, with three repeated measurements being performed over the temperature range of 293.15–333.15 K.

3.3.4 Viscosity

Viscosity measurements were carried out on a Brookfield RVDV-II+Pro viscometer using a Small Sample Adapter and Thermosel with a SC4-21 spindle. Three repeated measurements were performed over the temperature range of 293.15–333.15 K.

3.3.5 Electrical conductivity

Electrical conductivity measurements were carried out using a Hanna EC215 conductivity meter equipped with a 4-ring potentiometric probe. Three repeated measurements were recorded over the temperature range of 293.15–313.15 K. Manual single point calibration was performed with the appropriate conductivity standard.

3.4 LLE extraction studies

3.4.1 Test solution preparation

Multi-element aqueous solutions containing 30, 50, 20 mg L^{-1} of Cd(II), Cu(II), and Zn(II) were prepared by dilution of 1000 mg L^{-1} AAS standards using deionized water. The metal ion concentrations were selected according to ratios previously investigated (Leyma et al., 2016), as well as considering the metal ion concentration limits for industrial effluent (CCCT, 2013). CaCl$_2$ was added to increase the ionic strength of the mixture to 0.1 M CaCl$_2$, as was done with previous studies (Leyma et al., 2016; Fischer et al., 2011). NaOH was then added to neutralize the solution. This metal ion solution was used for all extraction experiments. All glassware (pipettes, flasks, beakers) and storage containers (vials, centrifuge tubes) were acid-washed before use using either 10% or 2% HNO$_3$.

3.4.2 Forward extraction of metal ions

The effect of extraction time on the metal uptake by the ILs was investigated using four different extraction times: 5, 15, 30, and 60 min. 2 g of IL and 4 mL of metal ion solution were added to 15 mL centrifuge tubes. The mixtures were then vigorously agitated using a vortex mixer at room temperature. After extraction, the mixtures were centrifuged for 10 min at 3000 rpm to facilitate phase separation. After separation, 2 mL of the resulting metal ion solution was immediately transferred into 15 mL centrifuge tubes, acidified with 10 mL of 2% HNO$_3$ for stabilization, and stored until measurement. Three repeated extraction experiments were performed for each investigated time.

3.4.3 Analysis

After extraction, the metal ion concentrations in the aqueous phase were determined using a Perkin Elmer AAnalyst 100 Flame Atomic Absorption Spectrometer (FAAS) *via* external standard calibration. The extraction efficiency for each metal i, E_i, was calculated using Eq. 3.1.

$$E_i(\%) = \left(\frac{C_{i,\text{aq}}^0 - C_{i,\text{aq}}}{C_{i,\text{aq}}^0}\right) \times 100 \tag{3.1}$$

where $C_{i,\text{aq}}^0$ and $C_{i,\text{aq}}$ are the initial and final metal ion concentrations of metal i in the aqueous phase, respectively. After equilibrium, distribution ratios, D_i, were calculated using Eq. 3.2.

$$D_i = \left(\frac{C_{i,\text{aq}}^0 - C_{i,\text{aq}}}{C_{i,\text{aq}}}\right)\left(\frac{V_{\text{aq}}}{V_{\text{IL}}}\right) \tag{3.2}$$

where V_{aq} and V_{IL} are the volumes of the aqueous and the IL phase, respectively.

3.4.4 Back-extraction

Back-extraction studies were conducted in order to investigate the recyclability of the studied ILs. First, 2 g of IL and 4 mL of metal ion solution were added to 15 mL centrifuge tubes. The mixtures were then agitated for 60 min. Afterwards, the amount of metals ions extracted by the IL was determined by analysing the metal ion solution using FAAS. The used IL and 4 mL of 0.1 M EDTA were then added to a 15 mL centrifuge tube. The mixture was agitated for 60 min. After regeneration, the metal ion concentration in the regenerating agent phase was also determined and used to determine final metal ion concentration in the IL phase. The back-extraction efficiency of the regenerating agent for metal i, S_i, was then calculated using Eq. 3.3

$$S_i(\%) = \left(\frac{C_{i,\text{IL}}^0 - C_{i,\text{IL}}}{C_{i,\text{IL}}^0}\right) \times 100 \tag{3.3}$$

where $C_{i,\text{IL}}^0$ and $C_{i,\text{IL}}$ are the metal ion concentrations of metal i in the IL phase before and after back-extraction, respectively.

CHAPTER 4 RESULTS AND DISCUSSION

4.1 Characterization

4.1.1 NMR spectroscopy

The synthesized ILs were characterized using ^{1}H and ^{13}C NMR spectroscopy, and the corresponding spectra are shown in Appendix B with the chemical shifts reported in Appendix A. ^{1}H NMR spectroscopy was not useful in confirming the proton transfer reaction for the ammonium dicarboxylate ILs. This is because the distinguishing structural differences between the reactants and products, namely the presence of the NH proton and the absence of the one OH proton, are not easily identified using ^{1}H NMR spectroscopy since signals for these protons are highly variable and broad (Foris, 2017).

A broad peak was noted in the ^{1}H NMR spectrum of [HTOA][adipate] at 4.44 ppm (Figure B-3). Although this peak is within the expected range of chemical shifts for NH protons, this peak was large and was not assigned. Furthermore, broad peaks were noted in the ^{1}H NMR spectra of [HTOA][phthalate] (Figure B-1) and [HTOA][suberate] (Figure B-4) between 9–12 ppm, which is characteristic of carboxyl protons. Integration of these peaks showed only one proton which may indicate that proton transfer had occurred. However, these peaks were not observed in the spectra of the other ILs.

The expected chemical shifts for the methyl protons of the octyl chains (0.82–0.87 ppm), the methylene protons of the octyl chains, (1.20–1.70 ppm), and the methyl protons adjacent to nitrogen (2.85–3.04 ppm) were noted for all the ILs. Additionally, the expected chemical shifts for the vinylic protons (2.25–2.32 ppm) and methylene protons (1.20–1.70 ppm) of the dicarboxylate anions were noted for [HTOA][succinate], [HTOA][adipate], [HTOA][suberate], and [HTOA][sebacate], with the chemical shifts of the benzene protons (7.48–7.50 and 8.29–8.32 ppm) being noted for [HTOA][phthalate]. The assignments of the different protons are provided in the ^{1}H NMR spectra in Appendix B. Similarly, expected chemicals shifts for the different carbon atoms were present for all the ILs, as shown by the assignments made in the ^{13}C NMR spectra shown in Appendix B.

4.1.2 FT-IR spectroscopy

The synthesized ILs were characterized using FT-IR spectroscopy, and the corresponding spectra are shown in Appendix B with the absorption bands reported in Appendix A. The proton transfer reaction for the ILs was confirmed using FT-IR spectroscopy as seen in Figure 4-1, which shows the partial, superimposed spectra for the [HTOA][adipate] system.
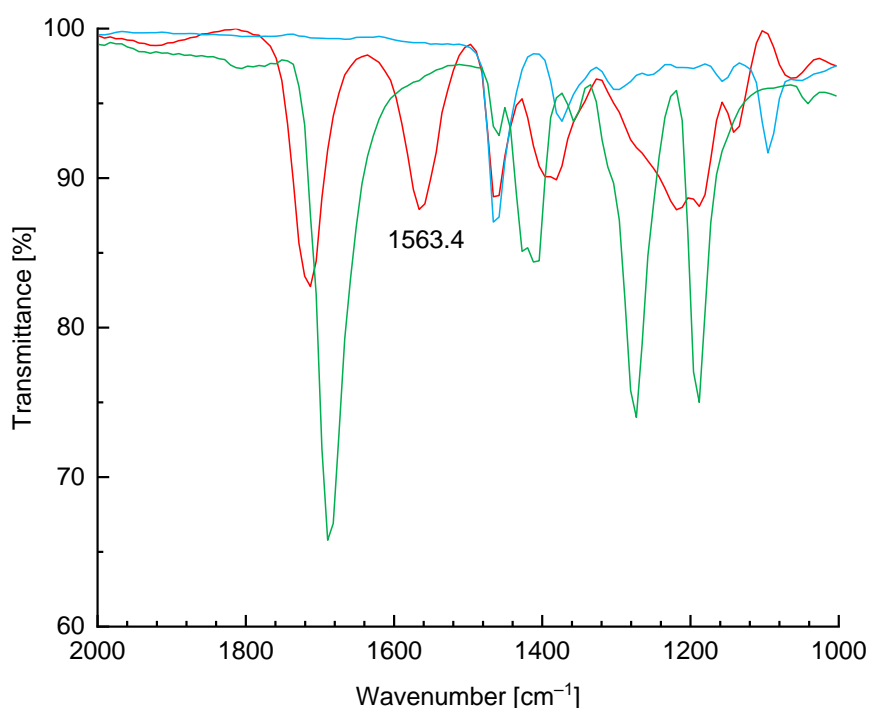
Figure 4-1 Partial FT-IR spectra of [HTOA][adipate] (—), TOA (—), and adipic acid (—).

The absorption band at 1563.4 cm^{-1} for [HTOA][adipate] is not present in either of the starting reagents and may indicate strong proton transfer. Absorption bands with similar wavenumbers were observed for PILs by Stoimenovski et al. (2012), who associated them with strong proton transfer. Similar absorption bands were present in the spectra of [HTOA][succinate], [HTOA][suberate], and [HTOA][sebacate]. This band could not be precisely identified in [HTOA][phthalate] as the benzene stretch occurs at a similar frequency, resulting in band overlap. Assigning this band is difficult as the only plausible bond to which this band may be assigned is the N–H bond, whose bend (1650–1580 cm^{-1}) is not normally observed in tertiary amine salts (Smith, 2019). Furthermore, the accompanying N–H stretch is not visible in the full spectra for any of the ILs (2700–2300 cm^{-1}). The characteristic O–H stretch of the

carboxylic acid (3300-2500 cm^{-1}) was also significantly reduced in all the IL spectra, possibly due to the proton transfer of one carboxyl hydrogen. This may further support strong proton transfer.

The expected absorption bands of the C–H stretches for the sp^3 carbons (2960–2850 cm^{-1}), the C=O stretch (1700–1650 cm^{-1}), and the C–H bends for the sp^3 carbons of the methylene group (1570–1560 cm^{-1}), were noted in the spectra for [HTOA][succinate], [HTOA][adipate], [HTOA][suberate], and [HTOA][sebacate]. The additional absorption bands of the benzene stretches (1600 and 1500–1430 cm^{-1}) could not be precisely identified in the spectrum of [HTOA][phthalate] since there was significant band overlap.

4.2 Physico-chemical properties of the studied ILs

A thorough understanding of the physico-chemical properties of ILs is vital to the design of the potential industrial applications in which they may be used. The physico-chemical properties were therefore investigated and the results of which are presented in the following sections. Table D-1 in Appendix D presents a summary of the results.

4.2.1 Melting point

Of the five synthesized ILs, [HTOA][phthalate], [HTOA][adipate], and [HTOA][sebacate] were liquid at room temperature (18 °C) with [HTOA][succinate] and [HTOA][suberate] being solid. The melting points for [HTOA][succinate] and [HTOA][suberate], determined using differential thermal analysis (DTA), were 20 and 26 °C, respectively. The DTA curves used to determine the melting points are given in Appendix C.

The trends in melting points for the dicarboxylate ILs did not match those noted for monocarboxylate ones. As shown by Yang et al. (2015), for the same cation, ILs with larger anions generally possess lower melting points. However, the melting points of the dicarboxylate ILs showed no clear trend. [HTOA][suberate] was solid while [HTOA][adipate] was liquid. [HTOA][suberate] being a solid can be explained by considering that intermolecular forces become significant as the size of the anion increases. However, [HOTA][sebacate], which contains a larger anion, was liquid.

4.2.2 Thermogravimetric analysis

The thermal stability of the studied ILs was investigated using thermogravimetric analysis (TGA), and the TGA curves are shown in Figure 4-2 with the corresponding construction plots given in Appendix C.
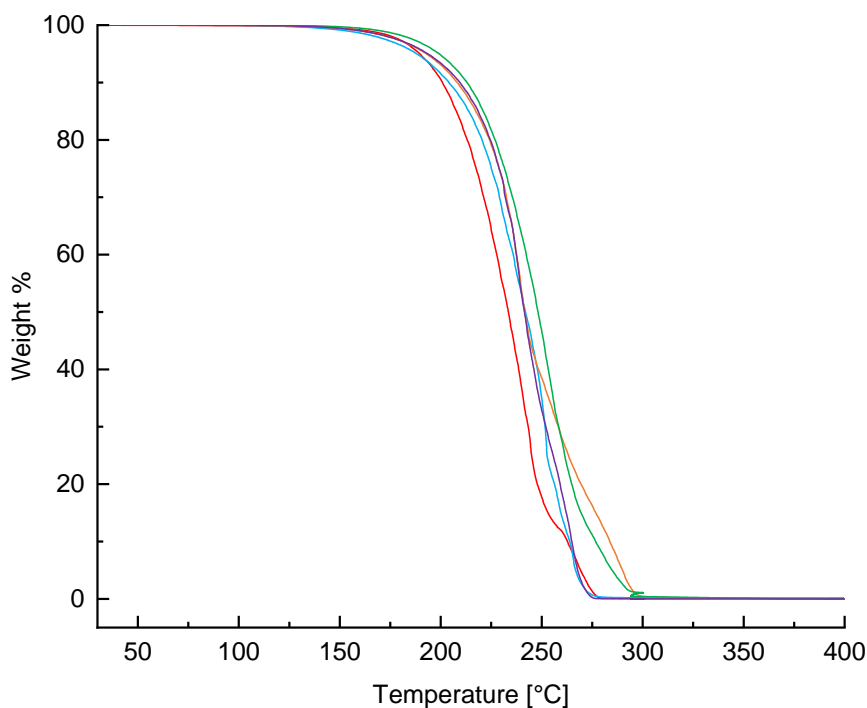
Figure 4-2 TGA curves for [HTOA][phthalate] (—), [HTOA][succinate] (—), [HTOA][adipate] (—), [HTOA][suberate] (—), and [HTOA][sebacate] (—).

 [HTOA][suberate] showed the highest thermal stability of the studied ILs with the following decreasing thermal stability sequence observed: [HTOA][suberate] > [HTOA][sebacate] > [HTOA][adipate] = [HTOA][succinate] > [HTOA][phthalate], with decomposition temperatures of 222, 221, 215, 215 and 205 °C, respectively. Although the thermal stabilities of the ILs were close, they were observed to be dependent on the size of the dicarboxylate anion with ILs having larger anions being more thermally stable. This is probably due to the increased Van der Waals interactions between the ions (Al Kaisy et al., 2017a).

The studied PILs had similar stabilities to HTOA ILs incorporating similar carboxylate ions (Al Kaisy et al., 2017a; Al Kaisy et al., 2017b). Furthermore, the thermal stabilities of the

studied ILs were greater than that of tetraoctylammonium oleate as shown in Table F-2 in Appendix F. The increased thermal stabilities may be due to the additional hydrogen bonding as a result of the dicarboxylate anion (Al Kaisy et al., 2017a).

4.2.3 Density

The density of the liquid ILs was investigated over the temperature range of 293.15–333.15 K at atmospheric pressure and the results are given in Table D-3 in Appendix D, with the corresponding plots shown in Figure 4-3. As expected, the density of the ILs decreased with an increase in temperature. This is in agreement with the general trend reported in the literature (Rocha et al., 2016; Al Kaisy et al., 2017a; Al Kaisy et al., 2017b).

Figure 4-3 Density as a function of temperature for [HTOA][phthalate] (●), [HTOA][adipate] (■), and [HTOA][sebacate] (▲). The solid lines represent the predicted values obtained using a linear model, Eq. (2.3).

[HTOA][phthalate] had the had the highest density of the three studied ILs with the following decreasing density sequence observed: [HTOA][phthalate] > [HTOA][adipate] > [HTOA][sebacate], with values of 0.9699, 0.9448, and 0.9257 g cm^{-3}, respectively, at 25 °C. The density of the ILs was observed to be dependent on the size of the dicarboxylate anion with ILs with smaller ions having larger densities. As explained in section 2.2.2, this is because larger ions occupy a larger volume and, therefore, have lower densities. Furthermore, smaller ions allow for increased hydrogen bonding which further reduces the density (Al Kaisy et al., 2017b). The larger density of [HTOA][phthalate] can be attributed to the smaller size of the phthalate ion arising from its cyclic structure.

The studied ammonium dicarboxylate ILs have higher densities than HTOA ILs with monocarboxylate anions, as shown in Table F-2 in Appendix F. The higher densities could be attributed to the additional carboxyl group present in the anion which increases the hydrogen bonding and results in increased densities.

As stated in section 2.2.2, a linear model, Eq. 2.3, is commonly used to investigate the dependence of density on temperature. This model was used to fit the density data and the best-fit parameters together with the coefficient of determination, R^2, are given in Table D-4 in Appendix D. As indicated by the solid lines in Figure 4-3 and R^2 values of 0.9997, 1.0000 (rounded off value), and 0.9997 for [HTOA][phthalate], [HTOA][adipate], and [HTOA][sebacate], respectively, Eq. 2.3 provided a satisfactory fit to the experimental data. The parameters of Eq. 2.3 are within range of those previously reported for similar HTOA ILs incorporating monocarboxylate anions (Al Kaisy et al., 2017a; Al Kaisy et al., 2017b).

4.2.4 Viscosity

The dynamic viscosity of the liquid ILs was investigated over the temperature range of 293.15–333.15 K at atmospheric pressure. The results are given in Table D-7 in Appendix D, with the corresponding plots shown in Figure 4-4. As expected, an increase in temperature was noted to significantly decrease the viscosity. This is in agreement with the general trend reported in the literature (Rocha et al., 2016; Al Kaisy et al., 2017a; Al Kaisy et al., 2017b).
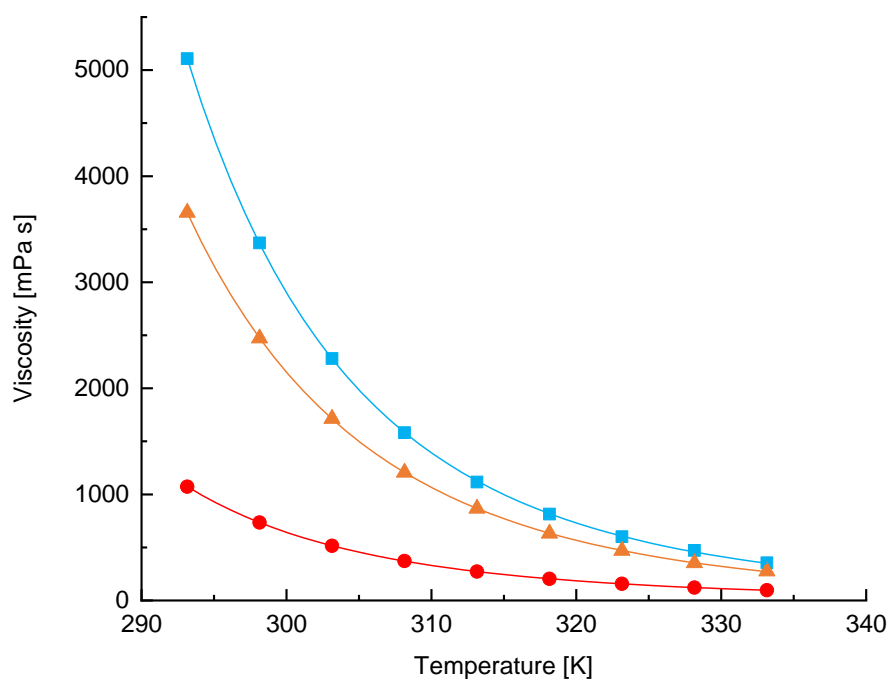
Figure 4-4 Viscosity as a function of temperature for [HTOA][phthalate] (●), [HTOA][adipate] (■), and [HTOA][sebacate] (▲). The solid lines represent the predicted values obtained using the Vogel–Fulcher–Tammann model.

[HTOA][phthalate] had the lowest viscosity of the three studied ILs with following decreasing viscosity sequence observed: [HTOA][adipate] > [HTOA][sebacate] > [HTOA][phthalate], with values of 3369.7, 2471.7, and 734.3 mPa s, respectively, at 25 °C. The viscosity of an IL is dependent on the size of the ions as well as the intermolecular forces (Van der Waals and hydrogen bonding) and electrostatic interactions between the constituent ions. The significantly lower viscosity of [HTOA][phthalate], therefore, could be attributed to the charge delocalization on the phthalate ring. This decreases the electrostatic interactions, resulting in decreased viscosities (MacFarlane et al., 2017).

[HTOA][sebacate] had a lower viscosity than [HTOA][adipate] despite [sebacate]$^-$ being larger than [adipate]$^-$. This is probably due to the smaller size of [adipate]$^-$ allowing for increased hydrogen bonding, which results in increased viscosities (Al Kaisy et al., 2017b). A similar result was reported by Rocha et al. (2016), who showed that the viscosities of ILs with larger anions were lower than the viscosities of those with smaller ones. They attributed this to smaller electrostatic interactions due to the larger anion size.

As a whole, the studied ammonium dicarboxylate ILs are highly viscous. The high viscosities of the studied ILs could be attributed to the additional carboxyl group present in the anion which increases hydrogen bonding and results in increased viscosity (Alcantara et al., 2018). [HTOA][phthalate] had similar viscosities to HTOA ILs incorporating similar anions with charge delocalization, as shown in Table F-2 in Appendix F. (Al Kaisy et al., 2017a)**.** Furthermore, the viscosities of [HTOA][sebacate] and [HTOA][adipate] were similar to that of [HTOA]$_2$[nonanedioate], indicating the dominant effect of the additional carboxyl group (Al Kaisy et al., 2017a).

As stated in section 2.2.3, the two commonly used models to investigate the dependence of viscosity on temperature are the Vogel–Fulcher–Tammann (VFT) and Arrhenius models These two models were used to fit the viscosity data and the best-fit parameters together with the coefficient of determination are given in Table D-8 and Table D-9, respectively, in Appendix D. The VFT model provided a better fit to the experimental data than did the Arrhenius model. The predicted values of the VFT model for the studied ILs, shown in Figure 4-4 as solid lines, are in good agreement with the experimental data, with R^2 being practically 1.0000 for all the ILs. The parameters of the VFT model are within range of those previously reported for similar HTOA ILs incorporating similar anions (Al Kaisy et al., 2017a; Al Kaisy et al., 2017b).

4.2.4.1 Viscosity of IL and molecular solvent mixtures

The high viscosities of the studied ILs (and ILs in general) are disadvantageous in that high viscosities result in larger pressure drops. As mentioned in section 2.2.3, a common method to alleviate the effect of the high viscosities of ILs is to mix them with molecular solvents. Table 4-1 shows the viscosities of IL mixtures formed by mixing each IL with varying amounts of methanol.

Table 4-1 Viscosities of IL mixtures with methanol as a function of methanol mass fraction at 328.15 K.

Methanol mass fraction	η [mPa s]		
	[HTOA][phthalate]	[HTOA][adipate]	[HTOA][sebacate]
0	1073.3	5108.3	3656.7
0.1	82.8	250.7	193.5
0.5	2.2	6.0	4.7

As can be seen in Table 4-1, adding a small amount of solvent is an effective way to significantly reduce the viscosity of the IL.

4.2.5 Electrical conductivity

The electrical conductivity of the liquid ILs was investigated over the temperature range of 293.15–313.15 K at atmospheric pressure and the results are given in Table D-11 in Appendix D, with the corresponding plots shown in Figure 4-5. As expected, the electrical conductivity of the ILs increased with increasing temperature. This is in agreement with the general trend reported in the literature (Litaiem and Dhahbi, 2012; Stoimenovski et al., 2012).

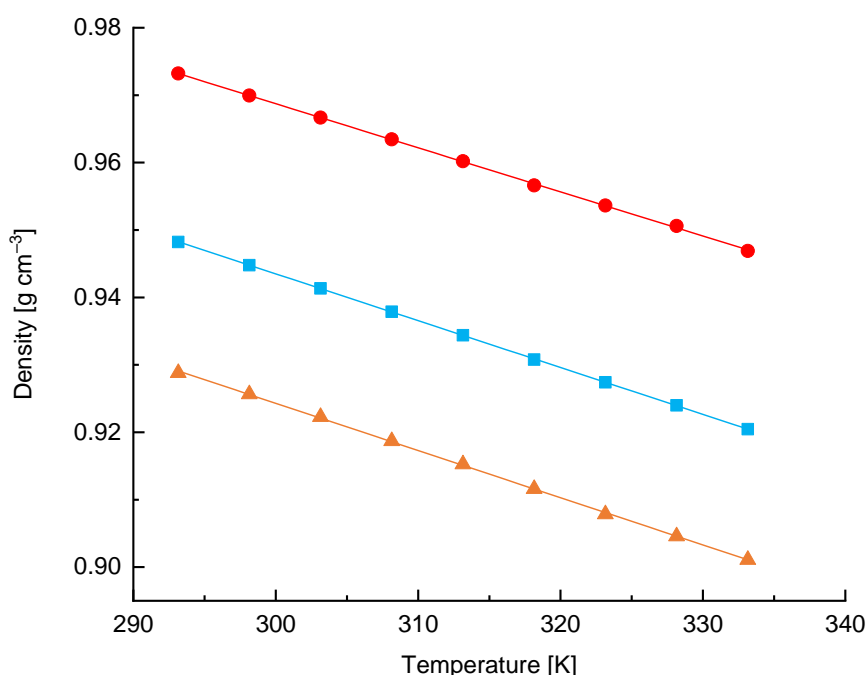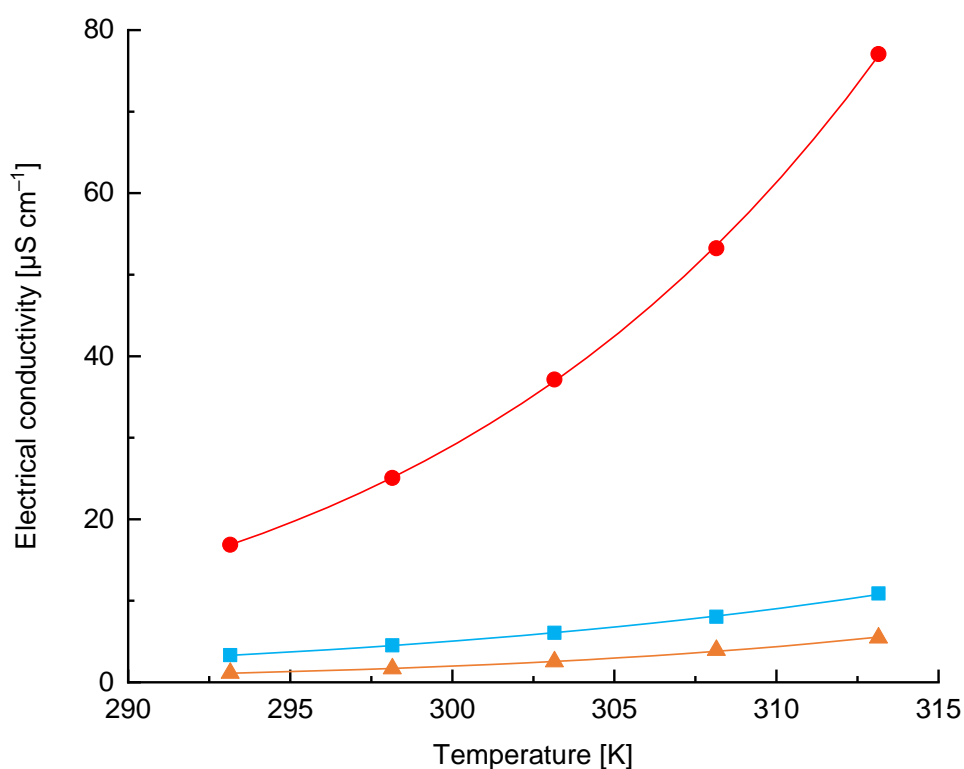**Figure 4-5 Electrical conductivity as a function of temperature for [HTOA][phthalate] (●), [HTOA][adipate] (■), and [HTOA][sebacate] (▲). The solid lines represent the predicted values obtained using the Arrhenius model.**

[HTOA][phthalate] had the highest electrical conductivity of the three studied ILs with the following decreasing conductivity sequence observed: [HTOA][phthalate] > [HTOA][sebacate] > [HTOA][adipate], with values of 25.1, 4.5, and 1.7 μS cm^{-1}, respectively, at 25 °C. As expected, the electrical conductivity of the ILs was observed to be dependent on its viscosity with ILs with lower viscosities having larger electrical conductivities.

The studied ILs have poor conductivities due to their high viscosities. In addition to their highly viscous nature, the poor conductivities may be a result of significant ion pairing or the formation of neutral aggregates. However, poor conductivity is common for ionic liquids (MacFarlane et al., 2009). The electrical conductivity of [HTOA][phthalate] was similar to that of Aliquat 336 which had a conductivity of 26.0 µS cm^{-1} at 25 °C (Litaiem and Dhahbi, 2012).

As stated in section 2.2.4, the Arrhenius model, Eq. 2.6, is commonly used to investigate the dependence of electrical conductivity on temperature. This model was used to fit the electrical conductivity data and the best-fit parameters together with the coefficient of determination are given in Table D-12 in Appendix D. As indicated by the solid lines in Figure 4-5 and R^2 values of 0.9992, 0.9953, and 0.9931 for [HTOA][phthalate], [HTOA][adipate], and [HTOA][sebacate], respectively, the Arrhenius model provided a satisfactory fit to the experimental data.

4.2.6 Ionicity

In order to determine the extent of proton transfer for the studied ILs, Walden curves were prepared by plotting the log of the molar conductivity, Λ_m, against that of the inverse of the viscosity, η^{-1}, over the temperature range of 293.15–313.15 K. The results are shown in Figure 4-6.
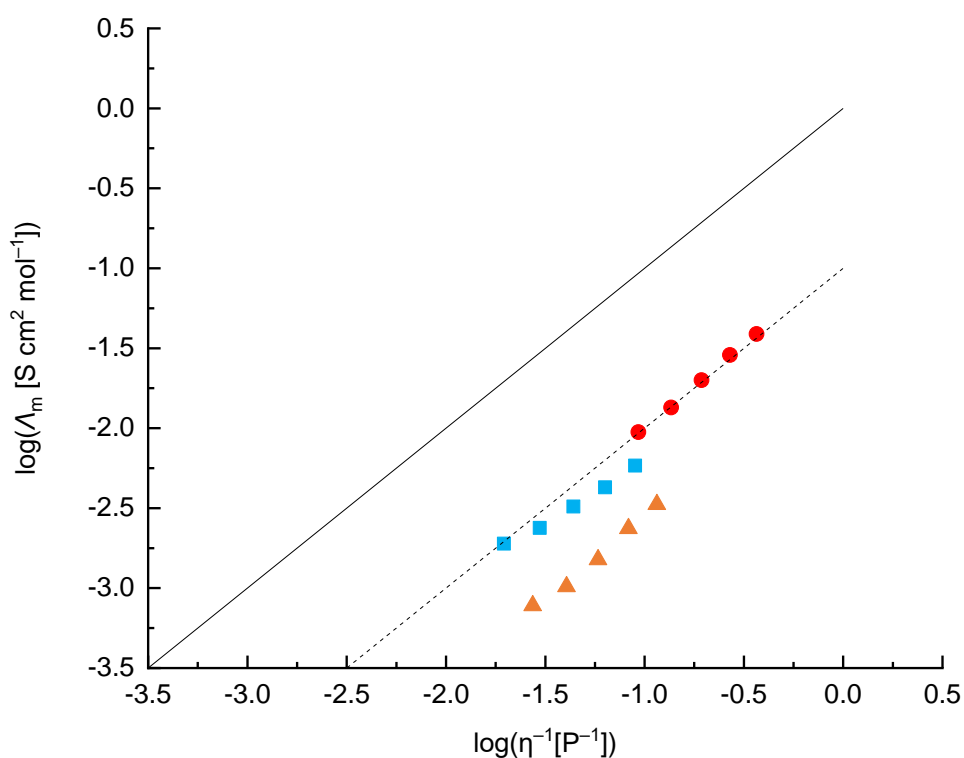
Figure 4-6 Walden plots for [HTOA][phthalate] (●), [HTOA][adipate] (■), and [HTOA][sebacate] (▲). The solid line represents the ideal 0.01 M KCl line. The dashed line represents the 10% ionization line.

The curves for [HTOA][adipate] and [HTOA][sebacate] fall below the 10% ionization line, indicating that [HTOA][adipate] and [HTOA][sebacate] have poor ionicity. However, proton transfer was confirmed using FT-IR spectroscopy. The low ionicity may, therefore, be indicative of significant ion pairing and ion association. [HTOA][phthalate] had slightly better ionicity as its curve was slightly above the 10% ionization line. This might be a result of a higher ΔpK_a^{aq} value for this system in addition to the lower viscosity of [HTOA][phthalate].

The low ionicity for the studied ILs might limit the use of these ILs in systems requiring a conductive solvent, such as electrochemistry applications. However, a low ionicity for LLE extraction is not an important factor.

The studied ILs had ionicities similar to methyltrioctylammonium ILs incorporating thioglycolate anions ILs, which were reported by Platzer et al. (2017a).

4.2.7 Solubility

The solubility of an IL in common molecular solvents is an important consideration since these solvents are sometimes added to reduce the viscosity of an IL. The solubility of the synthesized ILs in common solvents were investigated by mixing 1 mL of IL with 5 mL of the corresponding solvent at room temperature (18 °C). The results are given Table 4-2.

Table 4-2 Solubility data of the prepared ion liquids.

Ionic liquid	Solvent						
	H_2O	methanol	ethanol	acetone	cyclohexane	CH_2Cl_2	$CHCl_3$
[HTOA][succinate]	✗	✓	✓	✓	✓	✓	✓
[HTOA][phthalate]	✗	✓	✓	✓	✓	✓	✓
[HTOA][adipate]	✗	✓	✓	✓	✓	✓	✓
[HTOA][suberate]	✗	✓	✓	✓	✓	✓	✓
[HTOA][sebacate]	✗	✓	✓	✓	✓	✓	✓

As can be seen in the above table, the studied ILs are soluble in common solvents. This result is favourable as all of the above solvents are less viscous than the studied ILs and may be used to reduce their viscosities.

4.3 Metal extraction studies

The efficacy of the studied liquid ILs as extraction solvents in liquid-liquid extraction of Cd(II), Cu(II), and Zn(II) from aqueous solutions was determined by investigating the effect of extraction time on the extraction process. [HTOA][suberate] formed a solid substance after being in contact with water. Due to its water-stability, it was not investigated further.

4.3.1 Forward extraction

The extraction efficiency of [HTOA][phthalate] and [HTOA][adipate] as a function of extraction time was investigated, and the results are given Table E-16 in Appendix E with the corresponding plots given below. The uncertainties of the extraction efficiencies, represented by error bars, were calculated according to procedures shown in Appendix E.4.
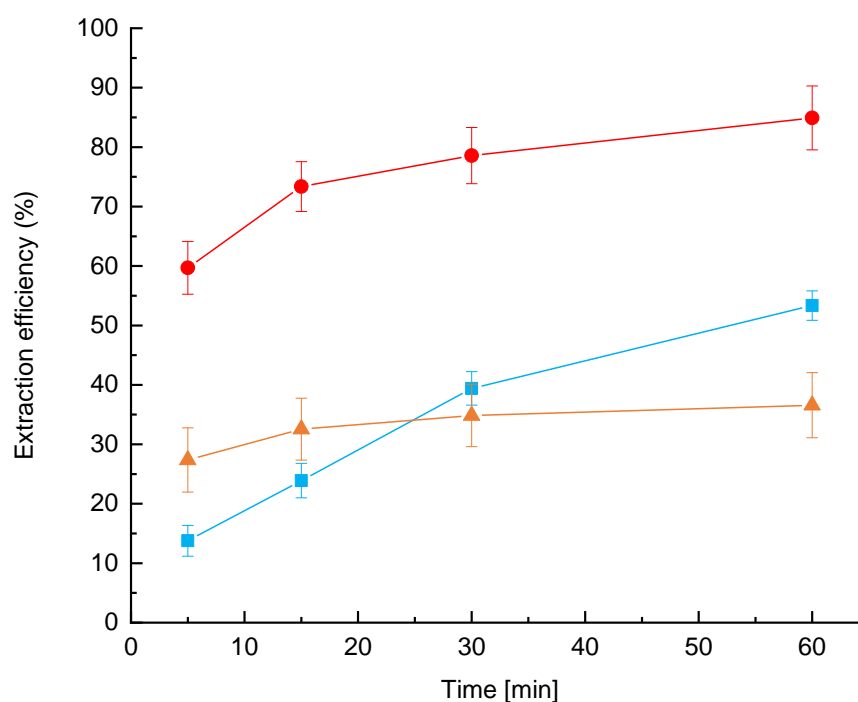
Figure 4-7 Extraction efficiencies of [HTOA][phthalate] for Cd(II) (—●—), Cu(II) (—■—), and Zn(II) (—▲—) as a function of extraction time.
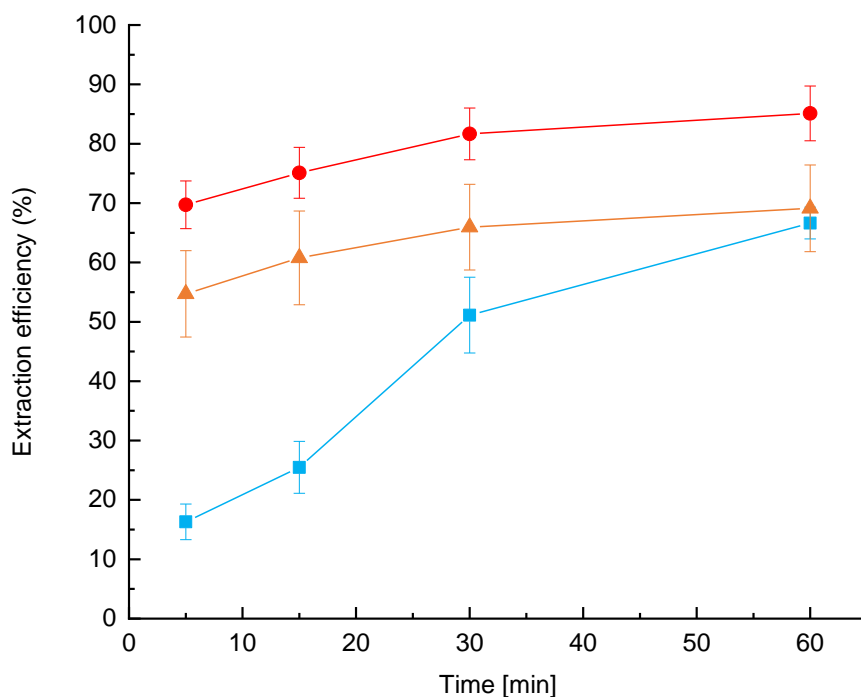
Figure 4-8 Extraction efficiencies of [HTOA][adipate] for Cd(II) (—●—), Cu(II) (—■—), and Zn(II) (—▲—) as a function of extraction time.

[HTOA][adipate] performed better than [HTOA][phthalate], having extraction efficiencies of 85, 67 and 69% for Cd(II), Cu(II), and Zn(II), respectively, after 60 min. In comparison, [HTOA][phthalate] had extraction efficiencies of 85, 53, and 37% for Cd(II), Cu(II), and Zn(II), respectively, after 60 min. The lower performance of [HTOA][phthalate] may be due to the steric hindrance exerted by the benzene ring present in the phthalate ion (Valdés Vergara et al., 2015). Both ILs showed a higher affinity for Cd(II) with extraction efficiencies for Cd(II) being significantly higher than those for Cu(II) and Zn(II).

The extraction efficiencies obtained for the studied ILs are within range of those obtained for aprotic ammonium and phosphonium ILs reported by Leyma et al. (2016), as shown in Table F-3 in Appendix F. Furthermore, the obtained extraction efficiencies were similar to those obtained for ILs containing similar dicarboxylate anions, with lower extraction efficiencies also being obtained for Zn(II) (Valdés Vergara et al., 2014).

For both ILs, the metal uptake of Cu(II) was slower than that of Cd(II) and Zn(II). Metal uptake of Cd(II) and Zn(II) after 30 min was not large, whereas that of Cu(II) was significant. Overall, the metal uptake observed for the studied ILs was much slower than that observed for similar

ILs. Valdés Vergara et al. (2014) observed maximum extraction after 15 min for ammonium ILs containing similar dicarboxylate anions. Moreover, Katsuta et al. (2011) did not observe further extraction of Pd(II) and Pt(IV) after 15 min for a mixture of 10 wt.% [HTOA][NO$_3$] in [HTOA][NTf$_2$].

Overall, [HTOA][adipate] performed well in extracting Cd(II), Cu(II), and Zn(II). However, its use in applications that require a higher degree of removal would require additional purification steps with the same IL or an alternative method to further reduce the concentration.

The calculated distribution ratios, assuming equilibrium after 60 min, are given in Table 4-3.

Table 4-3 Distribution ratios of the metal ions.

Ionic liquid	Distribution ratios		
	Cd(II)	Cu(II)	Zn(II)
[HTOA][phthalate]	11.2 ± 2.4	2.3 ± 0.1	1.2 ± 0.3
[HTOA][adipate]	11.4 ± 2.1	4.0 ± 0.2	4.5 ± 0.8

The distribution ratios achieved were much lower compared to those that are generally reported. Platzer et al. (2017a) reported distributions ratios between 100 to 1200 for thioglycolate based ammonium and phosphonium ILs in extraction of Cu(II) and Cd(II). However, most distribution ratios reported are for studies in which extraction was from an aqueous solution containing a single metal ion. In the present study, a multi-element solution was utilized. This could have reduced the individual extraction capabilities of the ILs.

4.3.2 Back-extraction

The recyclability of [HTOA][adipate] was investigated by using 0.1 M EDTA solution as the regenerating agent, and the back-extraction efficiencies achieved are given in Table 4-4. The EDTA solution was effective it extracting Cd(II) and Cu(II), with back-extraction efficiencies of 89 and 82%, respectively. Its extraction of Zn(II) was less effective with a back-extraction efficiency of 41% being achieved.

Table 4-4 Back-extraction efficiency of EDTA.

Ionic liquid	Back-extraction efficiency [%]		
	Cd(II)	Cu(II)	Zn(II)
[HTOA][adipate]	89 ± 7	82 ± 3	41 ± 7

This result agreed with the work done by Janssen et al. (2016), who obtained a back-extraction efficiency of 83% for Cu(II) in regenerating trioctylammonium ILs with 0.1 M EDTA solution. This result also agrees with the work done by (Zhou et al., 2015), who achieved almost complete back-extraction for Cu(II) using this regenerating agent in regenerating an IL containing the dicyanamide anion.

As the back-extraction efficiency was low for Zn(II), additional regeneration steps with the same regenerating agent or an alternative regenerating agent may be required.

CHAPTER 5 CONCLUSIONS AND RECOMMENDATIONS

5.1 Conclusions

The project aimed to synthesize ILs from TOA and dicarboxylic acids and evaluate their effectiveness as extraction solvents in extracting Cd(II), Cu(II), and Zn(II) from aqueous solutions. The ILs were successfully synthesized from the commercially available reagents in a one-pot synthesis procedure. This is highly advantageous as the cost of the starting materials was relatively competitive, and no additional solvent was required. The proton-transfer reaction was confirmed using FT-IR spectroscopy, with ^{1}H NMR and ^{13}C NMR confirming the structure of the ILs.

Of the five synthesized ionic liquids, [HTOA][phthalate], [HTOA][adipate], and [HTOA][sebacate] were liquid. The physico-chemical chemical properties of these ILs were investigated, revealing the ILs to be highly viscous. The viscosities of [HTOA][phthalate], [HTOA][adipate], and [HTOA][sebacate] were 734.3, 3369.7, and 2471.7 mPa s, respectively, at 25 °C. The high viscosity, unfortunately, limits the use of these ILs in most industrial processes. However, the addition of a molecular solvent was shown to be effective in reducing the viscosity as IL mixtures of [HTOA][phthalate], [HTOA][adipate], and [HTOA][sebacate] with 10 wt.% methanol had viscosities of 82.8, 250.7, and 193.5 mPa s, respectively, at 25 °C. This result significantly increases the range of industrial applications in which these solvents may be used. Furthermore, all five of the ILs were also shown to be soluble in common molecular solvents, which further increases their applicability.

All three liquid ILs were then investigated as extraction solvents. [HTOA][sebacate] was not water stable and was not investigated further. [HTOA][adipate] and [HTOA][phthalate] successfully extracted Cd(II), with both having extraction efficiencies of 85%. However, their performance in extracting Cu(II) and Zn(II) was less effective, with [HTOA][adipate] having extraction efficiencies of 67 and 69% and [HTOA][phthalate] having extraction efficiencies of 53 and 37% for Cu(II) and Zn(II), respectively. Their use in applications that require a higher degree of removal would require additional purification steps with the same ILs or an alternative method to reduce the concentration further.

The recyclability of [HTOA][adipate] was investigated using 0.1 M EDTA solution as the regenerating agent. The EDTA solution was effective it extracting Cd(II) and Cu(II), with back-extraction efficiencies of 89 and 82%, respectively. However, its extraction of Zn(II) was less effective with a back-extraction efficiency of 41% being achieved. Additional regeneration steps with the same regenerating agent or an alternative regenerating agent may be required to regenerate the IL after Zn(II) extraction.

5.2 Recommendations

In the present study, the volumes of the IL phase and aqueous phase were assumed to remain constant after extraction. Further work should verify this quantifiably using total organic carbon (TOC) analysis to determine the IL content in the water phase and Karl-Fischer titration to determine the water content in the IL phase.

As the studied ILs are highly viscous, utilizing an appropriate solvent to reduce the viscosity would be required. However, this may affect the extraction process. Further work should focus on obtaining extraction results for IL and solvent mixtures.

The recyclability of an ionic liquid is an important factor in determining its applicability. 0.1 M EDTA solution was selected as it was shown to yield effective results in a study by Janssen et al. (2016). However, it did not achieve complete back-extraction. Further work should focus on obtaining a better performing regenerating agent.

REFERENCES

Akpor, O. B., Ohiobor, G. O. & Olaolu, T. D. 2014. Heavy metal pollutants in wastewater effluents: Sources, effects and remediation. *Advances in Bioscience and Bioengineering*, 2(4), pp. 37-43.

Al Kaisy, G. M. J., Abdul Mutalib, M. I. & Rao, T. V. V. L. N. 2017a. Novel halogen free hydrophobic trioctylammonium-based protic ionic liquids with carboxylate anions: Synthesis, characterization, and thermophysical properties. *Journal of Molecular Liquids*, 242, pp. 349-356.

Al Kaisy, G. M. J., Mutalib, M. I. A., Leveque, J. M. & Rao, T. V. V. L. N. 2017b. Novel low viscosity ammonium-based ionic liquids with carboxylate anions: Synthesis, characterization, and thermophysical properties. *Journal of Molecular Liquids*, 230, pp. 565-573.

Alcantara, M. L., Santos, J. P., Loreno, M., Ferreira, P. I. S., Paredes, M. L. L., Cardozo-Filho, L., Silva, A. K., Lião, L. M., Pires, C. A. M. & Mattedi, S. 2018. Low viscosity protic ionic liquid for CO2/CH4 separation: Thermophysical and high-pressure phase equilibria for diethylammonium butanoate. *Fluid Phase Equilibria*, 459, pp. 30-43.

Anouti, M., Vigeant, A., Jacquemin, J., Brigouleix, C. & Lemordant, D. 2010. Volumetric properties, viscosity and refractive index of the protic ionic liquid, pyrrolidinium octanoate, in molecular solvents. *The Journal of Chemical Thermodynamics*, 42(7), pp. 834-845.

Barakat, M. A. 2011. New trends in removing heavy metals from industrial wastewater. *Arabian Journal of Chemistry*, 4(4), pp. 361-377.

Bruice, P. Y. 2016. *Organic Chemistry,* Upper Saddle River, NJ, Pearson Education, Inc.

Burrell, G. L., Burgar, I. M., Separovic, F. & Dunlop, N. F. 2010. Preparation of protic ionic liquids with minimal water content and 15N NMR study of proton transfer. *Physical Chemistry Chemical Physics*, 12(7), pp. 1571-1577.

Council of the City of Cape Town 2013. *City of Cape Town: Wastewater and Industrial Effluent By law, 2013*. Cape Town.

Cocalia, V. A., Visser, A. E., Rogers, R. D. & Holbrey, J. D. 2008. Solubility and Solvation in Ionic Liquids. *In:* WASSERSCHEID, P. & WELTON, T. (eds.) *Ionic Liquids in Synthesis: Second Edition.*

Davis, J. H. 2003. Synthesis of Task-specific Ionic Liquids. *In:* WASSERSCHEID, P. & WELTON, T. (eds.) *Ionic Liquids in Synthesis.* Weinheim: Wiley-VCH Verlag GmbH & Co. KGaA.

Department of Environmental Affairs 2014. *National Guideline for the Discharge of Effluent from Land-based Sources into the Coastal Environment*. Pretoria, South Africa.

Dietz, M. L. 2006. Ionic Liquids as Extraction Solvents: Where do We Stand? *Separation Science and Technology*, 41(10), pp. 2047-2063.

Fischer, L., Falta, T., Koellensperger, G., Stojanovic, A., Kogelnig, D., Galanski, M., Krachler, R., Keppler, B. K. & Hann, S. 2011. Ionic liquids for extraction of metals and metal containing compounds from communal and industrial waste water. *Water Research*, 45(15), pp. 4601-4614.

Foris, A. 2017. *On NH Chemical Shifts, Part V: NH and NH$_2$ Chemical Shifts of Hydrazides and Related Compounds*.

Gordon, C. M. & Muldoon, M. J. 2008. Synthesis of Ionic Liquids. *In:* WASSERSCHEID, P. & WELTON, T. (eds.) *Ionic Liquids in Synthesis: Second Edition.*

Gunatilake, S. K. 2015. Methods of Removing Heavy Metals from Industrial Wastewater. *Journal of Multidisciplinary Engineering Science Studies*, 1(1), pp. 12-18.

Harris, D. C. 2015. *Quantitative Chemical Analysis*, Macmillan Learning.

Janssen, C. H. C., Macías-Ruvalcaba, N. A., Aguilar-Martínez, M. & Kobrak, M. N. 2016. Copper extraction using protic ionic liquids: Evidence of the Hofmeister effect. *Separation and Purification Technology*, 168, pp. 275-283.

Katsuta, S., Okai, M., Yoshimoto, Y. & Kudo, Y. 2012. Extraction of Gallium(III) from Hydrochloric Acid Solutions by Trioctylammonium-based Mixed Ionic Liquids. *Analytical Sciences*, 28(10), pp. 1009-1012.

Katsuta, S. & Tamura, J. 2018. Extraction of Palladium(II) and Platinum(IV) from Hydrochloric Acid Solutions with Trioctylammonium Nitrate Ionic Liquid without Dilution. *Journal of Solution Chemistry*, 47(8), pp. 1293-1308.

Katsuta, S., Yoshimoto, Y., Okai, M., Takeda, Y. & Bessho, K. 2011. Selective Extraction of Palladium and Platinum from Hydrochloric Acid Solutions by Trioctylammonium-

Based Mixed Ionic Liquids. *Industrial & Engineering Chemistry Research*, 50(22), pp. 12735-12740.

Leyma, R., Platzer, S., Jirsa, F., Kandioller, W., Krachler, R. & Keppler, B. K. 2016. Novel thiosalicylate-based ionic liquids for heavy metal extractions. *Journal of Hazardous Materials*, 314, pp. 164-171.

Li, C.-P., Li, Z., Zou, B.-X., Liu, Q.-S. & Liu, X.-X. 2013. Density, Viscosity and Conductivity of Protic Ionic Liquid N,N-DimethylethanolammoniumPropionate. *Acta Physico-Chimica Sinica*, 29(10), pp. 2157-2161.

Litaiem, Y. & Dhahbi, M. 2012. Measurements and correlations of viscosity, conductivity and density of an hydrophobic ionic liquid (Aliquat 336) mixtures with a non-associated dipolar aprotic solvent (DMC). *Journal of Molecular Liquids*, 169, pp. 54-62.

MacFarlane, D. R., Forsyth, M., Izgorodina, E. I., Abbott, A. P., Annat, G. & Fraser, K. 2009. On the concept of ionicity in ionic liquids. *Physical Chemistry Chemical Physics*, 11(25), pp. 4962-4967.

MacFarlane, D. R., Kar, M. & Pringle, J. 2017. *Fundamentals of Ionic Liquids,* Weinheim Germany, Wiley-VCH Verlag GmbH & Co. KGaA.

Ohno, H. 2011. *Electrochemical Aspects of Ionic Liquids*, Wiley.

Parmentier, D., Metz, S. J. & Kroon, M. C. 2013. Tetraalkylammonium oleate and linoleate based ionic liquids: promising extractants for metal salts. *Green Chemistry*, 15(1), pp. 205-209.

Parmentier, D., Valia, Y. A., Metz, S. J., Burheim, O. S. & Kroon, M. C. 2015a. Regeneration of the ionic liquid tetraoctylammonium oleate after metal extraction. *Hydrometallurgy*, 158, pp. 56-60.

Parmentier, D., Vander Hoogerstraete, T., Metz, S. J., Binnemans, K. & Kroon, M. C. 2015b. Selective Extraction of Metals from Chloride Solutions with the Tetraoctylphosphonium Oleate Ionic Liquid. *Industrial & Engineering Chemistry Research*, 54(18), pp. 5149-5158.

Platzer, S., Kar, M., Leyma, R., Chib, S., Roller, A., Jirsa, F., Krachler, R., MacFarlane, D. R., Kandioller, W. & Keppler, B. K. 2017a. Task-specific thioglycolate ionic liquids for heavy metal extraction: Synthesis, extraction efficacies and recycling properties. *Journal of Hazardous Materials*, 324, pp. 241-249.

Platzer, S., Leyma, R., Wolske, S., Kandioller, W., Heid, E., Schröder, C., Schagerl, M., Krachler, R., Jirsa, F. & Keppler, B. K. 2017b. Thioglycolate-based task-specific ionic liquids: Metal extraction abilities vs acute algal toxicity. *Journal of Hazardous Materials*, 340, pp. 113-119.

Rocha, M. A. A., van den Bruinhorst, A., Schröer, W., Rathke, B. & Kroon, M. C. 2016. Physicochemical properties of fatty acid based ionic liquids. *The Journal of Chemical Thermodynamics*, 100, pp. 156-164.

Smith, B. C. 2019. Organic Nitrogen Compounds V: Amine Salts. *Spectroscopy*, 34(9), pp. 30-37.

Stoimenovski, J., Dean, P. M., Pas, E. & Macfarlane, D. R. 2012. Protic pharmaceutical ionic liquids and solids: aspects of protonics. *Faraday Discussions*, 15(Ionic Liquids), pp. 335-352.

Stoimenovski, J., Izgorodina, E. I. & MacFarlane, D. R. 2010. Ionicity and proton transfer in protic ionic liquids. *Physical Chemistry Chemical Physics*, 12(35), pp. 10341-10347.

Stojanovic, A. & Keppler, B. K. 2012. Ionic Liquids as Extracting Agents for Heavy Metals. *Separation Science and Technology*, 47(2), pp. 189-203.

Stojanovic, A., Kogelnig, D., Fischer, L., Hann, S., Galanski, M., Groessl, M., Krachler, R. & Keppler, B. K. 2010. Phosphonium and Ammonium Ionic Liquids with Aromatic Anions: Synthesis, Properties, and Platinum Extraction. *Australian Journal of Chemistry*, 63(3), pp. 511-524.

Taylor, B. N. & Kuyatt, C. E. 1994. Guidelines for Evaluating and Expressing the Uncertainty of NIST Measurement Results. *NIST Technical Note 1297*. Gaithersburg, MD: National Institute of Standards and Technology.

Theodore, L., Weiss, K. N., McKenna, J. D., Smith, F. L., Sharp, R. R., Santoleri, J. J. & McGowan, T. F. 2008. Waste Management. *In:* GREEN, D. W. & PERRY, R. H. (eds.) *Perry's Chemical Engineers' Handbook.* Chicago: McGraw-Hill.

Thomas, L. M., Jensen, L. J., Whittington, W. A., Barnes, D., Hall, E. P. & Goodwin, J. K. 1986. *Development document for effluent limitations guidelines and standards for the nonferrous metals forming and metal powders point source category,* Washington, DC, U.S. Environmental Protection Agency

Valdés Vergara, M. A., Lijanova, I. V., Likhanova, N. V., Olivares Xometl, O., Jaramillo Vigueras, D. & Morales Ramirez, A. J. 2015. Recycling and recovery of ammonium-

based ionic liquids after extraction of metal cations from aqueous solutions. *Separation and Purification Technology*, 155, pp. 110-117.

Valdés Vergara, M. A., Lijanova, I. V., Likhanova, N. V., Vigueras, D. J. & Xometl, O. O. 2014. The removal of heavy metal cations from an aqueous solution using ionic liquids. *The Canadian Journal of Chemical Engineering*, 92(11), pp. 1875-1881.

Visser, A. E., Swatloski, R. P., Reichert, W. M., Mayton, R., Sheff, S., Wierzbicki, A., Davis, J. H. & Rogers, R. D. 2002. Task-Specific Ionic Liquids Incorporating Novel Cations for the Coordination and Extraction of Hg^{2+} and Cd^{2+}: Synthesis, Characterization, and Extraction Studies. *Environmental Science & Technology*, 36(11), pp. 2523-2529.

Wagner, M. & Hilgers, C. 2008. Quality Aspects and Other Questions Related to Commercial Ionic Liquid Production. *In:* WASSERSCHEID, P. & WELTON, T. (eds.) *Ionic Liquids in Synthesis: Second Edition.*

Wasserscheid, P. & Welton, T. 2003. *Ionic Liquids in Synthesis,* Weinheim, Wiley-VCH Verlag GmbH & Co. KGaA.

Wasserscheid, P. & Welton, T. 2008. *Ionic Liquids in Synthesis: Second Edition.*

World Health Organization 2010. *Ten chemicals of major public health concern.* Geneva, Switzerland: WHO.

Wilkes, J. S. 2002. A short history of ionic liquids—from molten salts to neoteric solvents. *Green Chemistry*, 4(2), pp. 73-80.

Wilkes, J. S. 2003. Introduction. *In:* WASSERSCHEID, P. & WELTON, T. (eds.) *Ionic Liquids in Synthesis.* Weinheim: Wiley-VCH Verlag GmbH & Co. KGaA.

Wilkes, J. S. & Zaworotko, M. J. 1992. Air and water stable 1-ethyl-3-methylimidazolium based ionic liquids. *Journal of the Chemical Society, Chemical Communications*, (13), pp. 965-967.

Yang, Q., Xu, D., Zhang, J., Zhu, Y., Zhang, Z., Qian, C., Ren, Q. & Xing, H. 2015. Long-Chain Fatty Acid-Based Phosphonium Ionic Liquids with Strong Hydrogen-Bond Basicity and Good Lipophilicity: Synthesis, Characterization, and Application in Extraction. *ACS Sustainable Chemistry & Engineering*, 3(2), pp. 309-316.

Yoshizawa, M., Xu, W. & Angell, C. A. 2003. Ionic Liquids by Proton Transfer: Vapor Pressure, Conductivity, and the Relevance of ΔpKa from Aqueous Solutions. *Journal of the American Chemical Society*, 125(50), pp. 15411-15419.

Zhou, Y., Boudesocque, S., Mohamadou, A. & Dupont, L. 2015. Extraction of Metal Ions with Task Specific Ionic Liquids: Influence of a Coordinating Anion. *Separation Science and Technology*, 50(1), pp. 38-44.

APPENDIX A SYNTHESIS OF IONIC LIQUIDS

A.1 Synthesis procedure and spectroscopic results

A.1.1 Trioctylammonium phthalate [HTOA][phthalate]

TOA (20g, 56.55 mmol) and phthalic acid (10.33 g, 62.20 mmol) were added to a round-bottom flask. The mixture was then stirred for 24 h at room temperature using a magnetic stirrer. Afterwards, the mixture was left to settle for 2 h, resulting in the formation of three phases: a TOA phase (top), a liquid IL phase (middle), and an unreacted acid phase (bottom). The IL phase was then removed from the unreacted starting materials and dried over silica gel for 24 h, yielding a slightly yellow, viscous liquid. ^{1}H NMR (400 MHz, CDCl$_3$) δ 11.97 (s, 1H), 8.31 (dd, J = 5.9, 3.5 Hz, 2H), 7.49 (dd, J = 6.2, 3.4 Hz, 2H), 3.03 (t, J = 8.8 Hz, 6H), 1.73 – 1.62 (m, 6H), 1.42 – 1.09 (m, 30H), 0.83 (t, J = 7.3 Hz, 9H). ^{13}C NMR (100 MHz, CDCl$_3$) δ 171.11, 133.87, 133.13, 131.03, 52.18, 31.62, 28.99, 26.77, 23.24, 22.56, 14.03. IR (ATR) $\bar{v}_{max}$: 2924, 2856.9, 2485.2, 2366.4, 2053.8, 1927.2, 1692.9, 1456.7, 1356.8, 1165.6, 1044.7, 855.5, 789.4, 730.1, 629.4 cm^{-1}.

Figure A-1 Picture of trioctylammonium phthalate.

A.1.2 Trioctylammonium succinate [HTOA][succinate]

TOA (20g, 56.55 mmol) and succinic acid (7.35 g, 62.20 mmol) were added to a round-bottom flask. The mixture was then stirred for 24 h at room temperature using a magnetic stirrer. Afterwards, the mixture was left to settle for 2 h, resulting in the formation of three phases: a TOA phase, a liquid IL phase, and an unreacted acid phase. The IL phase was then removed from the unreacted starting materials and dried over silica gel for 24 h, yielding a clear, viscous liquid. ^{1}H NMR (400 MHz, CDCl$_3$) δ 2.97 – 2.85 (m, 6H), 2.52 (s, 4H), 1.66 – 1.52 (m, 6H), 1.34 – 1.18 (m, 30H), 0.83 (t, J = 6.6 Hz, 9H). ^{13}C NMR (100 MHz, CDCl$_3$) δ 178.05, 51.87, 32.29, 31.62, 29.69, 29.00, 26.79, 23.15, 22.56, 14.03. IR (ATR) $\bar{v}_{max}$: 2930.2, 2857.4, 2447.2, 2376.3, 2313.31721.0, 1567.5, 1462.1, 1380.8, 1324.8, 1168.3, 985.6, 875.5, 832.6, 721.8, 629.1 cm^{-1}.

Figure A-2 Picture of trioctylammonium succinate (solid).

A.1.3 Trioctylammonium adipate [HTOA][adipate]

TOA (20g, 56.55 mmol) and adipic acid (9.09 g, 62.20 mmol) were added to a round-bottom flask. The mixture was then stirred for 24 h at room temperature using a magnetic stirrer. Afterwards, the mixture was left to settle for 2 h, resulting in the formation of three phases: a TOA phase, a liquid IL phase, and an unreacted acid phase. The IL phase was then removed from the unreacted starting materials and dried over silica gel for 24 h, yielding a clear, viscous liquid. ^{1}H NMR (400 MHz, CDCl$_3$) δ 2.93 – 2.81 (m, 6H), 2.30 (t, J = 6.3 Hz, 4H), 1.68 (t, J = 6.7, 6.3 Hz, 4H), 1.65 – 1.50 (m, 6H), 1.35 – 1.13 (m, 30H), 0.85 (t, J = 6.7 Hz, 9H). ^{13}C NMR (100 MHz, CDCl$_3$) δ 178.49, 51.58, 35.44, 31.70, 29.12, 29.09, 26.95, 25.04, 23.34, 22.61, 14.07. IR (ATR) $\bar{v}_{max}$: 2923.5, 2857.5, 2473.5, 1714.0, 1563.4, 1460.0, 1384.7, 1215.7, 1063.0, 989.0, 891.6, 723.7, 627.2 cm^{-1}.

Figure A-3 Picture trioctylammonium adipate.

A.1.4 Trioctylammonium suberate [HTOA][suberate]

TOA (20g, 56.55 mmol) and suberic acid (10.84 g, 62.20 mmol) were added to a round-bottom flask. The mixture was then placed in a water bath where the temperature of the mixture was increased and maintained at 40 °C. The mixture was then left for 24 h under continuous stirring. Afterwards, the mixture was left to settle for 2 h. The IL phase was then removed from the unreacted starting materials and dried over silica gel for 24 h, yielding a white solid. ^{1}H NMR (400 MHz, CDCl$_3$) δ 9.65 (s, 1H), 2.95 – 2.84 (m, 6H), 2.21 (t, J = 7.5 Hz, 4H), 1.63 – 1.49 (m, 10H), 1.44 – 1.09 (m, 34H), 0.83 (t, J = 6.4 Hz, 9H). ^{13}C NMR (100 MHz, CDCl$_3$) δ 178.81, 51.30, 35.68, 31.69, 29.70, 29.08, 26.89, 25.44, 23.09, 22.59, 14.06. IR (ATR) $\bar{v}_{max}$: 2923.8, 2856.7, 1715.2, 1563.0, 1460.2, 1394.1, 1199.4, 1083.1, 983.8, 878.0, 817.7, 724.0, 630.0 cm^{-1}.

Figure A-4 Picture of trioctylammonium suberate (solid).

A.1.5 Trioctylammonium sebacate [HTOA][sebacate]

TOA (20g, 56.55 mmol) and sebacic acid (12.58 g, 62.20 mmol) were added to a round-bottom flask. The mixture was then stirred for 24 h at room temperature using a magnetic stirrer. Afterwards, the mixture was left to settle for 2 h resulting in the formation of three phases: a TOA phase, a liquid IL phase, and an unreacted acid phase. The IL phase was then removed from the unreacted starting materials and dried over silica gel for 24 h, yielding a clear, viscous liquid. ^{1}H NMR (400 MHz, CDCl$_3$) δ 2.93 – 2.84 (m, 6H), 2.20 (t, J = 6.8 Hz, 4H), 1.64 – 1.49 (m, 10H), 1.24 (d, J = 14.1 Hz, 38H), 0.83 (t, J = 5.0 Hz, 9H). ^{13}C NMR (100 MHz, CDCl$_3$) δ 178.90, 178.88, 51.30, 35.78, 31.70, 29.69, 29.37, 29.23, 29.10, 29.08, 26.91, 25.56, 23.12, 22.60, 14.06. IR (ATR) $\bar{v}_{max}$: 2921.9, 2855.3, 2364.2, 1715.3, 1563.3, 1460.3, 1395.5, 1196.6, 1091.2, 989.8, 885.2, 721.3, 658.1 cm^{-1}.

Figure A-5 Picture trioctylammonium sebacate.

APPENDIX B SPECTROSCOPIC DATA

The following sections present the NMR and FT-IR spectra of the synthesized ILs.

B.1 NMR spectra
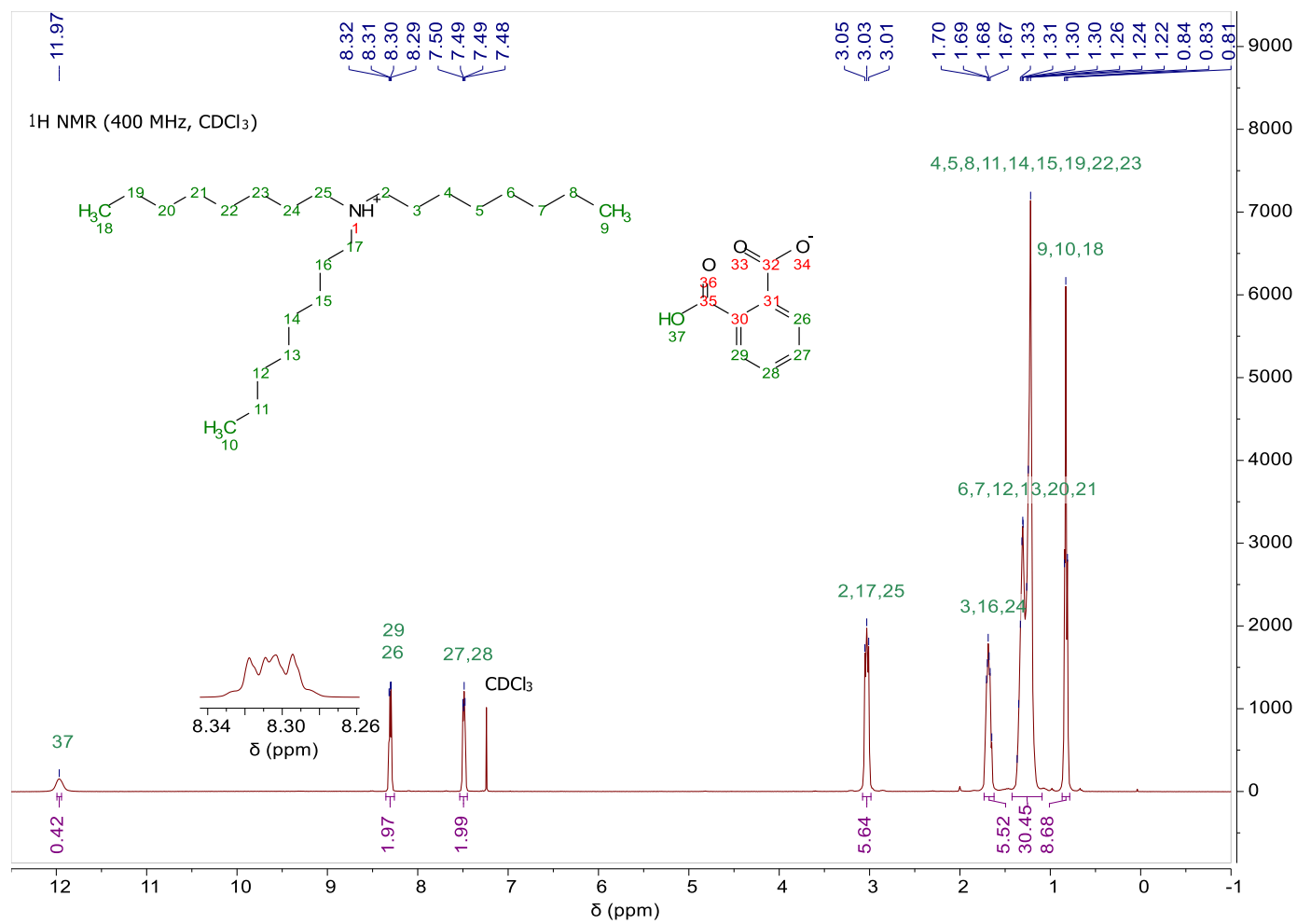
Figure B-1 ^{1}H NMR spectrum of [HTOA][phthalate] in CDCl$_3$.
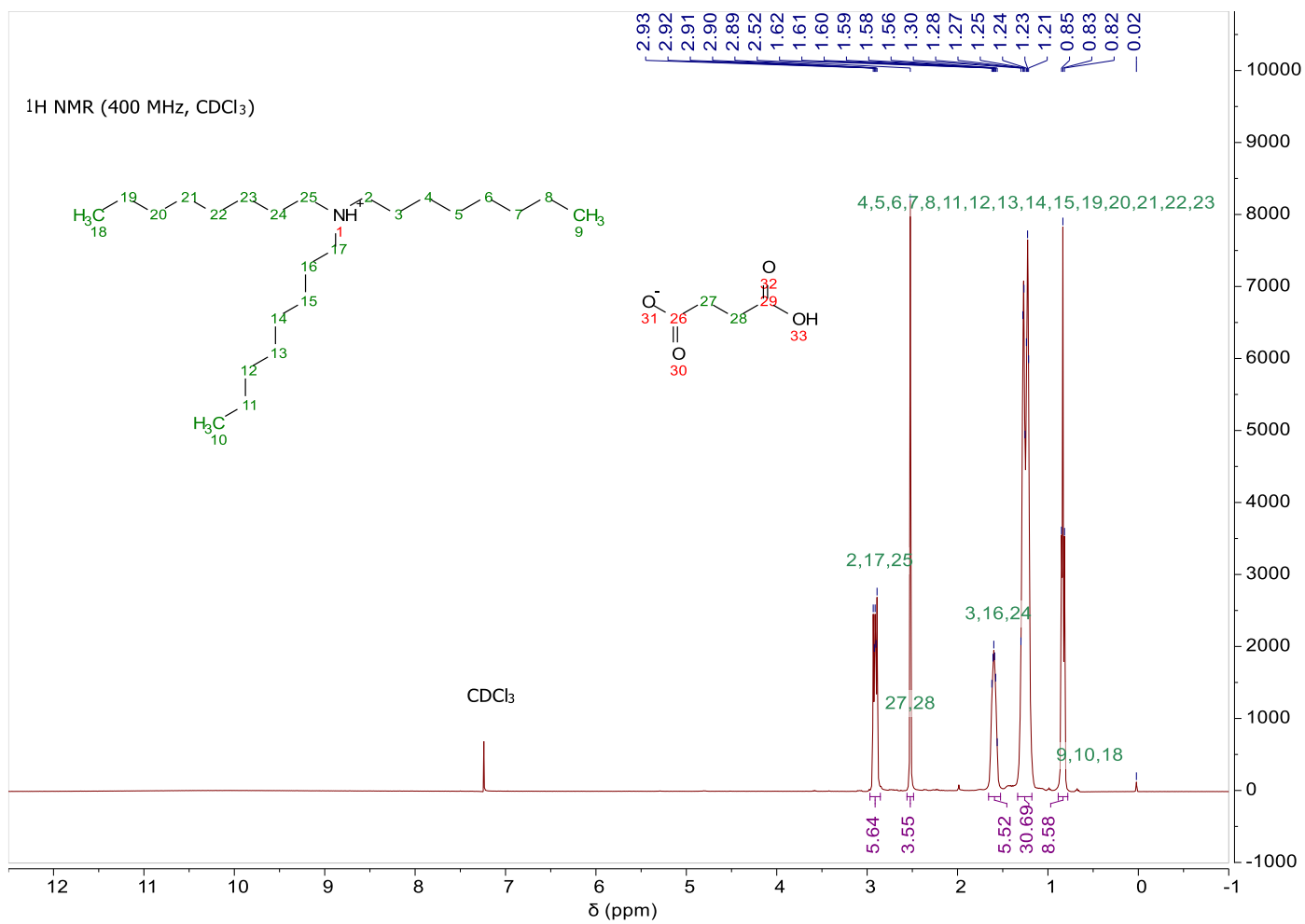
Figure B-2 ^{1}H NMR spectrum of [HTOA][succinate] in CDCl$_3$.
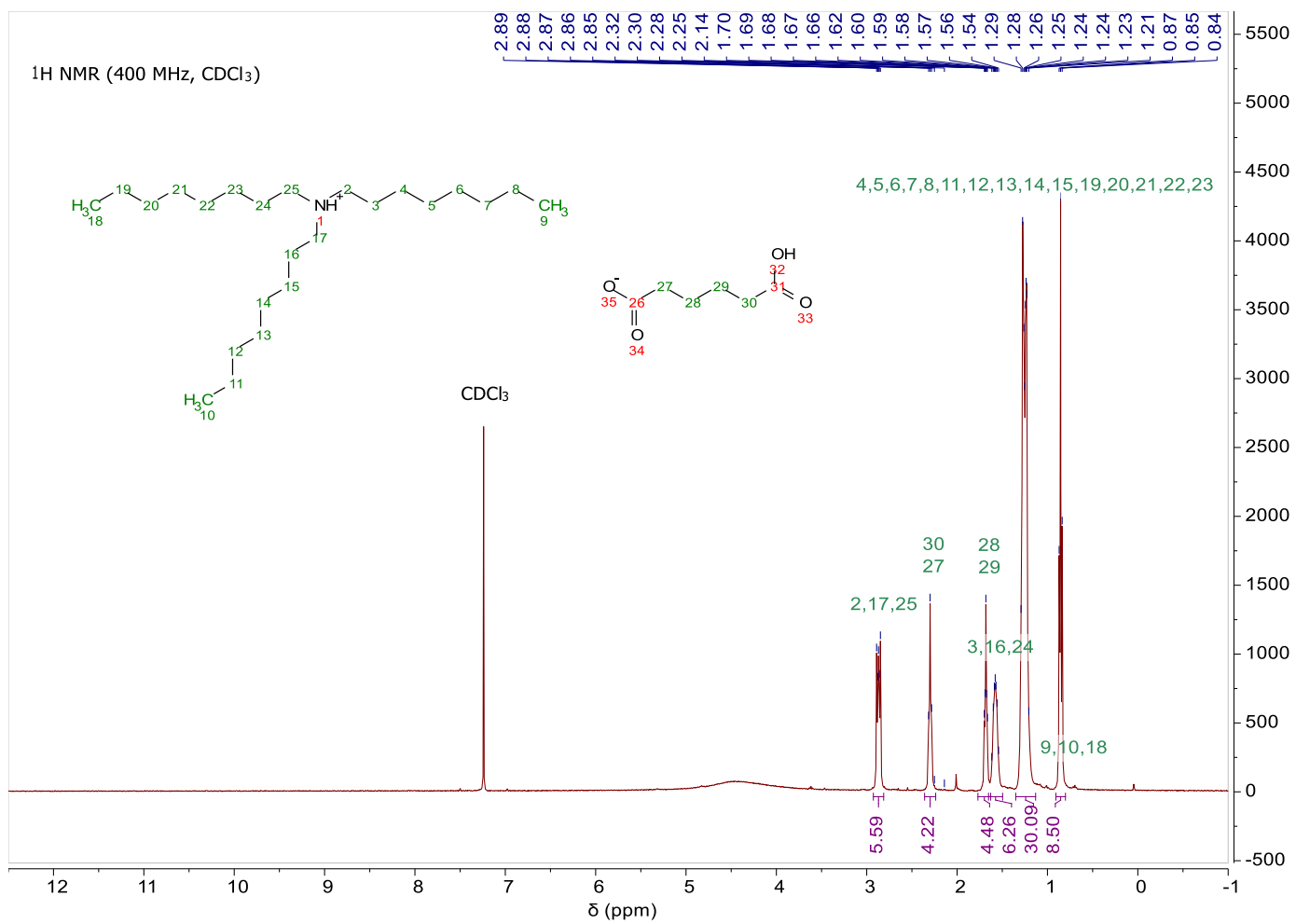
Figure B-3 ^{1}H NMR spectrum of [HTOA][adipate] in CDCl$_3$.
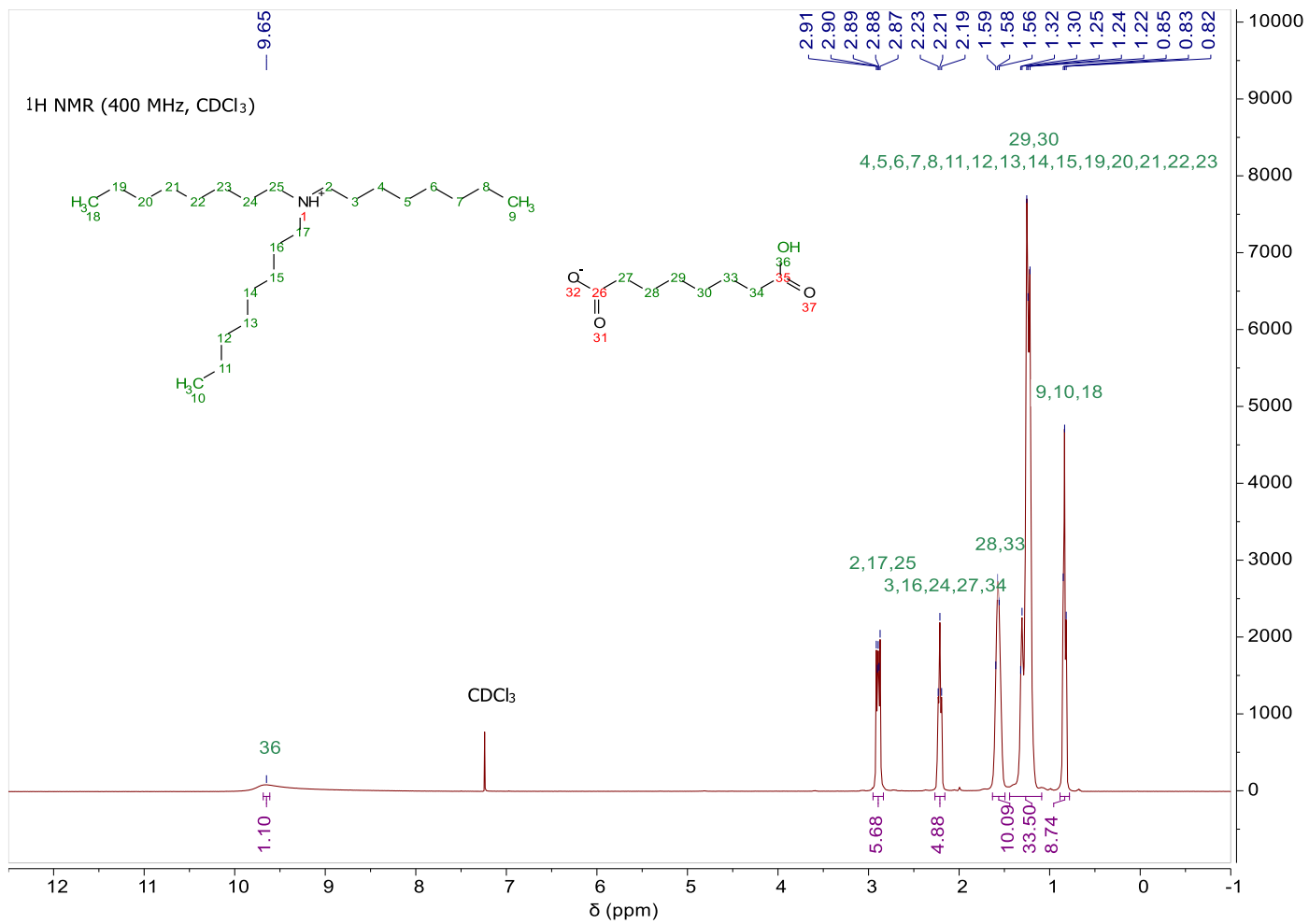
Figure B-4 ^{1}H NMR spectrum of [HTOA][suberate] in CDCl$_3$.
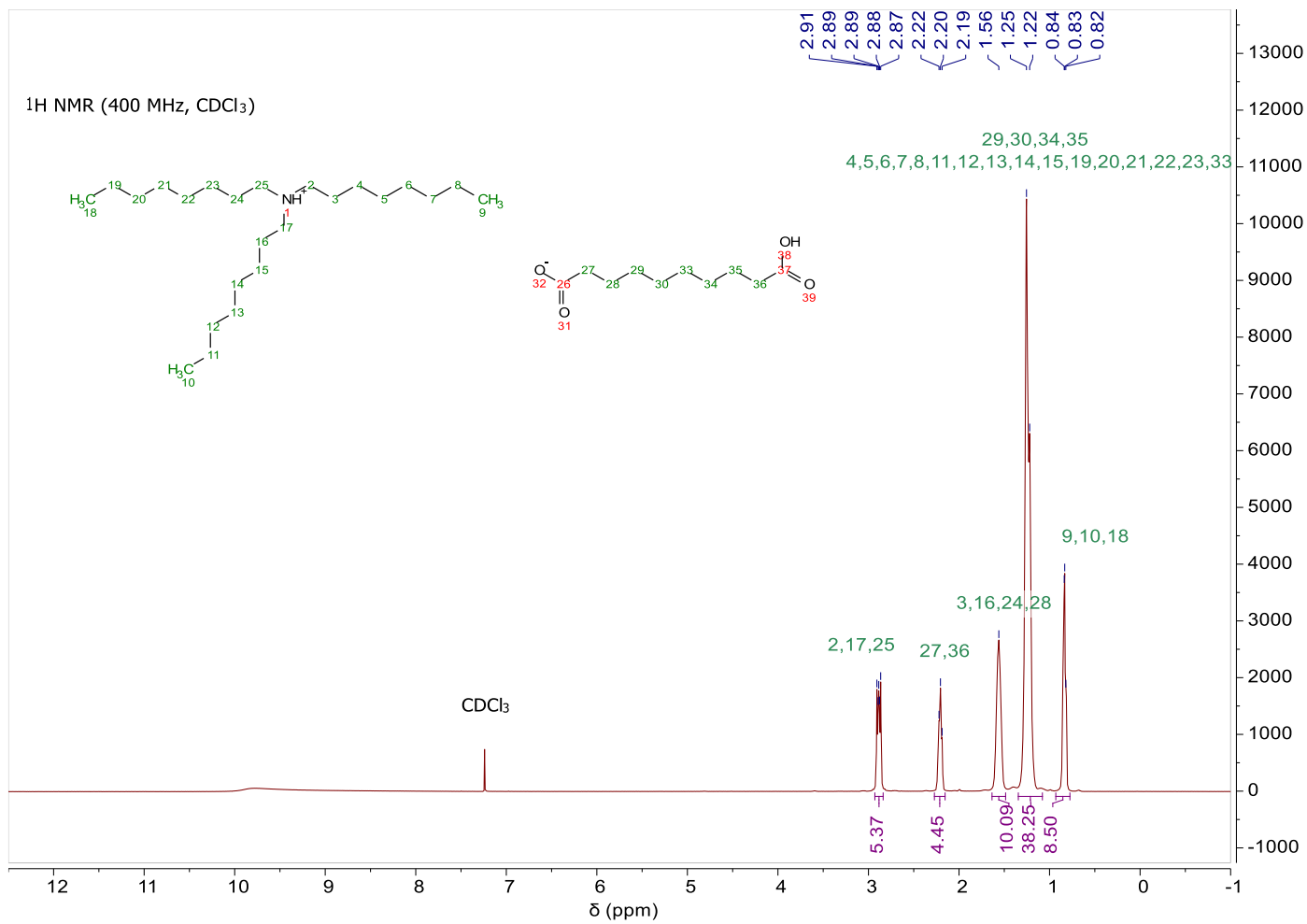
Figure B-5 ^{1}H NMR spectrum of [HTOA][sebacate] in CDCl$_3$.
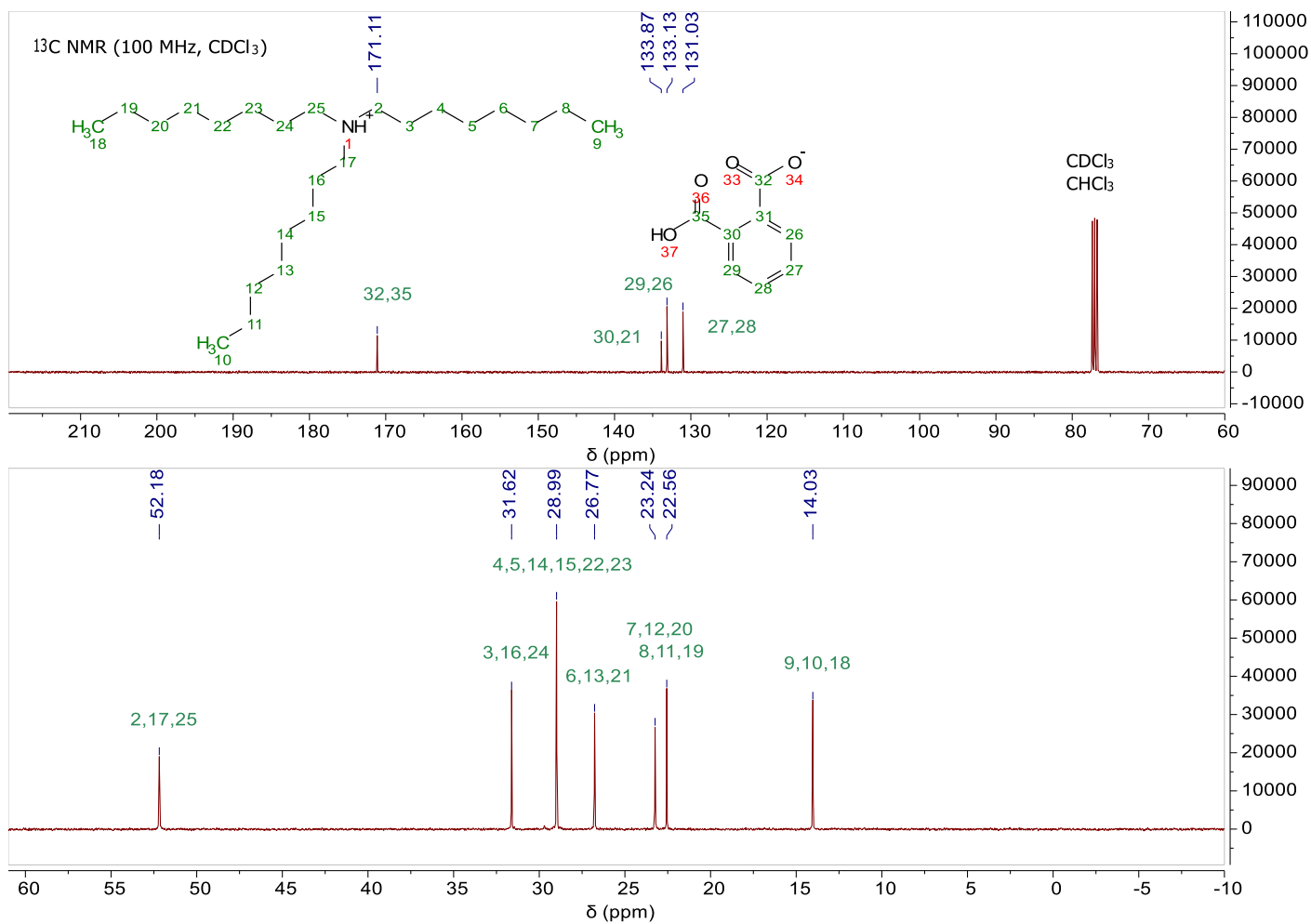
Figure B-6 ^{13}C NMR spectrum of [HTOA][phthalate] in CDCl$_3$.
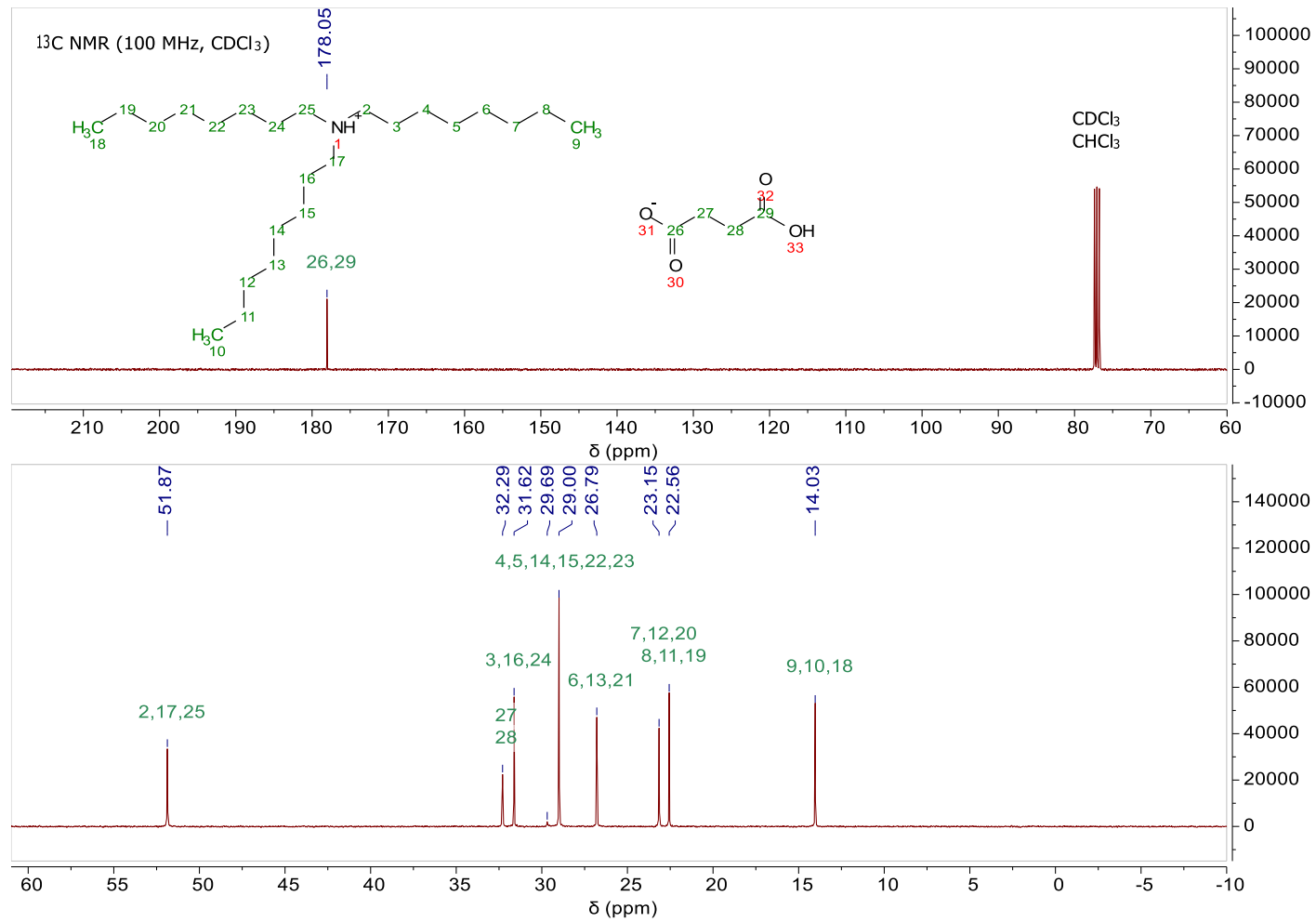
Figure B-7 ^{13}C NMR spectrum of [HTOA][succinate] in CDCl$_3$.
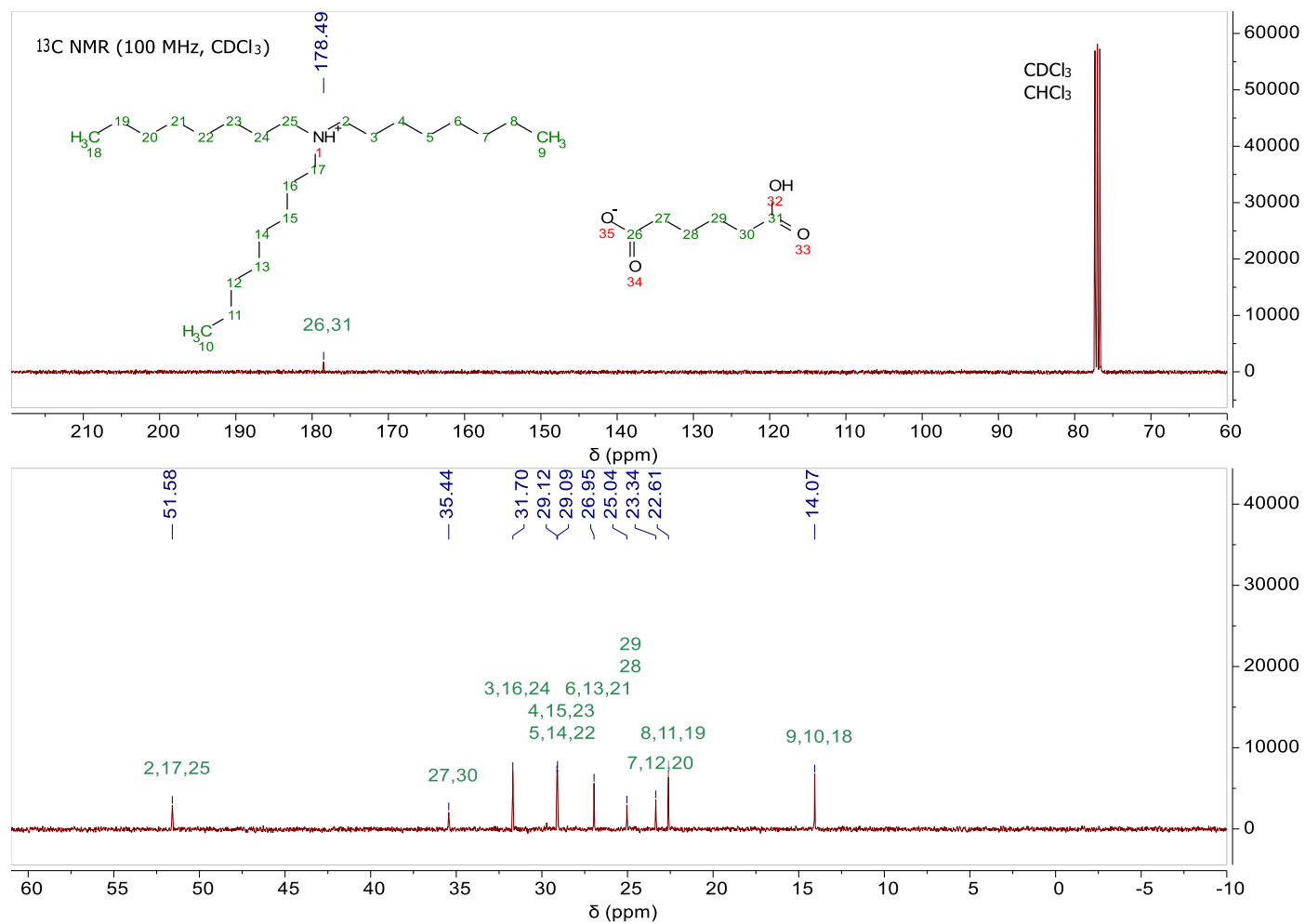
Figure B-8 ^{13}C NMR spectrum of [HTOA][adipate] in CDCl$_3$.
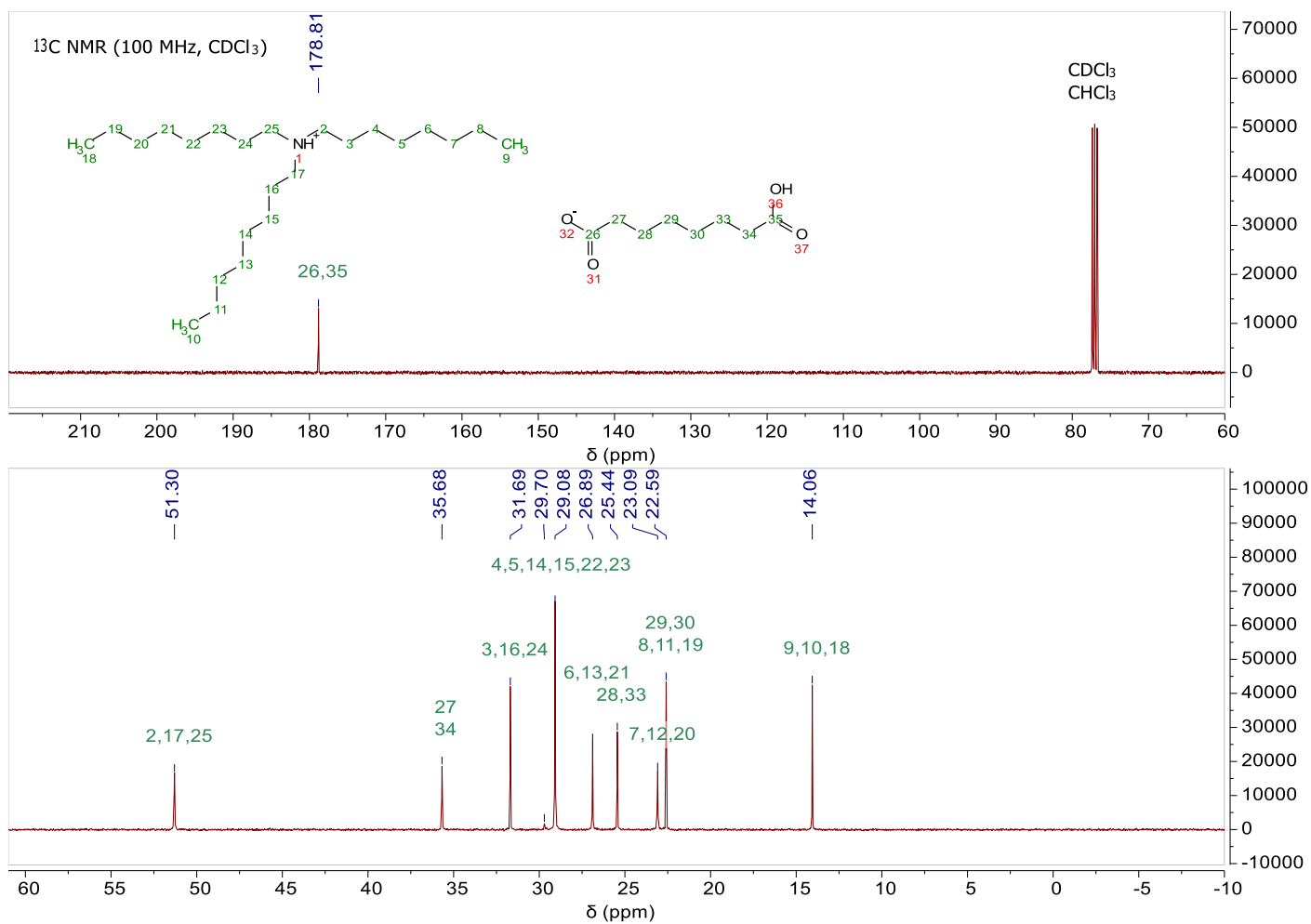
Figure B-9 ^{13}C NMR spectrum of [HTOA][suberate] in CDCl$_3$.
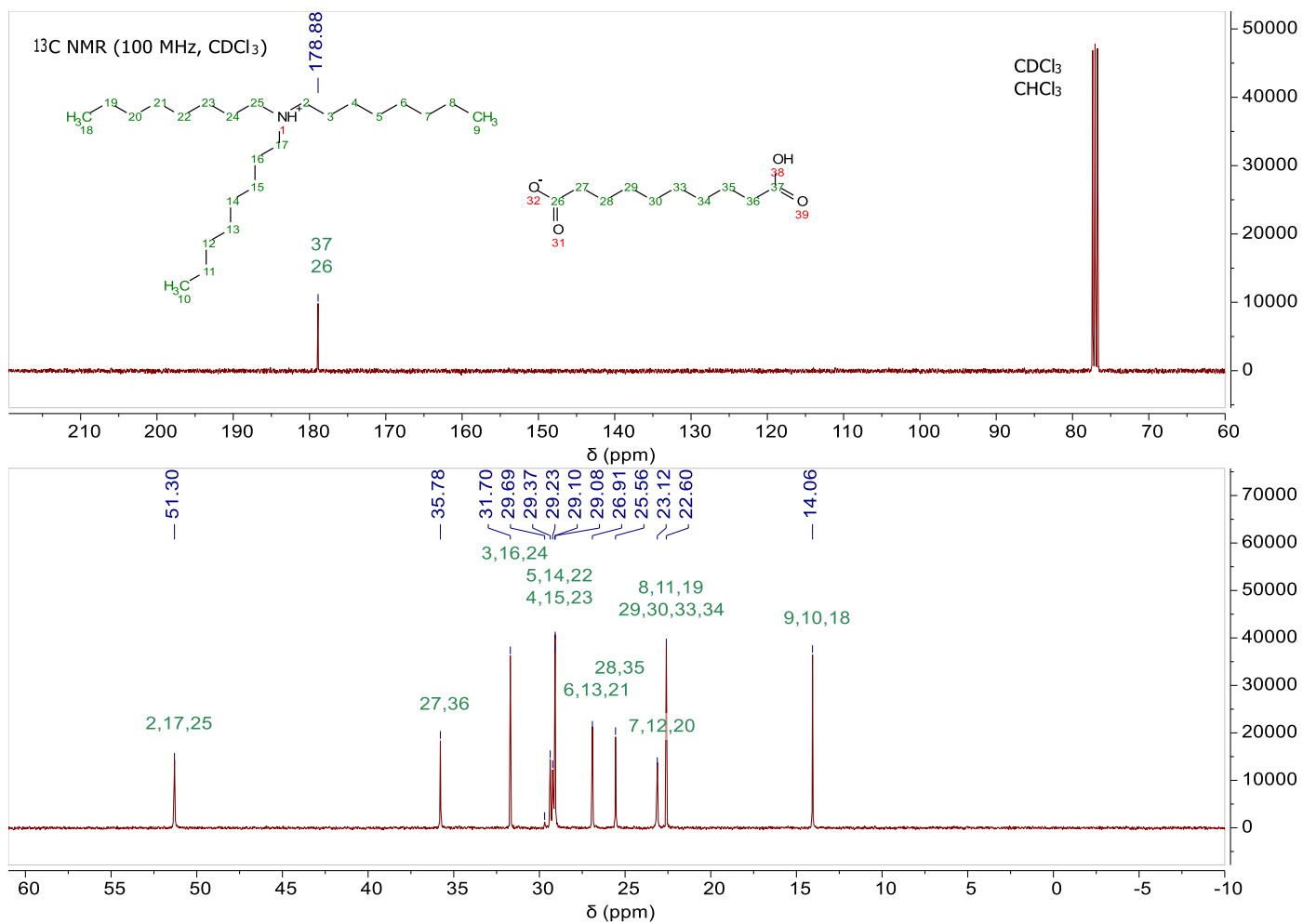
Figure B-10 ¹³C NMR spectrum of [HTOA][sebacate] in CDCl₃.

B.2 FT-IR spectra
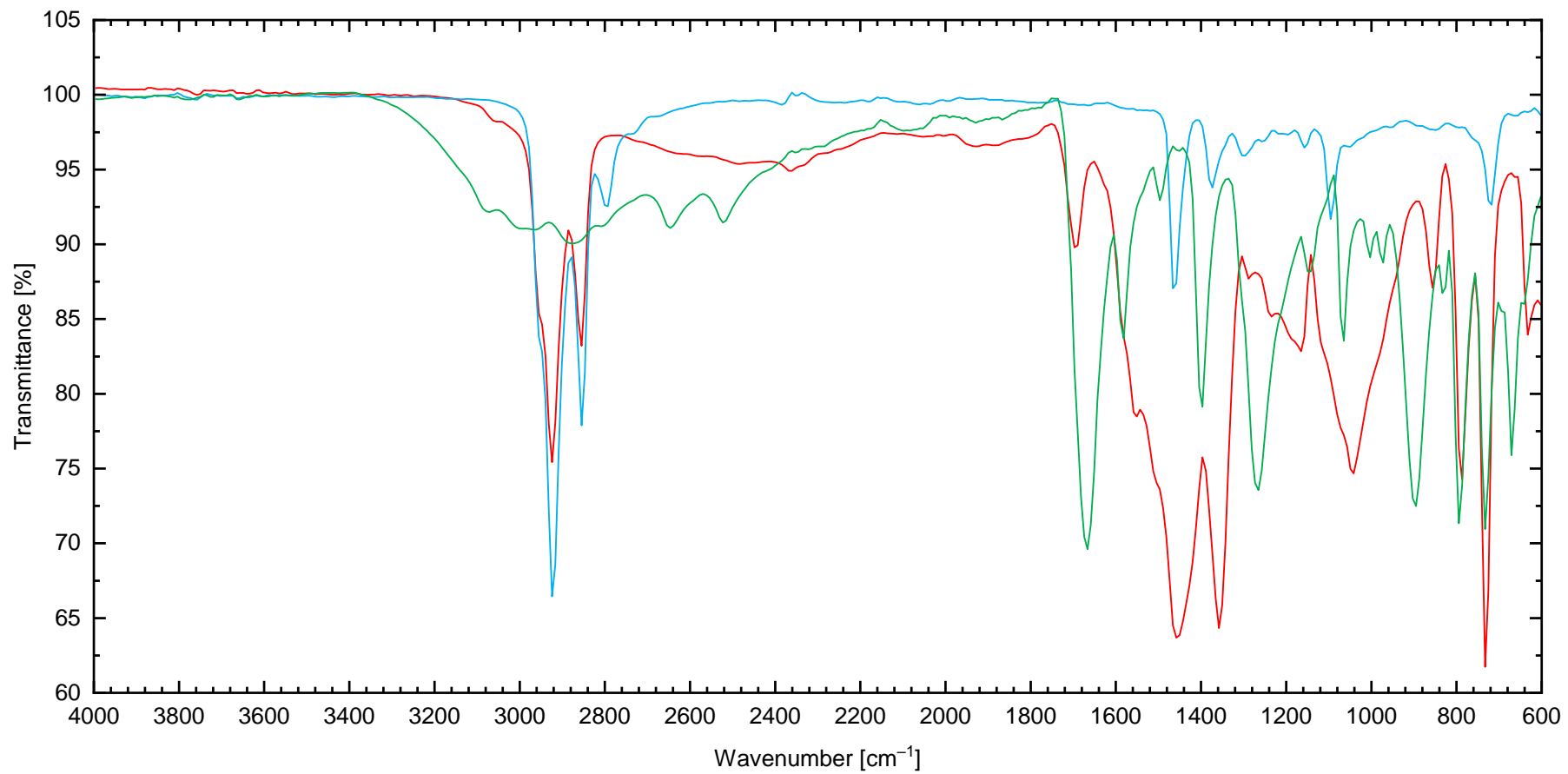
Figure B-11 FT-IR spectra of [HTOA][phthalate] (—), TOA (—), and phthalic acid (—).
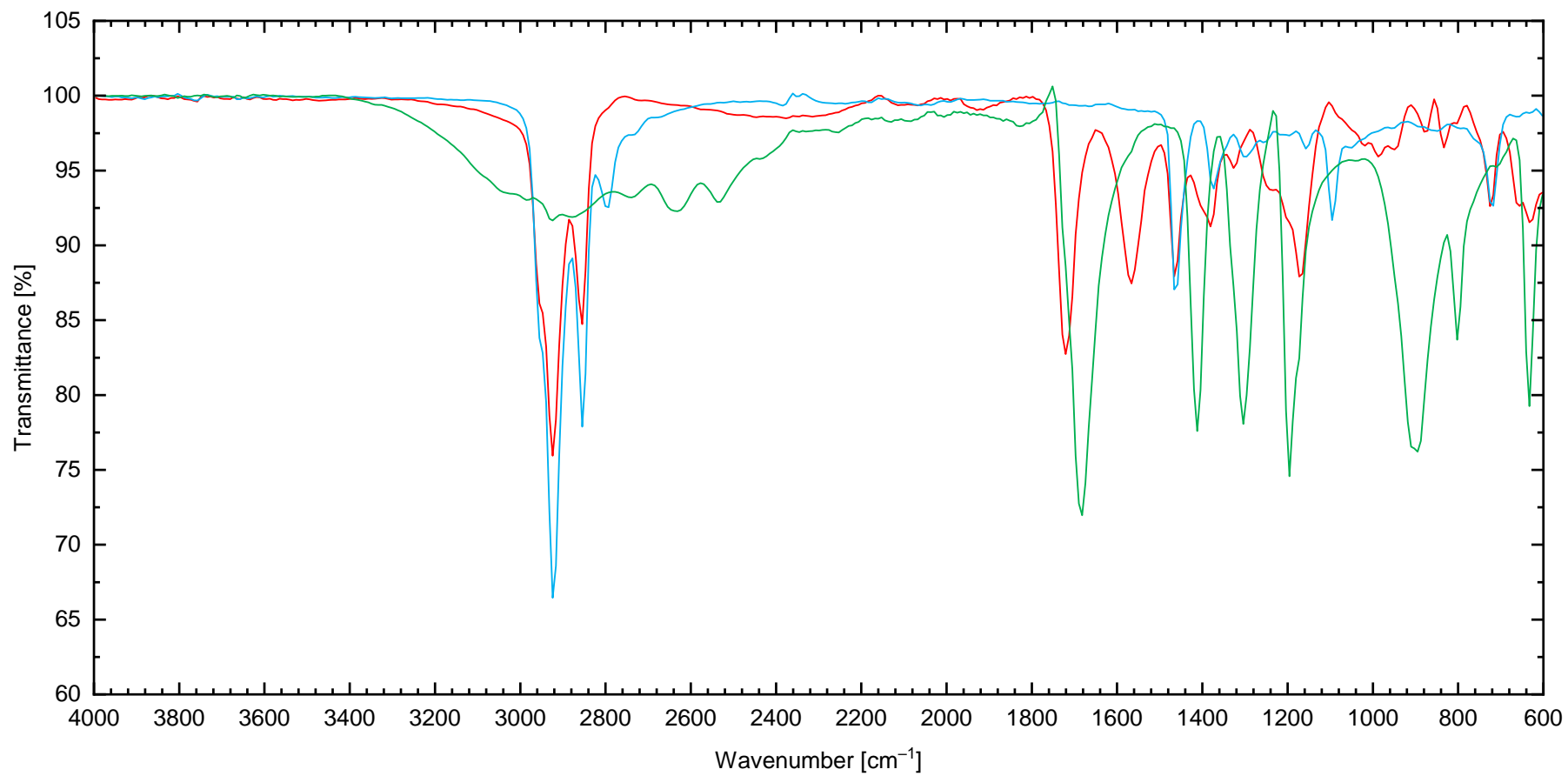
Figure B-12 FT-IR spectra of [HTOA][succinate] (—), TOA (—), and succinic acid (—).
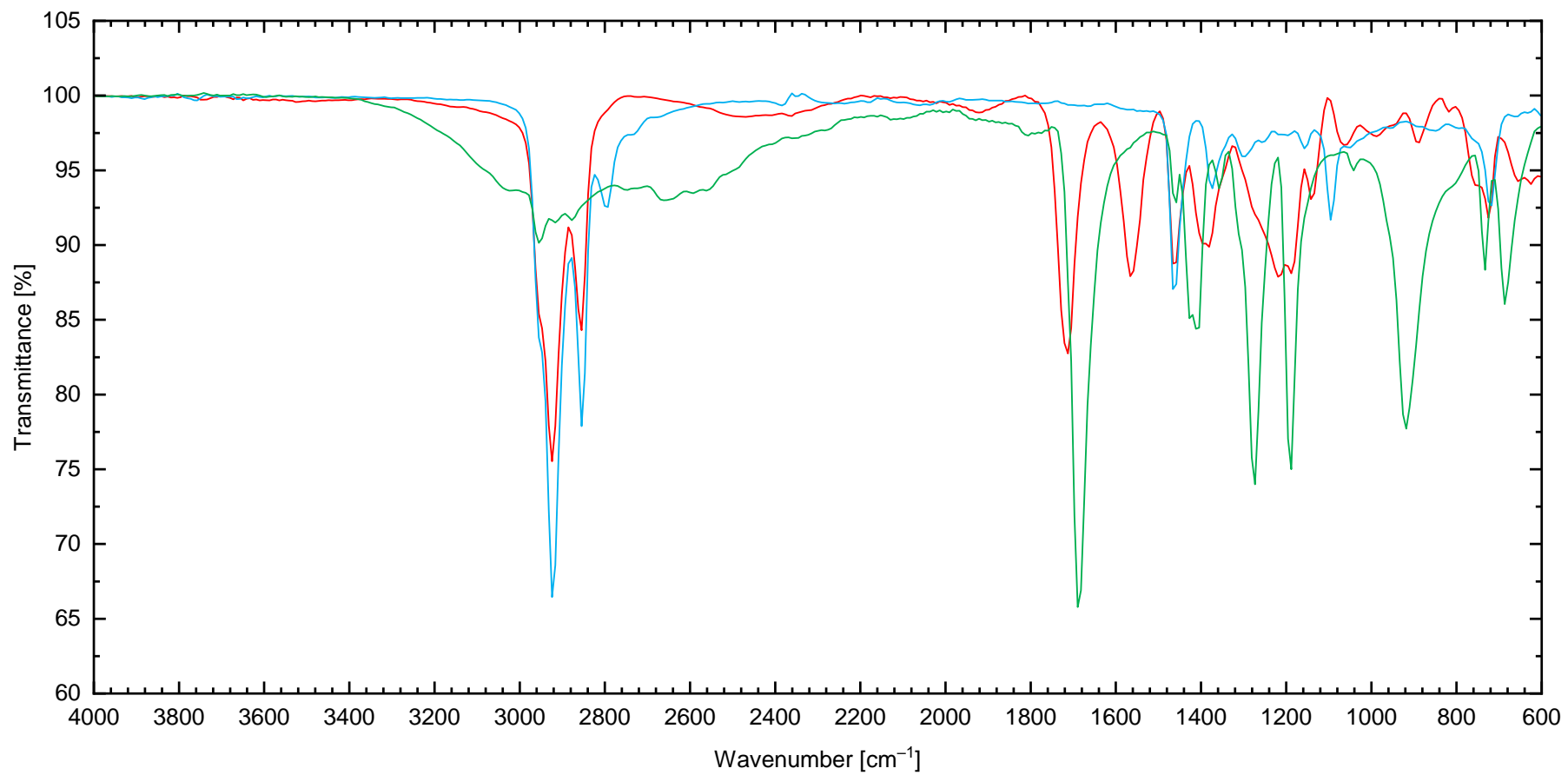
Figure B-13 FT-IR spectra of [HTOA][adipate] (—), TOA (—), and adipic acid (—).
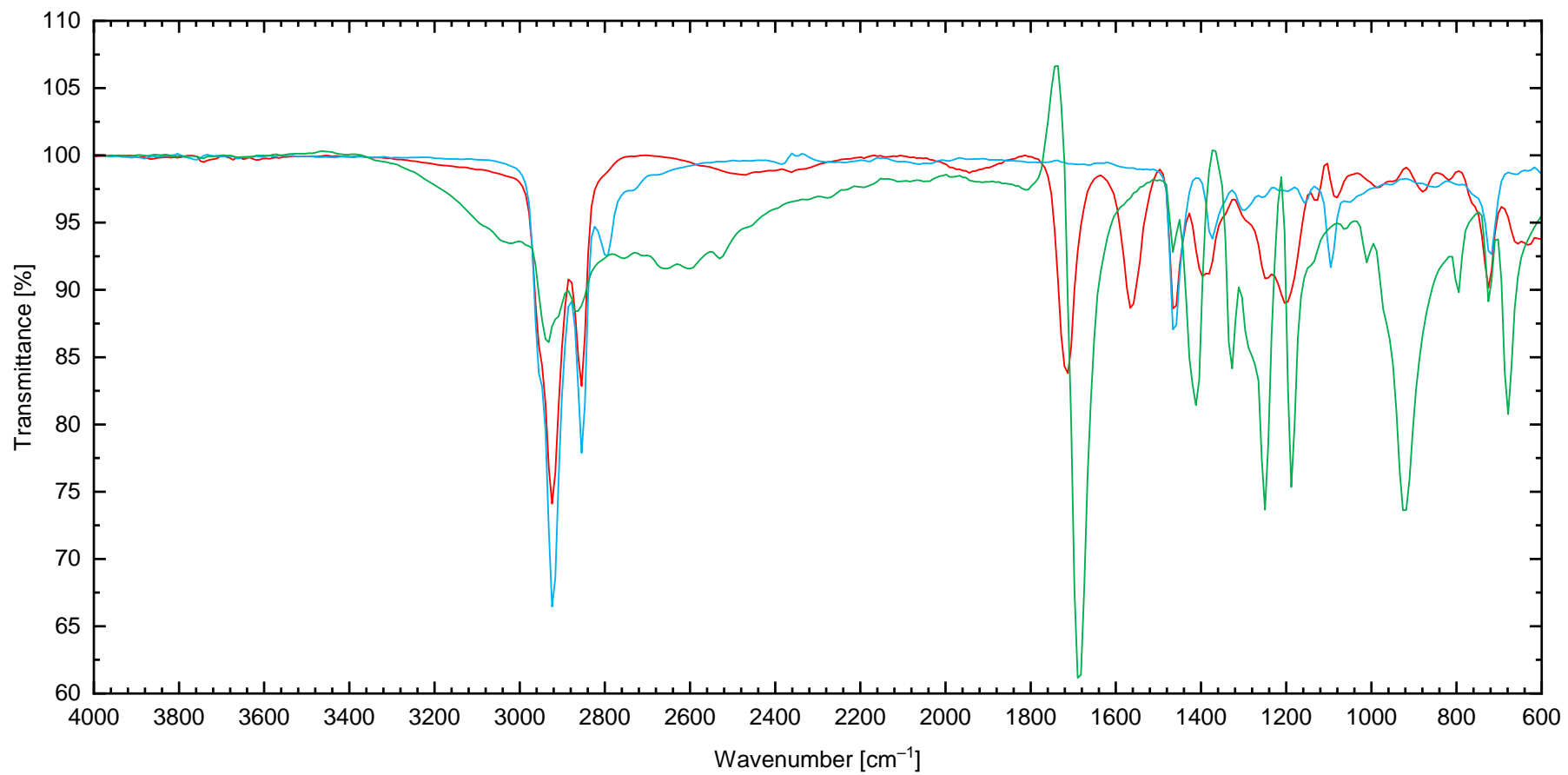
Figure B-14 FT-IR spectra of [HTOA][suberate] (—), TOA (—), and suberic acid (—).
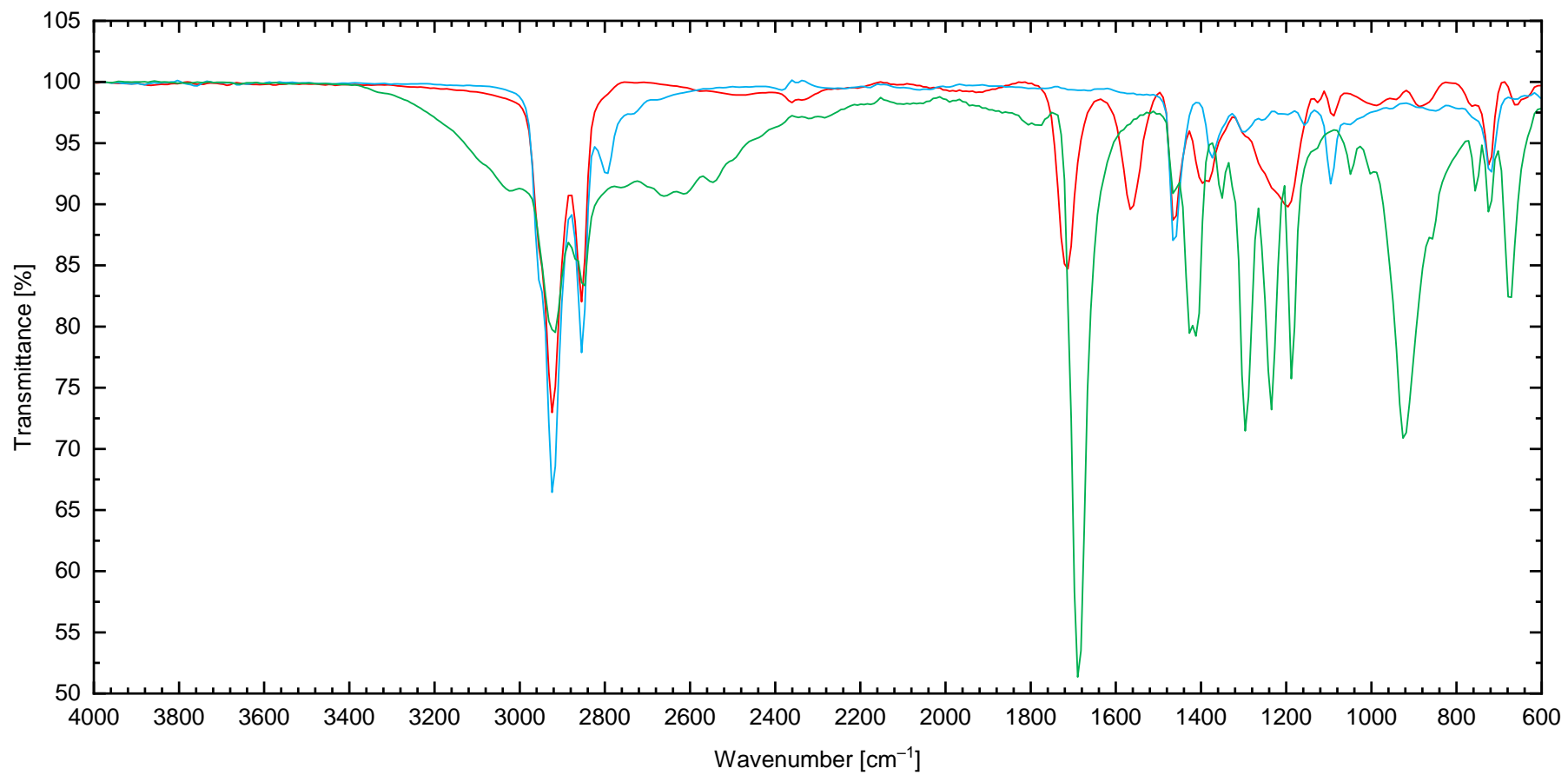
Figure B-15 FT-IR spectra of [HTOA][sebacate] (—), TOA (—), and sebacic acid (—).

APPENDIX C THERMAL ANALYSIS

C.1 Thermogravimetric analysis curves

The following constructions were used to determine the onset of decomposition temperatures.
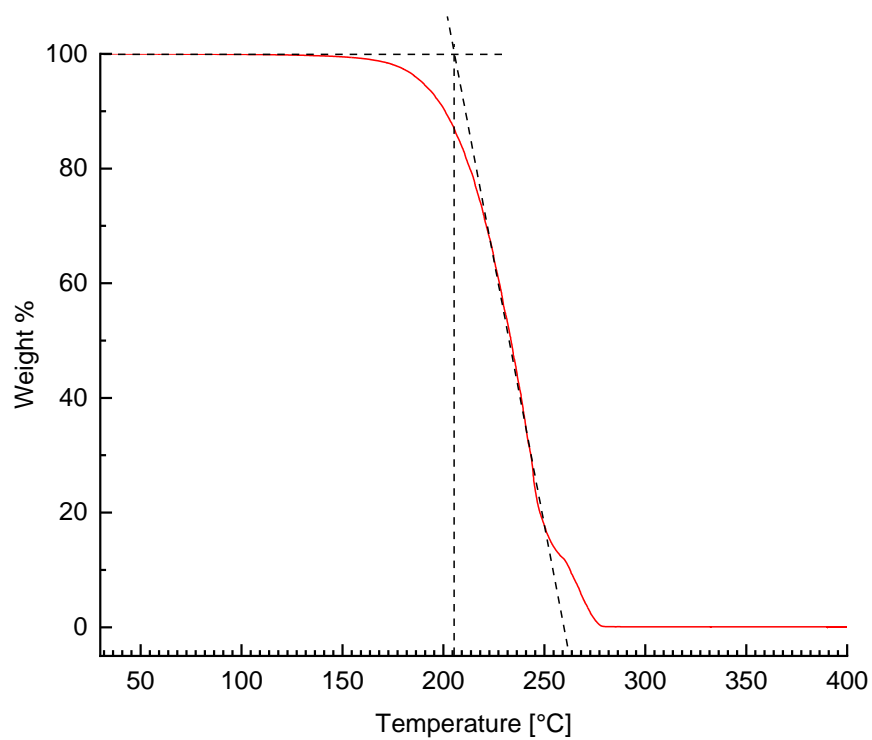
Figure C-1 TGA curve for [HTOA][phthalate].
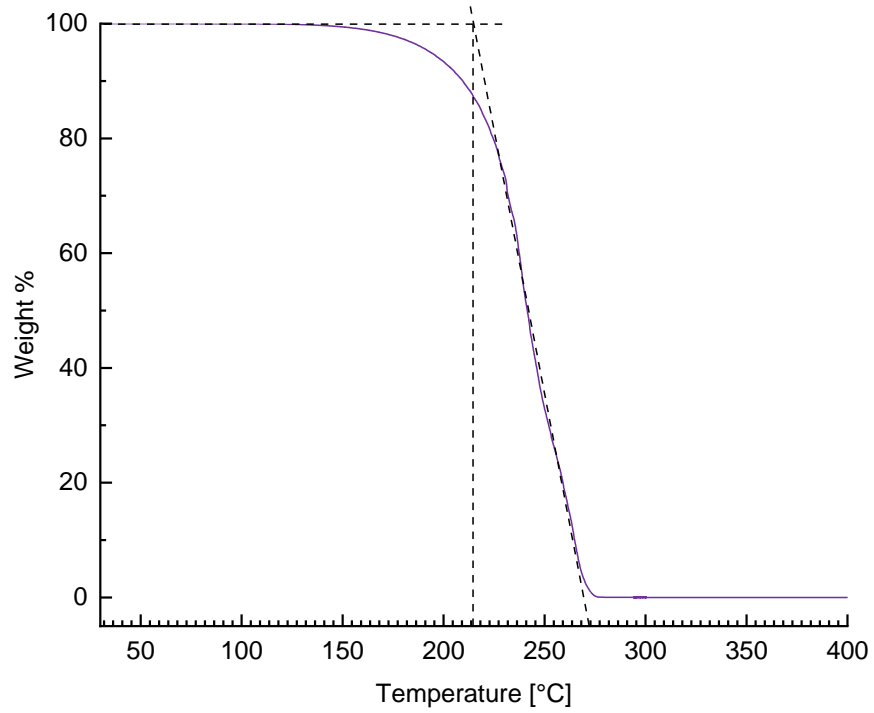
Figure C-2 TGA curve for [HTOA][succinate].
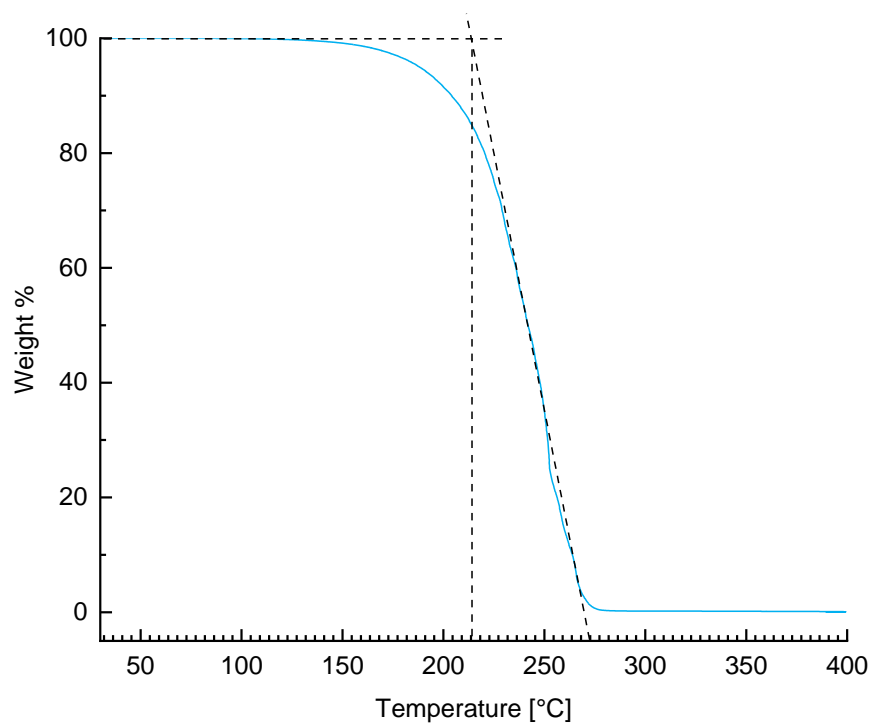
Figure C-3 TGA curve for [HTOA][adipate].
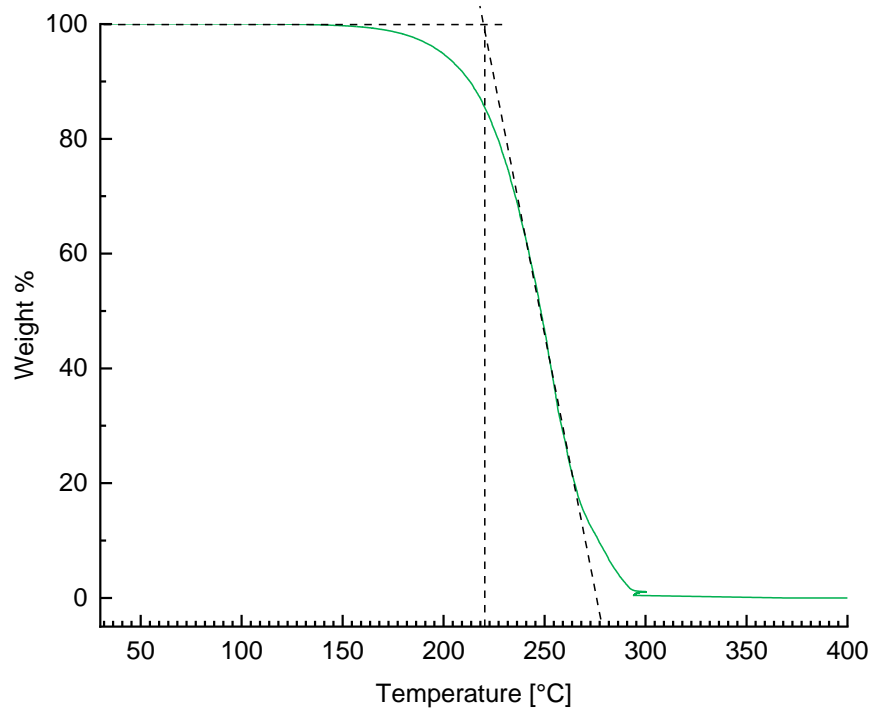
Figure C-4 TGA curve for [HTOA][suberate].
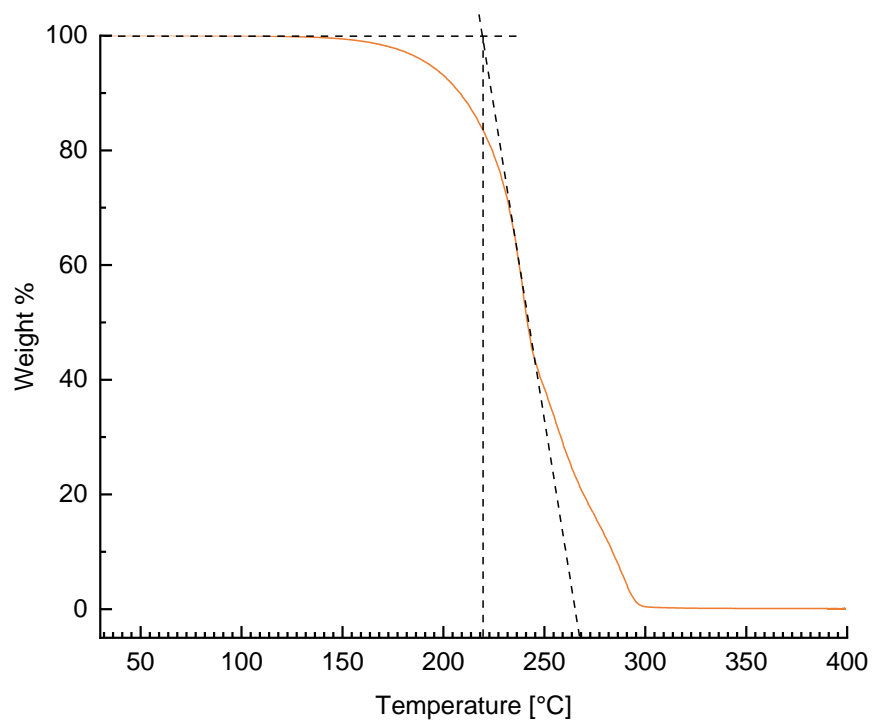
Figure C-5 TGA curve for [HTOA][sebacate].

C.2 Differential thermal analysis curves

The following curves were used to determine the melting points of [HTOA][succinate] and [HTOA][suberate].
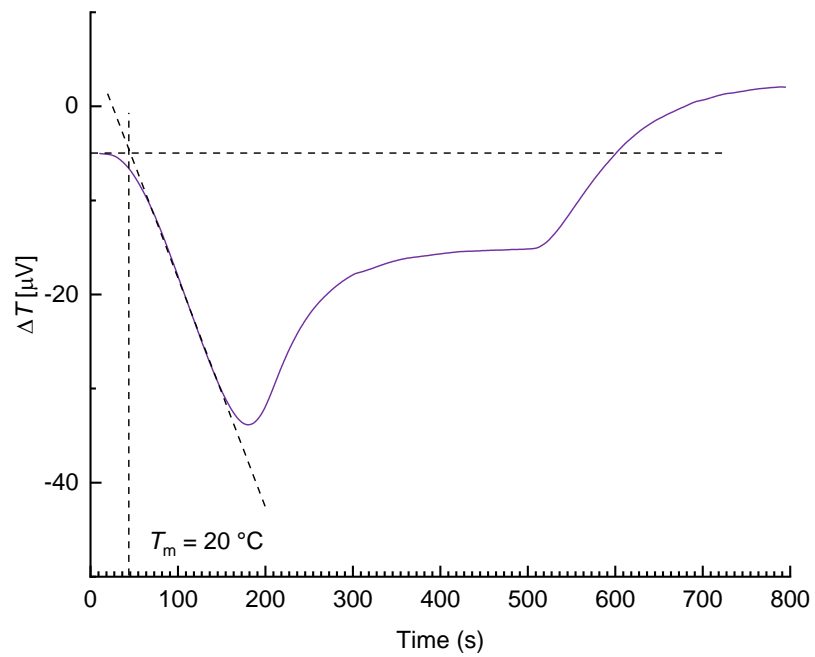
Figure C-6 DTA curve for [HTOA][succinate].
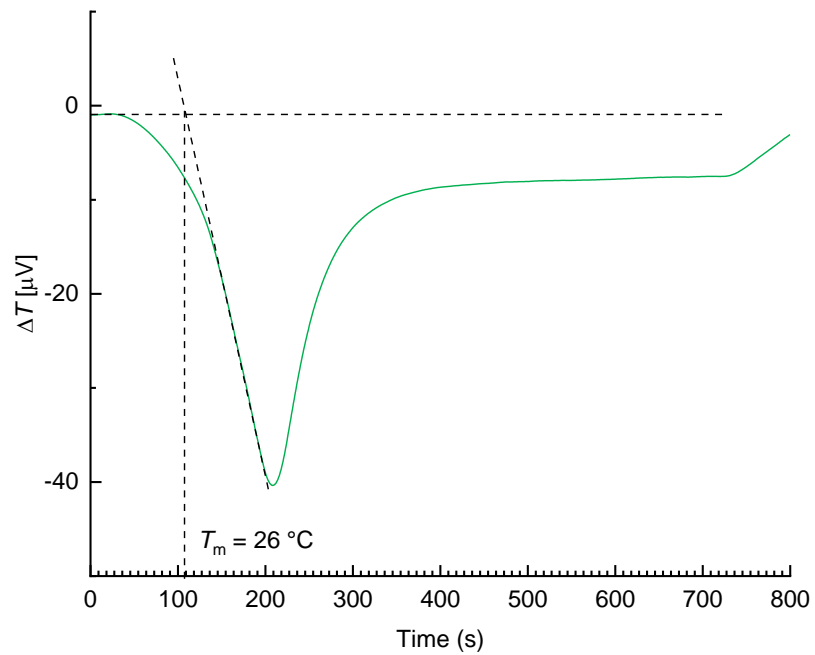
Figure C-7 DTA curve for [HTOA][suberate].

APPENDIX D PHYSICO-CHEMICAL PROPERTY DATA

Table D-1 Properties of trioctylammonium dicarboxylate ionic liquids.

Ionic liquid	Appearance [a]	Density [g cm^{-3}] [a]	Viscosity [mPa s] [a]	Electrical conductivity [S cm^{-1}][a]	Refractive index	Melting point [°C]	Decomposition temperature [°C]
[HTOA][phthalate]	Slightly yellow liquid	0.9699	734.3	25.1	1.4921	20	205
[HTOA][succinate]	clear liquid	–	–	–	–	–	215
[HTOA][adipate]	clear liquid	0.9448	3369.7	4.5	14659		215
[HTOA][suberate]	white solid	–	–	–	–	26	222
[HTOA][sebacate]	clear liquid	0.9257	2471.7	1.7	14654	–	221

[a] Determined at 25 °C.

D.1 Density data

D.1.1 Raw data

Table D-2 Raw density data, ρ, as a function of temperature at atmospheric pressure for the studied ILs.

T [K]	ρ [g cm^{-3}]								
	[HTOA][phthalate]			[HTOA][adipate]			[HTOA][sebacate]		
	Measurement			Measurement			Measurement		
	1	2	3	1	2	3	1	2	3
293.15	0.973207	0.973190	0.973213	0.948221	0.948218	0.948229	0.928810	0.928809	0.928813
298.15	0.969943	0.969924	0.969950	0.944789	0.944770	0.944799	0.925650	0.925638	0.925665
303.15	0.966667	0.966651	0.966679	0.941344	0.941326	0.941351	0.922280	0.922279	0.922299
308.15	0.963436	0.963433	0.963452	0.937884	0.937867	0.937898	0.918688	0.918687	0.918704
313.15	0.960195	0.960185	0.960199	0.934380	0.934365	0.934399	0.915246	0.915227	0.915260
318.15	0.956621	0.956602	0.956639	0.930777	0.930758	0.930795	0.911601	0.911590	0.911620
323.15	0.953636	0.953618	0.953656	0.927412	0.927395	0.927425	0.907840	0.907831	0.907841
328.15	0.950591	0.950581	0.950598	0.924000	0.923985	0.924005	0.904583	0.904564	0.904600
333.15	0.946898	0.946891	0.946902	0.920448	0.920446	0.920456	0.901082	0.901078	0.901102

D.1.2 Experimental data

Table D-3 Experimental density data, ρ, as a function of temperature at atmospheric pressure for the studied ILs.

T [K]	ρ [g cm^{-3}]		
	[HTOA][phthalate]	[HTOA][adipate]	[HTOA][sebacate]
293.15	0.9732 ± 0.0000	0.9482 ± 0.0000	0.9288 ± 0.0000
298.15	0.9699 ± 0.0000	0.9448 ± 0.0000	0.9257 ± 0.0000
303.15	0.9667 ± 0.0000	0.9413 ± 0.0000	0.9223 ± 0.0000
308.15	0.9634 ± 0.0000	0.9379 ± 0.0000	0.9187 ± 0.0000
313.15	0.9602 ± 0.0000	0.9344 ± 0.0000	0.9152 ± 0.0000
318.15	0.9566 ± 0.0000	0.9308 ± 0.0000	0.9116 ± 0.0000
323.15	0.9536 ± 0.0000	0.9274 ± 0.0000	0.9078 ± 0.0000
328.15	0.9506 ± 0.0000	0.9240 ± 0.0000	0.9046 ± 0.0000
333.15	0.9469 ± 0.0000	0.9204 ± 0.0000	0.9011 ± 0.0000

D.1.3 Model parameters

Table D-4 Best-fit parameters of the linear model for the density data of the studied ILs.

Ionic liquid	A_0 [g cm^{-3}]	A_1 [g cm^{-3} K^{-1}]	R^2
[HTOA][phthalate]	1.165	-6.539×10^{-4}	0.9997
[HTOA][adipate]	1.152	-6.948×10^{-4}	1.0000
[HTOA][sebacate]	1.134	-7.004×10^{-4}	0.9997

D.2 Viscosity data

D.2.1 Raw data

Table D-5 Raw viscosity data, η, as a function of temperature at atmospheric pressure for the studied ILs.

T [K]	η [mPa s]								
	[HTOA][phthalate]			[HTOA][adipate]			[HTOA][sebacate]		
	Measurement			Measurement			Measurement		
	1	2	3	1	2	3	1	2	3
293.15	1075.0	1075.0	1070.0	5105.0	5110.0	5110.0	3655.0	3655.0	3660.0
298.15	735.0	733.0	735.0	3375.0	3367.0	3367.0	2470.0	2470.0	2475.0
303.15	516.0	516.0	516.0	2279.0	2283.0	2279.0	1712.0	1712.0	1717.0
308.15	371.0	372.0	371.0	1583.0	1579.0	1583.0	1207.0	1205.0	1207.0
313.15	273.0	272.5	273.0	1117.0	1115.0	1117.0	866.7	866.7	866.7
318.15	204.5	204.5	205.0	815.0	812.5	815.0	633.0	632.0	632.0
323.15	157.0	157.0	157.0	600.0	600.0	601.0	469.2	470.0	469.2
328.15	122.0	122.0	122.0	471.7	470.8	471.7	353.3	352.5	352.5
333.15	96.0	96.0	96.0	355.0	355.0	355.0	276.0	276.0	276.0

Table D-6 Raw viscosities of IL mixtures with methanol as a function of methanol mass fraction at 328.15 K.

Methanol mass fraction	η [mPa s]								
	[HTOA][phthalate]			[HTOA][adipate]			[HTOA][sebacate]		
	Measurement			Measurement			Measurement		
	1	2	3	1	2	3	1	2	3
0.1	83.0	82.5	83.0	252.0	250.0	250.0	194.0	192.5	194.0
0.5	2.0	2.5	2.0	6.0	6.0	6.0	4.5	4.5	5.0

D.2.2 Experimental data

Table D-7 Experimental viscosity data, η, as a function of temperature at atmospheric pressure for the studied ILs.

T [K]	η [mPa s]		
	[HTOA][phthalate]	[HTOA][adipate]	[HTOA][sebacate]
293.15	1073.3 ± 29	5108.3 ± 96	3656.7 ± 58
298.15	734.3 ± 19	3369.7 ± 58	2471.7 ± 58
303.15	516.0 ± 12	2280.3 ± 58	1713.7 ± 48
308.15	371.3 ± 12	1581.7 ± 48	1206.3 ± 29
313.15	272.8 ± 10	1116.3 ± 29	866.7 ± 19
318.15	204.7 ± 6	814.2 ± 19	632.3 ± 12
323.15	157.0 ± 6	600.3 ± 12	469.5 ± 10
328.15	122.0 ± 6	471.4 ± 10	352.8 ± 10
333.15	96.0 ± 6	355.0 ± 10	276.0 ± 10

D.2.3 VFT and Arrhenius model parameters

Table D-8 Best-fit parameters of the VFT model for the viscosity data of the studied ILs.

Ionic liquid	η_0 [mPa s]	B [K]	T_0 [K]	R^2
[HTOA][phthalate]	4.141×10^{-2}	1305	164.8	1.0000
[HTOA][adipate]	3.922×10^{-2}	1599	157.4	1.0000
[HTOA][sebacate]	4.974×10^{-3}	2266	125.4	1.0000

Table D-9 Best-fit parameters of the Arrhenius model for the viscosity data of the studied ILs.

Ionic liquid	η_∞ [mPa s]	E_η [kJ mol^{-1}]	R^2
[HTOA][phthalate]	1.980×10^{-6}	48.89	0.9984
[HTOA][adipate]	1.148×10^{-6}	54.01	0.9979
[HTOA][sebacate]	1.466×10^{-6}	52.65	0.9992

D.2.4 Arrhenius predictions
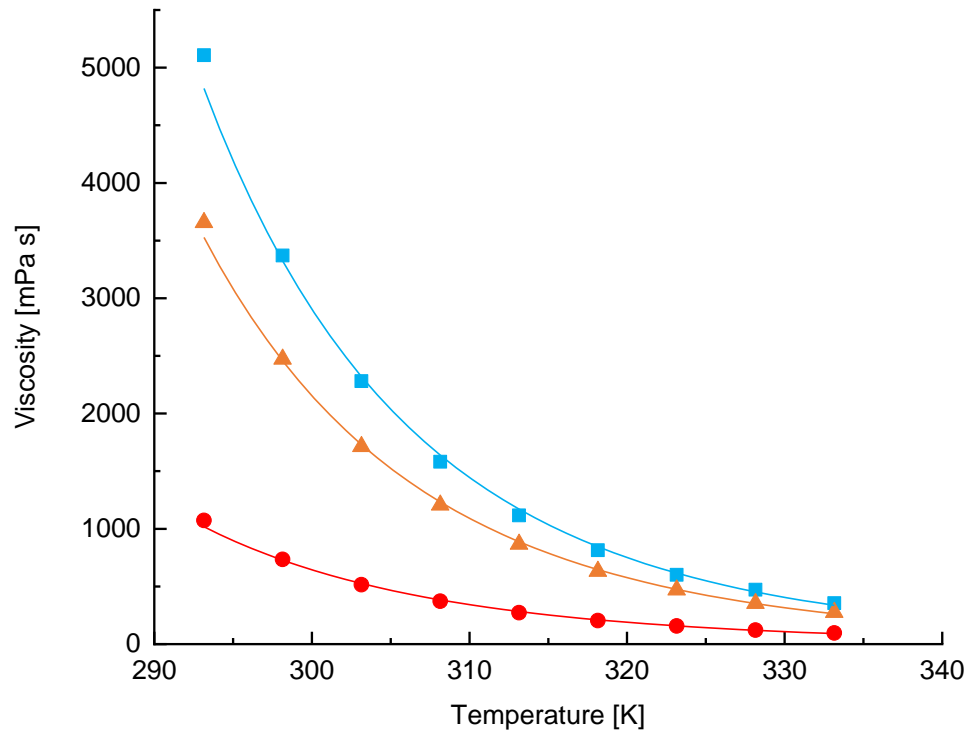
Figure D-1 Viscosity as a function of temperature for [HTOA][phthalate] (●), [HTOA][adipate] (■), and [HTOA][sebacate] (▲). The solid lines represent the predicted values obtained using the Arrhenius model.

D.3 Electrical conductivity data

D.3.1 Raw data

Table D-10 Raw electrical conductivity data, σ, as a function of temperature at atmospheric pressure for the studied ILs.

T [K]	σ [S cm^{-1}]								
	[HTOA][phthalate]			[HTOA][adipate]			[HTOA][sebacate]		
	Measurement			Measurement			Measurement		
	1	2	3	1	2	3	1	2	3
293.15	16.8	16.9	16.9	3.3	3.4	3.3	1.1	1.1	1.2
298.15	25.0	25.1	25.1	4.5	4.6	4.5	1.7	1.7	1.6
303.15	37.1	37.1	37.2	6.1	6.0	6.1	2.5	2.6	2.5
308.15	53.2	53.2	53.3	7.9	8.1	8.1	3.9	3.9	4.0
313.15	77.1	77.1	77.0	11.0	10.8	10.9	5.5	5.5	5.4

D.3.2 Experimental data

Table D-11 Experimental electrical conductivity data, σ, as a function of temperature at atmospheric pressure for the studied ILs.

T [K]	σ [μS cm^{-1}]		
	[HTOA][phthalate]	[HTOA][adipate]	[HTOA][sebacate]
293.15	16.9 ± 0.1	3.3 ± 0.1	1.1 ± 0.1
298.15	25.1 ± 0.1	4.5 ± 0.1	1.7 ± 0.1
303.15	37.1 ± 0.1	6.1 ± 0.1	2.5 ± 0.1
308.15	53.2 ± 0.1	8.0 ± 0.1	3.9 ± 0.1
313.15	77.1 ± 0.1	10.9 ± 0.1	5.5 ± 0.1

D.3.3 Arrhenius model parameters

Table D-12 Best-fit parameters of the Arrhenius model for the electrical conductivity data of the studied ILs.

Ionic liquid	σ_∞ [μS cm^{-1}]	E_∞ [kJ mol^{-1}]	R^2
[HTOA][phthalate]	3.485×10^{11}	57.89	0.9992
[HTOA][adipate]	3.468×10^{11}	45.01	0.9953
[HTOA][sebacate]	8.826×10^{11}	61.16	0.9931

D.4 Uncertainty analysis

The following is an outline of the procedure followed in calculating the uncertainties in the property measurements.

D.4.1 Density and viscosity

For density and viscosity measurements, uncertainties were estimated using the manufacturer's specifications and the measurement repeatability. These two uncertainties were combined ,using Eq. D1 , into a combined standard uncertainty $u_c(y)$,which calculates the uncertainty for a quantity y by combining all possible sources of uncertainty (Taylor and Kuyatt, 1994).

$$u_c(y) = \sqrt{\sum_i u_i(y)} \tag{D1}$$

$$u_c(y) = \sqrt{u_{spec}(y)^2 + u_{rep}(y)^2}$$

A rectangular distribution was assumed for the uncertainty specified by the manufacturer (b), and the standard uncertainty was evaluated using Eq. D2

$$u_{spec}(y) = \frac{b}{\sqrt{3}} \tag{D2}$$

The uncertainty due to repeatability was estimated by the standard deviation of the mean (Taylor and Kuyatt, 1994).

$$u_{rep}(y) = \frac{s}{\sqrt{n}}$$

$$= \sqrt{\left(\frac{1}{n(n-1)}\sum_{j=1}^{n}(y_j - \bar{y})^2\right)} \tag{D3}$$

where n is the number of repeated measurements, s is the standard deviation of the measurements, and $\bar{y}$ is the arithmetic mean of the measured values y . $u_c(y)$ was calculated using Eq. D1 and expanded using a coverage factor, $k = 2$, to obtain an expanded uncertainty U.

$$U = \pm k u_c(y) \qquad (D4)$$

Assuming y follows a normal distribution, a coverage factor of 2 defines a confidence interval with a confidence level of approximately 95%.

D.4.2 Conductivity

As the conductivity meter was calibrated, uncertainties in the conductivity measurements were estimated by multiplying the standard deviation of the mean by a coverage factor of two.

$$U = \pm k u_{\mathrm{rep}}(y) \qquad (D5)$$

APPENDIX E LIQUID-LIQUID EXTRACTION DATA

E.1 Calibration data

E.1.1 FAAS absorbance data

Table E-1 Absorbance data for the Cd(II) calibration curve.

Standard concentration [mg L^{-1}]	Corrected absorbance		
	Measurement		
	1	2	3
blank	0.001	–	–
0.1	0.005	0.004	0.005
0.3	0.016	0.017	0.017
0.5	0.029	0.028	0.029
0.7	0.040	0.042	0.042
0.9	0.052	0.050	0.054

Table E-2 Absorbance data for the Cu(II) calibration curve.

Standard concentration [mg L^{-1}]	Corrected absorbance		
	Measurement		
	1	2	3
blank	0.001	0.001	0.001
0.1	0.004	0.004	0.004
0.3	0.009	0.009	0.008
0.5	0.014	0.013	0.013
0.7	0.017	0.018	0.018
0.9	0.022	0.022	0.022
2	0.044	0.045	0.044

Table E-3 Absorbance data for the Zn(II) calibration curve.

Standard concentration [mg L^{-1}]	Corrected absorbance		
	Measurement		
	1	2	3
blank	−0.001	−0.001	−
0.1	0.006	0.007	0.008
0.3	0.017	0.017	0.018
0.5	0.029	0.028	0.027
0.9	0.049	0.049	0.049

E.1.2 Calibration curves
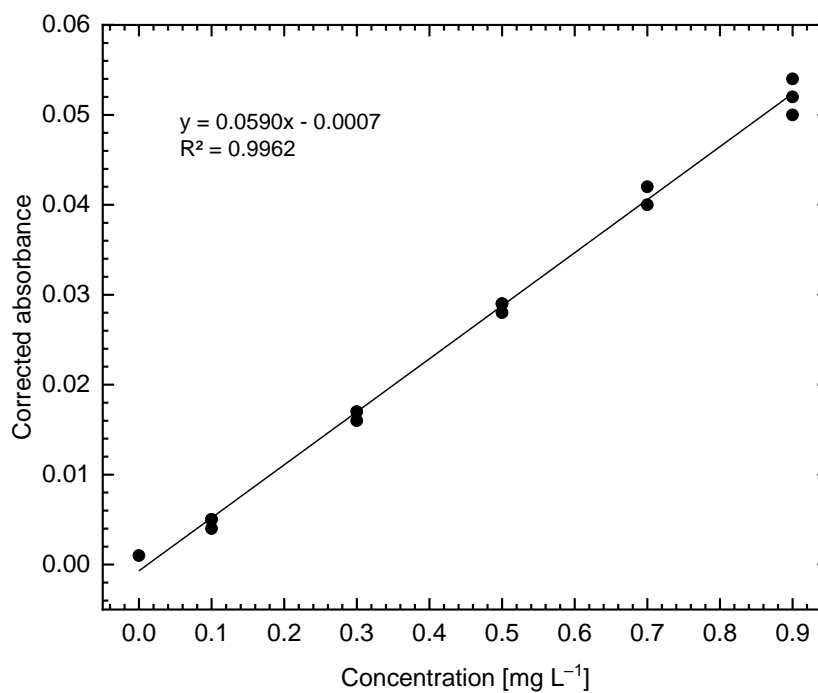
Figure E-1 Calibration curve for Cd(II) analysis. The equation of the solid straight line fitting the data points (●) was determined by the method of least squares.
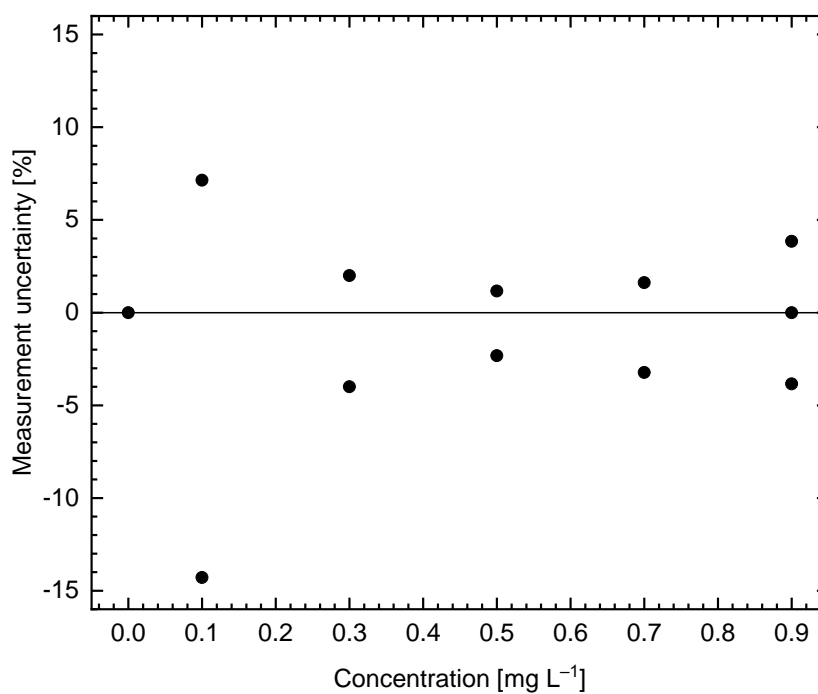
Figure E-2 Measurement uncertainty for the Cd(II) calibration curve defined as the percentage deviation from the measurement average.
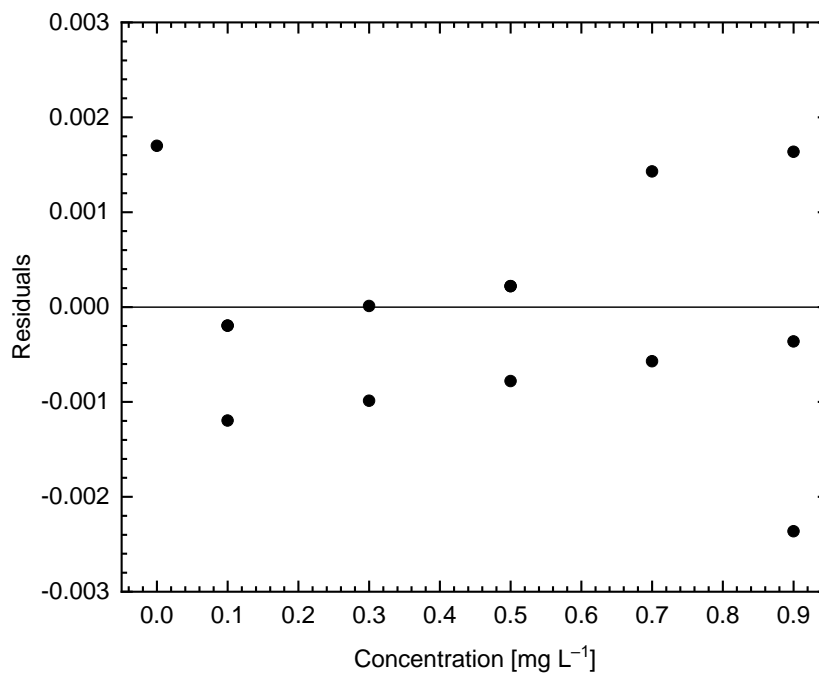
Figure E-3 Residuals as a function of standard concentration for the Cd(II) calibration curve.

Table E-4 Regression statistics for the Cd(II) calibration curve.

Parameter	Value
slope	5.896×10^{-2}
uncertainty of the slope	$\pm 9.7 \times 10^{-4}$
intercept	-7.0×10^{-3}
uncertainty of the intercept	$\pm 5.4 \times 10^{-4}$
R^2	0.9962
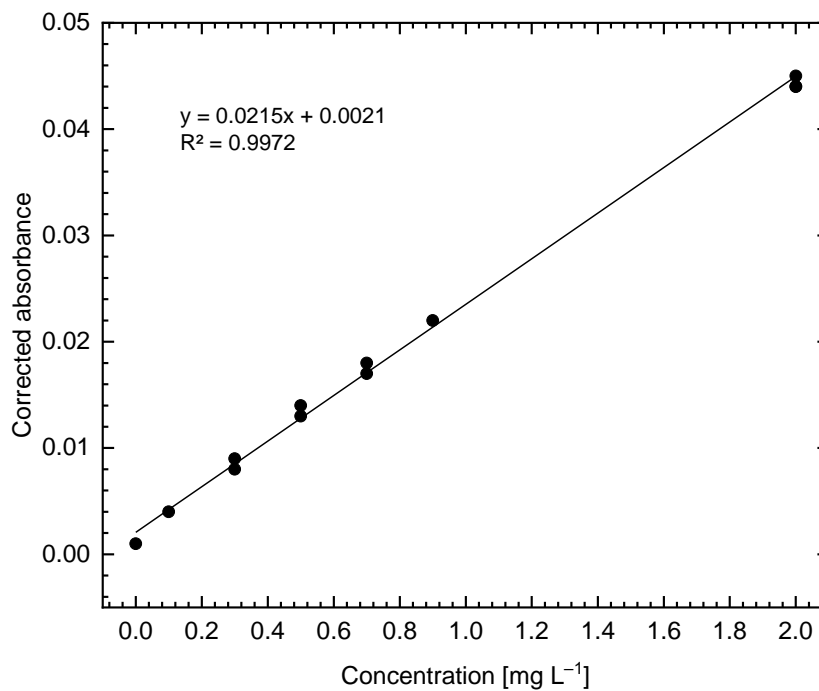
Figure E-4 Calibration curve for Cu(II) analysis. The equation of the solid straight line fitting the data points (●) was determined by the method of least squares.
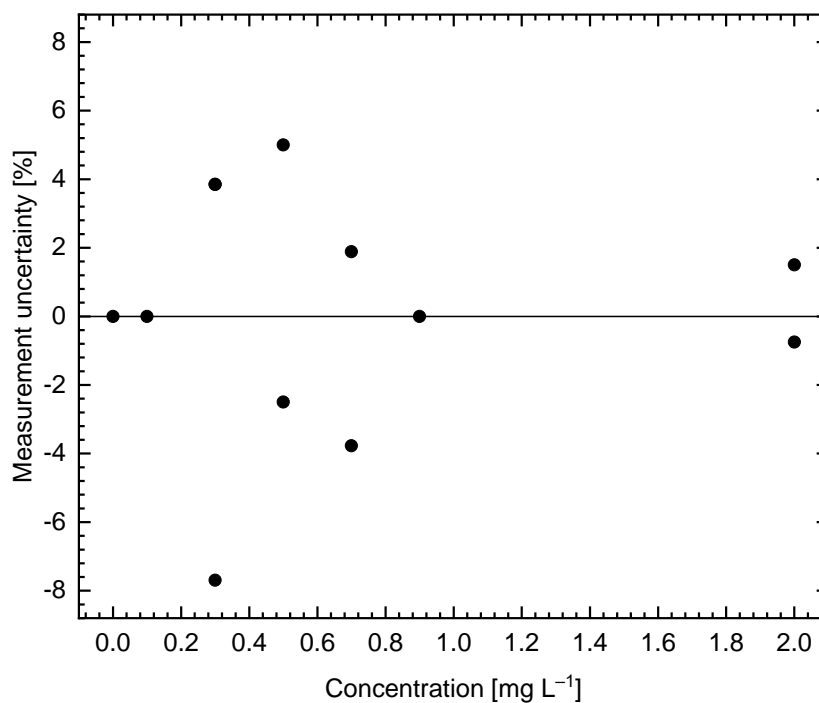
Figure E-5 Measurement uncertainty for the Cu(II) calibration curve defined as the percentage deviation from the measurement average.
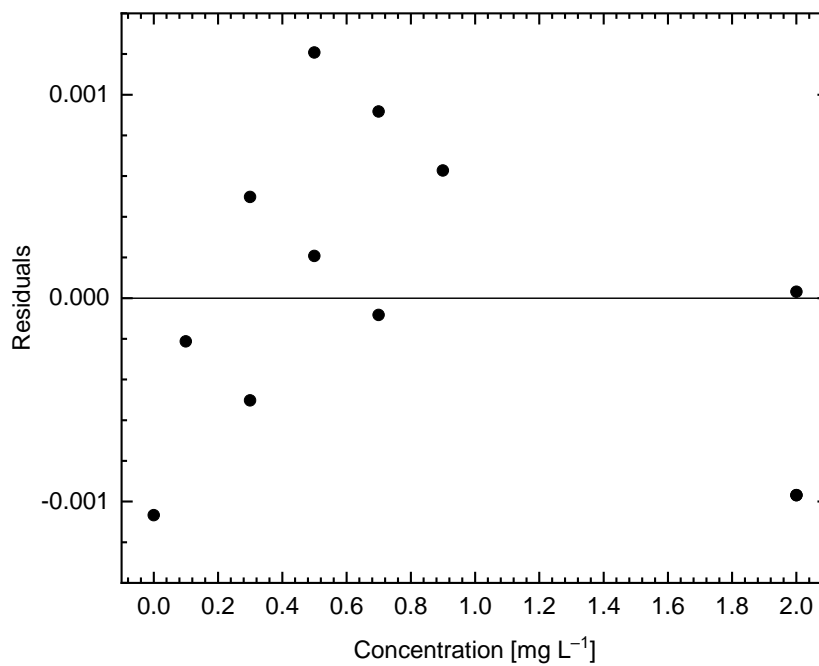
Figure E-6 Residuals as a function of standard concentration for the Cu(II) calibration curve.

Table E-5 Regression statistics for the Cu(II) calibration curve.

Parameter	Value
slope	2.145×10^{-2}
uncertainty of the slope	$\pm 2.6 \times 10^{-4}$
intercept	2.1×10^{-3}
uncertainty of the intercept	$\pm 2.3 \times 10^{-4}$
R^2	0.9972
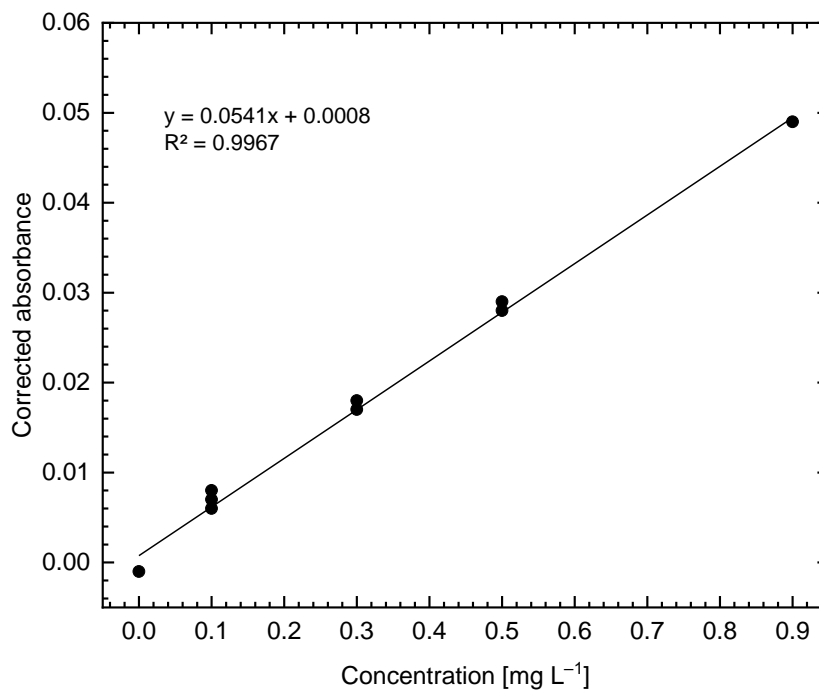
Figure E-7 Calibration curve for Zn(II) analysis. The equation of the solid straight line fitting the data points (●) was determined by the method of least squares.
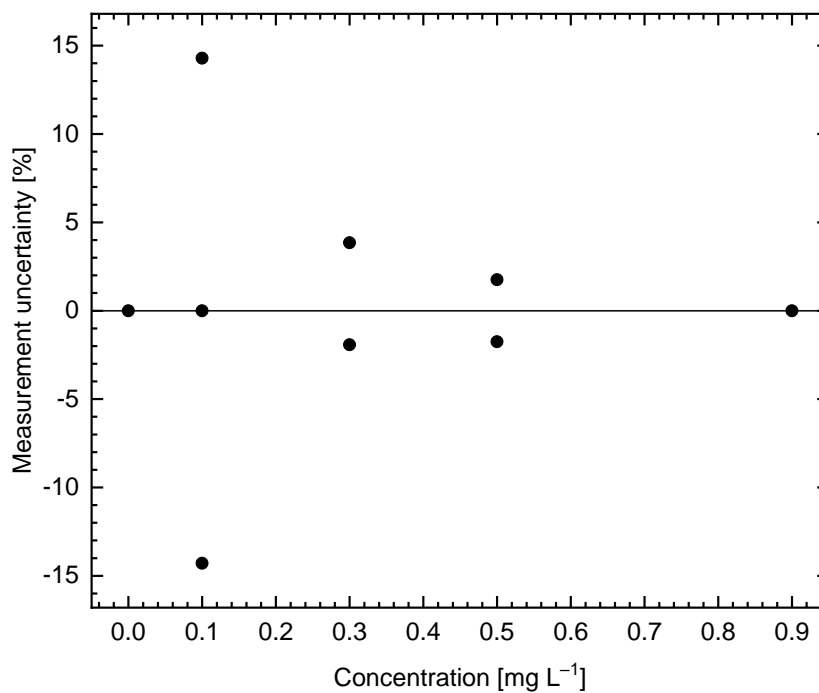
Figure E-8 Measurement uncertainty for the Zn(II) calibration curve defined as the percentage deviation from the measurement average.
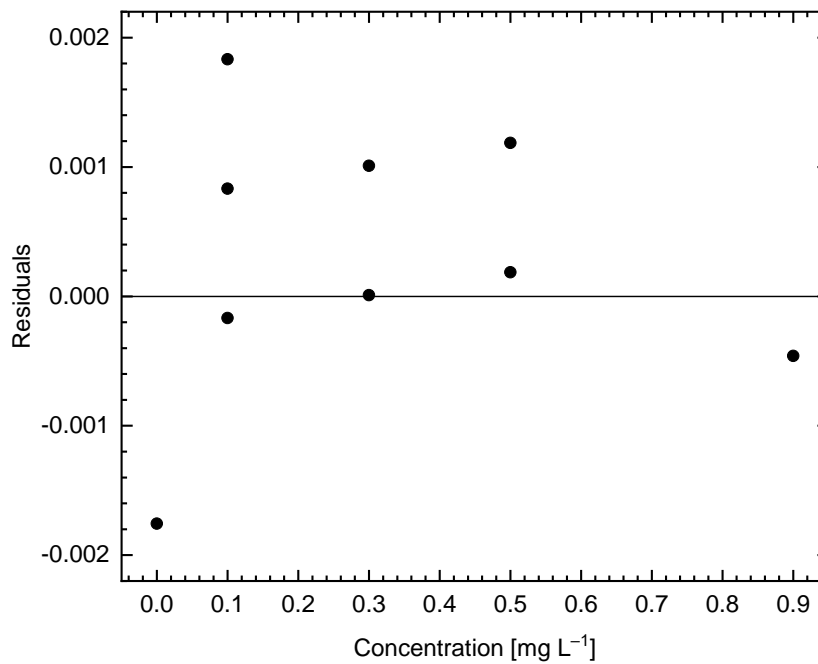
Figure E-9 Residuals as a function of standard concentration for the Zn(II) calibration curve.

Table E-6 Regression statistics for the Zn(II) calibration curve.

Parameter	Value
slope	5.421×10^{-2}
uncertainty of the slope	$\pm\, 9.4 \times 10^{-4}$
intercept	7.6×10^{-4}
uncertainty of the intercept	$\pm\, 4.7 \times 10^{-4}$
R^2	0.9967

E.2 Experimental data

E.2.1 FAAS absorbance data

Table E-7 Absorbance data for the test solutions before extraction.

Test solution	Corrected absorbance								
	Cd(II)			Cu(II)			Zn(II)		
	Measurement			Measurement			Measurement		
	1	2	3	1	2	3	1	2	3
1	0.055	0.058	0.056	0.036	0.037	0.037	0.041	0.040	0.039
2 (repeated)	0.059	0.057	0.057	0.037	0.038	0.038	0.039	0.038	0.039

Table E-8 Forward extraction absorbance data for [HTOA][phthalate].

Time[min]	Experiment	Corrected absorbance								
		Cd(II)			Cu(II)			Zn(II)		
		Measurement			Measurement			Measurement		
		1	2	3	1	2	3	1	2	3
5	1	0.022	0.024	0.022	0.033	0.033	0.033	0.030	0.030	0.029
	2	0.024	0.022	0.022	0.032	0.033	0.032	0.030	0.029	0.028
	3	0.021	0.022	0.024	0.032	0.031	0.032	0.029	0.027	0.027
15	1	0.016	0.014	0.016	0.030	0.030	0.030	0.026	0.027	0.028
	2	0.013	0.015	0.015	0.028	0.029	0.028	0.028	0.026	0.027
	3	0.014	0.015	0.014	0.028	0.028	0.028	0.024	0.027	0.028
30	1	0.013	0.013	0.012	0.024	0.025	0.025	0.024	0.029	0.025
	2	0.012	0.011	0.011	0.023	0.023	0.022	0.026	0.025	0.027
	3	0.009	0.012	0.012	0.023	0.022	0.023	0.028	0.025	0.024
60	1	0.01	0.009	0.009	0.018	0.018	0.020	0.028	0.025	0.023
	2	0.011	0.007	0.008	0.019	0.018	0.018	0.026	0.025	0.025
	3	0.006	0.005	0.007	0.019	0.019	0.017	0.027	0.027	0.021

Table E-9 Forward extraction absorbance data for [HTOA][adipate].

Time [min]	Experiment	Corrected absorbance								
		Cd(II)			Cu(II)			Zn(II)		
		Measurement			Measurement			Measurement		
		1	2	3	1	2	3	1	2	3
5	1	0.016	0.017	0.016	0.032	0.031	0.032	0.018	0.019	0.018
	2	0.017	0.017	0.017	0.031	0.031	0.033	0.018	0.018	0.019
	3	0.017	0.016	0.018	0.031	0.030	0.032	0.019	0.017	0.018
15	1	0.013	0.014	0.013	0.030	0.030	0.030	0.018	0.016	0.015
	2	0.013	0.013	0.014	0.029	0.029	0.028	0.015	0.015	0.017
	3	0.016	0.013	0.014	0.026	0.026	0.026	0.018	0.013	0.016
30	1	0.010	0.010	0.009	0.022	0.023	0.023	0.017	0.013	0.014
	2	0.010	0.010	0.009	0.019	0.017	0.019	0.014	0.014	0.013
	3	0.010	0.010	0.011	0.016	0.017	0.017	0.013	0.012	0.015
60	1	0.007	0.009	0.008	0.015	0.015	0.013	0.012	0.014	0.012
	2	0.007	0.009	0.008	0.014	0.014	0.014	0.013	0.012	0.013
	3	0.008	0.008	0.007	0.014	0.012	0.013	0.014	0.010	0.014

Table E-10 Back-extraction absorbance data for [HTOA][adipate].

	Experiment	Corrected absorbance								
		Cd(II)			Cu(II)			Zn(II)		
		Measurement			Measurement			Measurement		
		1	2	3	1	2	3	1	2	3
Before extraction	1	0.004	0.007	0.006	0.009	0.008	0.009	0.007	0.007	0.006
	2	0.007	0.007	0.007	0.009	0.009	0.009	0.007	0.006	0.006
After extraction	1	0.048	0.047	0.048	0.027	0.027	0.027	0.017	0.017	0.018
	2	0.051	0.049	0.052	0.028	0.029	0.028	0.018	0.016	0.016
	3	0.051	0.052	0.052	0.029	0.029	0.03	0.017	0.017	0.019

E.2.2 Raw sample concentration data

Table E-11 Metal ion concentrations of the test solution.

Test solution	Concentration [mg L^{-1}]								
	Cd(II)			Cu(II)			Zn(II)		
	Measurement			Measurement			Measurement		
	1	2	3	1	2	3	1	2	3
1	29.3	30.9	29.8	49.0	50.5	50.5	23.1	22.5	21.9
2 (repeated sample)	31.4	30.3	30.3	50.5	51.9	51.9	21.9	21.3	21.9

Table E-12 Forward extraction concentration data (after adjustments for the dilutions) for [HTOA][phthalate].

Time [min]	Experiment	Concentration [mg L^{-1}]								
		Cd(II)			Cu(II)			Zn(II)		
		Measurement			Measurement			Measurement		
		1	2	3	1	2	3	1	2	3
5	1	11.9	13.0	11.9	44.7	44.7	44.7	16.8	16.8	16.2
	2	13.0	11.9	11.9	43.3	44.7	43.3	16.8	16.2	15.6
	3	11.4	11.9	13.0	43.3	41.8	43.3	16.2	15.0	15.0
15	1	8.8	7.7	8.8	40.4	40.4	40.4	14.5	15.0	15.6
	2	7.2	8.3	8.3	37.5	38.9	37.5	15.6	14.5	15.0
	3	7.7	8.3	7.7	37.5	37.5	37.5	13.3	15.0	15.6
30	1	7.2	7.2	6.7	31.7	33.1	33.1	13.3	16.2	13.9
	2	6.7	6.2	6.2	30.3	30.3	28.8	14.5	13.9	15.0
	3	5.1	6.7	6.7	30.3	28.8	30.3	15.6	13.9	13.3
60	1	5.6	5.1	5.1	23.0	23.0	25.9	15.6	13.9	12.7
	2	6.2	4.0	4.6	24.5	23.0	23.0	14.5	13.9	13.9
	3	3.5	3.0	4.0	24.5	24.5	21.6	15.0	15.0	11.6

Table E-13 Forward extraction concentration data (after adjustments for the dilutions) for [HTOA][adipate].

Time [min]	Experiment	Concentration [mg L^{-1}]								
		Cd(II)			Cu(II)			Zn(II)		
		Measurement			Measurement			Measurement		
		1	2	3	1	2	3	1	2	3
5	1	8.8	9.3	8.8	43.3	41.8	43.3	9.9	10.5	9.9
	2	9.3	9.3	9.3	41.8	41.8	44.7	9.9	9.9	10.5
	3	9.3	8.8	9.8	41.8	40.4	43.3	10.5	9.3	9.9
15	1	7.2	7.7	7.2	40.4	40.4	40.4	9.9	8.7	8.2
	2	7.2	7.2	7.7	38.9	38.9	37.5	8.2	8.2	9.3
	3	8.8	7.2	7.7	34.6	34.6	34.6	9.9	7.0	8.7
30	1	5.6	5.6	5.1	28.8	30.3	30.3	9.3	7.0	7.6
	2	5.6	5.6	5.1	24.5	21.6	24.5	7.6	7.6	7.0
	3	5.6	5.6	6.2	20.1	21.6	21.6	7.0	6.4	8.2
60	1	4.0	5.1	4.6	18.7	18.7	15.8	6.4	7.6	6.4
	2	4.0	5.1	4.6	17.2	17.2	17.2	7.0	6.4	7.0
	3	4.6	4.6	4.0	17.2	14.4	15.8	7.6	5.3	7.6

Table E-14 Back-extraction concentration data (after adjustments for the dilutions) for [HTOA][adipate].

Time [min]	Experiment	Concentration [mg L^{-1}]								
		Cd(II)			Cu(II)			Zn(II)		
		Measurement			Measurement			Measurement		
		1	2	3	1	2	3	1	2	3
Before extraction	1	2.5	4.0	3.5	10.0	8.6	10.0	3.6	3.6	3.0
	2	4.0	4.0	4.0	10.0	10.0	10.0	3.6	3.0	3.0
After extraction	1	25.6	25.1	25.6	36.0	36.0	36.0	9.3	9.3	9.9
	2	27.2	26.1	27.7	37.5	38.9	37.5	9.9	8.7	8.7
	3	27.2	27.7	27.7	38.9	38.9	40.4	9.3	9.3	10.5

E.2.3 Sample concentrations

The test solution was determined to contain 30.3 ± 1.2, 50.7 ± 0.6, and $22.1 + 1.4$ mg L^{-1} of Cd (II), Cu(II), and Zn(II), respectively. However, for simplicity, these concentrations are stated as 50, 30, and 20 mg L^{-1}, respectively. The actual concentrations were used in determining the extraction efficiencies and distribution ratios.

Table E-15 Final metal ion concentrations used to determine the extraction efficiencies and distribution ratios.

Ionic liquid	Time [min]	Final concentration [mg L^{-1}]		
		Cd(II)	Cu(II)	Zn(II)
[HTOA][phthalate]	5	12.2 ± 0.5	43.7 ± 0.4	16.1 ± 0.6
	15	8.1 ± 0.6	38.6 ± 0.6	14.9 ± 0.6
	30	6.5 ± 0.7	30.7 ± 0.7	14.4 ± 0.7
	60	4.6 ± 0.8	23.7 ± 0.8	14.0 ± 0.8
[HTOA][adipate]	5	9.2 ± 0.5	42.5 ± 0.6	10.0 ± 0.5
	15	7.6 ± 0.6	37.8 ± 1.0	8.7 ± 0.7
	30	5.6 ± 0.6	24.8 ± 1.6	7.5 ± 0.6
	60	4.5 ± 0.7	16.9 ± 0.6	6.8 ± 0.7

E.3 Extraction efficiency data

Table E-16 Extraction efficiencies of [HTOA][phthalate] and [HTOA][adipate] as a function of extraction time.

Ionic liquid	Time [min]	Extraction efficiency [%]		
		Cd(II)	Cu(II)	Zn(II)
[HTOA][phthalate]	5	60 ± 4	14 ± 3	27 ± 5
	15	73 ± 4	24 ± 3	33 ± 5
	30	79 ± 5	39 ± 3	35 ± 5
	60	85 ± 5	53 ± 2	37 ± 5
[HTOA][adipate]	5	70 ± 4	16 ± 3	55 ± 7
	15	75 ± 4	25 ± 4	61 ± 8
	30	82 ± 4	51 ± 6	66 ± 7
	60	85 ± 5	67 ± 3	69 ± 7

E.4 Uncertainty analysis

The following is an outline of the procedure followed in calculating the uncertainties of the extraction efficiencies and distribution ratios.

The extraction efficiency of the IL for each metal i, E_i, was calculated using Eq. E1.

$$E_i(\%) = \left(\frac{C_{i,\text{aq}}^0 - C_{i,\text{aq}}}{C_{i,\text{aq}}^0} \right) \times 100 \tag{E1}$$

where $C_{i,\text{aq}}^0$ and $C_{i,\text{aq}}$ are the initial and final metal ion concentrations of metal i in the aqueous phase, respectively. Three repeated experiments were carried out for each extraction time experiment, and the average final concentration was used to determine the extraction efficiency.

$$C_{i,\text{aq}} = \frac{1}{n} \sum_{j=1}^{n} C_{i,\text{aq},j} \tag{E2}$$

The combined standard uncertainty of the extraction efficiency, $u_c(E_i)$, was obtained using Eq. E3, the law of propagation of uncertainty (Taylor and Kuyatt, 1994). This law estimates the combined standard uncertainty of E_i by using the uncertainties of the inputs on which E_i depends.

$$y = f(x_1, x_2, \ldots, x_n)$$

$$u_c^2(y) = \sum_{i=1}^{n} \left(\frac{\partial f}{\partial x_i} \right)^2 u^2(x_i) + 2 \sum_{i=1}^{n-1} \sum_{j=i+1}^{n} \frac{\partial f}{\partial x_i} \frac{\partial f}{\partial x_j} u(x_i, x_j) \tag{E3}$$

For E_i, the second term vanishes since the inputs on which it depends are uncorrelated. Therefore,

$$u_c(E_i) = \sqrt{\left[\left(\frac{\partial E_i}{C_{i,aq}^0}\right)_{C_{i,aq}} u(C_{i,aq}^0)\right]^2 + \left[\left(\frac{\partial E_i}{C_{i,aq}}\right)_{C_{i,aq}^0} u(C_{i,aq})\right]^2} \qquad (E4)$$

$$u_c(E_i) = \sqrt{\left[\left(\frac{C_{i,aq}}{C_{i,aq}^{0}{}^2} \times 100\right) u(C_{i,aq}^0)\right]^2 + \left[\left(\frac{-1}{C_{i,aq}^0} \times 100\right) u(C_{i,aq})\right]^2} \qquad (E5)$$

For the final concentrations, uncertainties arose from the measurement process (i.e., the calibration and instrument precision) and the variability of the multiple experiments. These two uncertainties were combined using Eq. D1 to give Eq. E6.

$$u_c(C_i) = \sqrt{u_{meas}(C_i)^2 + u_{exper}(C_i)^2} \qquad (E6)$$

The measurement uncertainties comprised uncertainties arising from the calibration and the precision of the FAAS.

$$u_{meas}(C_i) = \sqrt{u_{calib}(C_i)^2 + u_{prec}(C_i)^2} \qquad (E7)$$

The calibration uncertainty was calculated using Eq. E8 (Harris, 2015).

$$u_{calib}(C_{i,aq}) = \frac{s_y}{|b|} \sqrt{\frac{1}{m} + \frac{1}{n} + \frac{(y - \bar{y})^2}{b^2 \Sigma (x_i - \bar{x}_i)^2}} \qquad (E8)$$

where y is the (average) corrected response (absorbance) for the unknown, s_y is standard deviation in y, $|b|$ is the absolute value of the slope of the calibration curve, m is the number of replicate measurements of the unknown, n is the number of data points for the calibration

curve, $\bar{y}$ is the average of the responses for the calibration standards, x_i is the concentration of the standards, and $\bar{x}_i$ is the average of the concentrations for the calibration standards.

The uncertainty arising from the precision of the FAAS was estimated by the standard deviation of the mean for the three replicate measurements (Taylor and Kuyatt, 1994).

$$u_{\text{prec}}(C_{i,\text{aq}}) = \frac{s_{\text{meas}}}{\sqrt{n}}$$

$$= \sqrt{\left(\frac{1}{n(n-1)} \sum_{j=1}^{n} (C_{i,\text{aq},j} - C_{i,\text{aq}})^2\right)} \tag{E9}$$

where n is the number of replicate measurements, s_{meas} is the standard deviation of the final concentrations for the three replicate measurements, $C_{i,\text{aq},j}$ is the final concentration of metal i for measurement j, and $C_{i,\text{aq}}$ is the average concentration of the three experiments.

As the final concentration for each experiment had an associated measurement uncertainty, the highest uncertainty of the experiments was taken as $u_{\text{meas}}(C_{i,\text{aq}})$.

The uncertainty arising from the variability of repeated experiments was estimated by the standard deviation of the mean for the three repeated experiments (Taylor and Kuyatt, 1994).

$$u_{\text{exper}}(C_{i,\text{aq}}) = \frac{s_{\text{exper}}}{\sqrt{n}}$$

$$= \sqrt{\left(\frac{1}{n(n-1)} \sum_{j=1}^{n} (C_{i,\text{aq},j} - C_{i,\text{aq}})^2\right)} \tag{E10}$$

where n is the number of repeated experiments, s_{exper} is the standard deviation of the final concentrations for the three repeated experiments, $C_{i,\text{aq},j}$ is the final concentration of metal i for experiment j, and $C_{i,\text{aq}}$ is the average concentration of the three experiments. The uncertainty of the initial concentration was determined in a similar manner by considering the variability of the duplicate samples, the calibration uncertainties, and the instrument precision.

$u_c(E_i)$ was then calculated using Eq. E5 and expanded using a coverage factor, $k = 2$, to obtain an expanded uncertainty U for the extraction efficiency.

$$U = \pm k u_c(E_i) \tag{E11}$$

Assuming E_i follows a normal distribution, a coverage factor of 2 defines a confidence interval with a confidence level of approximately 95%.

A similar procedure was used in calculating the uncertainties of the distribution ratios, with the standard uncertainty calculated using Eq. E12.

$$u_c(D_i) = \sqrt{\left[\left(\frac{-C^0_{i,\text{aq}}}{C_{i,\text{aq}}{}^2} \times \frac{V_{\text{aq}}}{V_{\text{IL}}}\right) u(C_{i,\text{aq}})\right]^2 + \left[\left(\frac{1}{C_{i,\text{aq}}} \times \frac{V_{\text{aq}}}{V_{\text{IL}}}\right) u(C^0_{i,\text{aq}})\right]^2} \tag{E12}$$

APPENDIX F DATA FOR THE REFERENCED ILS

Table F-1 Ion abbreviations.

Ion abbreviation	Description
Cations	
[HTOA]$^+$	Trioctylammonium
[N$_{8888}$]$^+$	Tetraoctylammonium
[N$_{6666}$]$^+$	Tetrahexylammonium
[N$_{1888}$]$^+$	Methyltrioctylammonium
[P$_{66614}$]$^+$	Trihexyltetradecylphosphonium
[P$_{1888}$]$^+$	Methyltrioctylphosphonium
[A336]$^+$	Tricaprylylmethylammonium
Anions	
[NTf$_2$]$^-$	Bis(trifluoromethanesulfonyl)imide
[BTB]$^-$	2-(benzylthio)benzoate
[ETB]$^-$	2-(ethylthio)benzoate
[PTB]$^-$	2-(propylthio)benzoate
[TS]$^-$	Thiosalicylate
[C$_4$SAc]$^-$	Butylsulfanyl acetate
[C$_5$SAc]$^-$	Pentylsulfanyl acetate
[C$_6$SAc]$^-$	Hexylsulfanyl acetate
[BnSAc]$^-$	Benzylsulfanyl acetate

F.1 Physical properties

Table F-2 Physico-chemical properties of similar ILs.

Ionic liquid	ρ [g cm^{-3}][a]	η [mPa s][a]	σ [μS cm^{-1}][a]	n_D [a]	T_m [°C]	T_onset [°C]	Reference
Trioctylammonium							
[HTOA][salicylate]	0.9352	348.2	–	1.486	–	212.5	(Al Kaisy et al., 2017a)
[HTOA]$_2$[nonanedioate]	0.9262	3202	–	1.449	–	227.0	(Al Kaisy et al., 2017a)
[HTOA][dimethylbenzoate]	0.9009	126.6	–	1.480	–	189.1	(Al Kaisy et al., 2017a)
[HTOA][2-naphthoate]	0.9198	248.2	–	1.501	–	224.7	(Al Kaisy et al., 2017b)
[HTOA][4-tert-butylbenzoate]	0.8904	151.5	–	1.476	–	199.5	(Al Kaisy et al., 2017b)
[HTOA][2-hexyldecanoate]	0.8456	43.3	–	1.451	–	211.3	(Al Kaisy et al., 2017b)
[HTOA][4-phenylbutanoate]	0.8864	37.3	–	1.471	–	194.8	(Al Kaisy et al., 2017b)
[HTOA][NTf$_2$]	1.1043	200.4	–	–	3.7	–	(Katsuta et al., 2011)
Tetraalkylammonium							
[A336][Cl]	0.8875	1502	26.0	–	–	–	(Litaiem and Dhahbi, 2012)

Continued on next page

[N$_{8888}$][oleate]	0.8753	1153	–	–	-24.6	448	(Rocha et al., 2016)
[N$_{6666}$][oleate]	0.8879	1624	–	–	-29.4	442	(Rocha et al., 2016)
[N$_{1888}$][oleate]	0.8885	1971	–	–	-0.8	458	(Rocha et al., 2016)
[N$_{1888}$][4-ethyloctanoate]	0.8901	3733	–	–	-5.8	450	(Rocha et al., 2016)
[A336][BTB]	0.99	–	–	–	–	–	(Leyma et al., 2016)
[P$_{66614}$][BTB]	0.97	3120	–	–	–	–	(Leyma et al., 2016)
[A336][ETB]	0.98	4558	–	–	–	–	(Leyma et al., 2016)
[P$_{66614}$][ETB]	0.97	1947	–	–	–	–	(Leyma et al., 2016)
[A336][PTB]	0.97	5510	–	–	–	–	(Leyma et al., 2016)
[P$_{66614}$][PTB]	0.96	1814	–	–	–	–	(Leyma et al., 2016)
[A336][TS]	0.95	3220	–	–	–	–	(Leyma et al., 2016)
[P$_{66614}$][TS]	0.93	3875	–	–	–	–	(Leyma et al., 2016)

[a] Measured at 25 °C.

F.2 Extraction efficiency and distribution ratio data

Table F-3 Extraction efficiency and distribution ratio data.

Ionic liquid	Metals ions	Concentration [mg L^{-1}]	Extraction time [min]	Extraction efficiency [%]	Distribution ratio	Reference
[HTOA][octanoate]	Cu	1271	30	75	2.51	(Janssen et al., 2016)
[N$_{6661}$][methyl carbonate]	Cu, Zn [a]	25	15	74.4, 80.1	–	(Valdés Vergara et al., 2014)
[N$_{6661}$][adipate]	Cu, Zn [a]	25	15	96.8, 20.4	–	(Valdés Vergara et al., 2014)
[N$_{6661}$][salicylate]	Cu, Zn [a]	25	15	87.7, 88.6	–	(Valdés Vergara et al., 2014)
[N$_{6661}$][azelate]	Cu, Zn [a]	25	15	92.0, 42.5	–	(Valdés Vergara et al., 2014)
[N$_{1888}$][dodecanedioate]	Cu, Zn [a]	25	15	98.9, 88.1	–	(Valdés Vergara et al., 2014)
[N$_{1888}$][oxalate]	Cu, Zn [a]	25	15	99.9, 88.6	–	(Valdés Vergara et al., 2014)
[N$_{1888}$][azelate]	Cu, Zn [a]	25	15	86.8, 35.0	–	(Valdés Vergara et al., 2014)
[N$_{1888}$][thiosalicylate]	Cu, Zn [a]	25	15	76.2, 92.8	–	(Valdés Vergara et al., 2014)
[N$_{1888}$][methyl carbonate]	Cu, Zn [a]	25	15	54.1, 80.6	–	(Valdés Vergara et al., 2014)
[N$_{1888}$][camphorate]	Cd, Cu [a]	50	30	96.0, 93.9		(Valdés Vergara et al., 2015)
[N$_{1888}$][dodecanedioate]	Cd, Cu [a]	50	30	93.8, 99.8		(Valdés Vergara et al., 2015)

Continued on next page

[N$_{1888}$][camphorate]	Cd, Cu [a]	100	30	93.2, 89.4		(Valdés Vergara et al., 2015)
[N$_{1888}$][dodecanedioate]	Cd, Cu [a]	1000	30	92.8, 99.7		(Valdés Vergara et al., 2015)
[A336][BTB]	Cd, Cu, Zn [a]	4, 5, 1	240	42.3, 77.0, 50.9	–	(Leyma et al., 2016)
[P$_{66614}$][BTB]	Cd, Cu, Zn [a]	4, 5, 1	240	80.1, 90.2, 74.6	–	(Leyma et al., 2016)
[A336][ETB]	Cd, Cu, Zn [a]	4, 5, 1	240	64.2, 64.3, 23.7	–	(Leyma et al., 2016)
[P$_{66614}$][ETB]	Cd, Cu, Zn [a]	4, 5, 1	240	71.0, 86.5, 26.0	–	(Leyma et al., 2016)
[A336][PTB]	Cd, Cu, Zn [a]	4, 5, 1	240	66.0, 78.9, 37.4	–	(Leyma et al., 2016)
[P$_{66614}$][PTB]	Cd, Cu, Zn [a]	4, 5, 1	240	69.0, 93.6, 56.0	–	(Leyma et al., 2016)
[A336][TS]	Cd, Cu, Zn [a]	–	120	<5.0, 95.0, <5.0	–	(Leyma et al., 2016)
[P$_{66614}$][TS]	Cd, Cu, Zn [a]	–	120	14.0, 81.0, 24.0	–	(Leyma et al., 2016)
[N$_{1888}$][C$_4$SAc]	Cd, Cu [a]	2, 5	120	–	950, 144	(Platzer et al., 2017a)
[N$_{1888}$][C$_5$SAc]	Cd, Cu [a]	2, 5	120	–	943, 721	(Platzer et al., 2017a)
[N$_{1888}$][C$_6$SAc]	Cd, Cu [a]	2, 5	120	–	820, 1200	(Platzer et al., 2017a)
[N$_{1888}$][BnSAc]	Cd, Cu [a]	2, 5	120	–	731, 849	(Platzer et al., 2017a)
[P$_{1888}$][C$_4$SAc]	Cd, Cu [a]	2, 5	120	–	950, 882	(Platzer et al., 2017a)
[P$_{1888}$][C$_5$SAc]	Cd, Cu [a]	2, 5	120	–	950, 1200	(Platzer et al., 2017a)

Continued on next page

[P$_{1888}$][C$_6$SAc]	Cd, Cu [a]	2, 5	120	–	950, 1200	(Platzer et al., 2017a)
[P$_{1888}$][BnSAc]	Cd, Cu [a]	2, 5	120	–	950, 1045	(Platzer et al., 2017a)

[a] Single element aqueous solutions.